NTNU

Norwegian University of
Science and Technology

Displacement ventilation in Zero Emission Office Buildings (ZEB)

Hanne Jorunn Trydal

Master of Energy and Environmental Engineering
Submission date: July 2017
Supervisor: Hans Martin Mathisen, EPT
Co-supervisor: Maria Justo Alonso, EPT

Norwegian University of Science and Technology
Department of Energy and Process Engineering

NTNU

Norwegian University
of Science and Technology

Department of Energy
and Process Engineering

EPT-M-2017-89

MASTER THESIS

for

Student
Hanne Jorunn Trydal

Spring 2017

Displacement ventilation in Zero Emission Office Buildings (ZEB)
Fortrengningsventilasjon i nullutslipps kontorbygninger

Background and objective

Zero Emission Buildings require energy efficient ventilation to fulfil requirements for low energy use. Displacement ventilation has high ventilation effectiveness and the air can be even distributed with low pressure (low SFP). One challenge with this solution is to ventilate all parts of larger premises with high effectiveness, without using a high number of supply devices. In order to study the effectiveness of the displacement of Powerhouse Kjorbø a scala model has been constructed. The student's work should be based on measurement in the scaled model of an open office landscape in the laboratory.

The project is connected to the research program for Zero Emission Buildings (FME ZEB). Among the research activities FME ZEB are studies of so-called pilot buildings. One of these is Powerhouse Kjørbo, which is an older office building that has been renovated to become a zero emission building. The scaled model is a part of one floor at Powerhouse Kjørbo. See http://www.powerhouse.no/prosjekter/kjorbo/ for more information about the building.

The final goal of the work is to study whether the applied solutions for ventilation and cooling can provide good thermal environment and indoor air quality. If the solutions have weaknesses, the student is to provide improvement suggestions. It should be discussed if the solutions in general are well suited for ZEB.

The master thesis is a continuation of the student's project work.

The following tasks can be considered:

1. Conduct a literature study on state of the art solutions for ventilation and indoor climate, relevant for super insulated office buildings
2. Study how to apply displacement ventilation in larger open office areas and compare with the current solution at Kjørbo.
3. Discuss the theoretical basis for scaled models and their limitations.
4. Calibrate the model against the prototype

5. Perform measurements in the model for different conditions
6. Make test for possible alternative solutions

-- " --

Within 14 days of receiving the written text on the master thesis, the candidate shall submit a research plan for his project to the department.

When the thesis is evaluated, emphasis is put on processing of the results, and that they are presented in tabular and/or graphic form in a clear manner, and that they are analyzed carefully.

The thesis should be formulated as a research report with summary both in English and Norwegian, conclusion, literature references, table of contents etc. During the preparation of the text, the candidate should make an effort to produce a well-structured and easily readable report. In order to ease the evaluation of the thesis, it is important that the cross-references are correct. In the making of the report, strong emphasis should be placed on both a thorough discussion of the results and an orderly presentation.

The candidate is requested to initiate and keep close contact with his/her academic supervisor(s) throughout the working period. The candidate must follow the rules and regulations of NTNU as well as passive directions given by the Department of Energy and Process Engineering.

Risk assessment of the candidate's work shall be carried out according to the department's procedures. The risk assessment must be documented and included as part of the final report. Events related to the candidate's work adversely affecting the health, safety or security, must be documented and included as part of the final report. If the documentation on risk assessment represents a large number of pages, the full version is to be submitted electronically to the supervisor and an excerpt is included in the report.

Pursuant to "Regulations concerning the supplementary provisions to the technology study program/Master of Science" at NTNU §20, the Department reserves the permission to utilize all the results and data for teaching and research purposes as well as in future publications.

The final report is to be submitted digitally in DAIM. An executive summary of the thesis including title, student's name, supervisor's name, year, department name, and NTNU's logo and name, shall be submitted to the department as a separate pdf file. Based on an agreement with the supervisor, the final report and other material and documents may be given to the supervisor in digital format.

☒ Work to be done in lab (Water power lab, Fluids engineering lab, Thermal engineering lab)
☒ Field work

Department of Energy and Process Engineering, 22. January 2017

Hans Martin Mathisen
Academic Supervisor

Research Advisor:
Maria Justo Alonso

Preface

This thesis is part of the Master of Science Degree in Energy and Environmental Engineering, with specialization in Energy Planning and Environmental Analysis. It is written for the Department of Energy and Process Engineering (EPT) at the Norwegian University of Science and Technology (NTNU). The thesis is connected to the NTNU-SINTEF Zero Emission Building (ZEB) research activity on pilot buildings.

This thesis is a study into the indoor climate and ventilation of super insulated buildings, where the displacement ventilated system at Powerhouse Kjørbo has been investigated. The building is connected to the research programme for Zero Emission Buildings (FME ZEB). A reduced scale model of Powerhouse Kjørbo was been built by a previous student in the laboratory in the thermal building (VATL) at NTNU. The purpose of this thesis is to investigate how well suited the applied solution for ventilation is at Powerhouse Kjørbo. This thesis is a continuation of the project work, Autumn 2016.

Hanne Jorunn Trydal

Kristiansand, July 2 2017

Acknowledgements

I would like to thank my supervisor Hans Martin Mathisen for good guidance throughout this thesis. I would also like to thank Odin B. Søgnen for quick and good answer to my questions on Powerhouse Kjørbo, and access to files from his field work measurements and access to his files downloaded from Projectplace. To Magnus O. Sagnes for access to his files used for his master work, and to Lars Konrad Sørensen and the other laboratory workers for helping to improve the model. Lastly, I would like to thank my parents, for inspiration and guidance through the final stages of the construction of this thesis.

Abstract

This thesis investigates the ventilation efficiency and thermal climate of Powerhouse Kjørbo, located in Sandvika, Norway. Powerhouse Kjørbo consists of two buildings in a building complex of nine buildings, where building 4 and 5 have been renovated to zero-emission office buildings. They were renovated from conventional office buildings to plus houses, producing more energy than they consume in their operational lifetime, minus the equipment load. Building 4 is further investigated in this thesis. The ventilation principle used is displacement ventilation, supplied by few large diffusers in a large open office landscape. Several previous studies have examined the indoor climate of Powerhouse Kjørbo. Tracer gas measurements have shown the ventilation efficiency was lower than expected, looking more like mixing ventilation than displacement ventilation. CO_2 concentration measurements showed the overall air quality was good. However, concentration measurements from the east corner suggest this location as a stagnant zone, as the concentration was equal in height, and higher than the exhaust concentration. The east corner is almost completely enclosed by bookshelves placed directly on the floor. This can hinder the displacement supply flow significantly.

A scaled model has been built of half the 2nd floor of Powerhouse Kjørbo, to investigate ventilation efficiency and temperature distribution. Air velocity measurements have been performed on a supply diffuser, mapping the supply air velocities. Smoke experiments have been conducted at several locations in the model, to get a better overview of the air flow patterns. Temperature and tracer gas measurements have been conducted simultaneously for three different experimental cases, where the internal heat loads were changed. The temperature distribution and ventilation efficiency for different conditions were measured. The results have been compared to values from the prototype when available.

The velocity of a supply diffusers in the model was mapped. The results were compared to measurements from the corresponding supply diffuser in the prototype. The velocity mapping show the air distribution in the model and prototype differ. The model results show the negative buoyant effect expected for displacement ventilation. The prototype results indicate the supply air may be too warm. Smoke visualization of the air flow patterns in the model generally show the air behaves as for displacement ventilation. Some smoke experiments show the air flow patterns are unstable. The east corner gets a notably smaller supply air flow at floor level, compared to the south corner. This is confirmed by the tracer gas measurements.

The local air change index in the east corner is 95 %-units to 159 %-units smaller than the south corner, depending on the internal heat gain and local presence. However, both the east and south corner measurements show values consistent with good displacement ventilation. The minimum measurement at floor level was 161 %-units (East 25, Case II). The local air change efficiency increased with an increased presence. The east corner was almost completely enclosed by two large bookshelves. To see if the local air change index increased with a smaller bookshelf, the one facing north was halved in size. The tracer gas experiments showed a small increase in the local air change index (13 %-units at 25mm height), though the uncertainty of the measurements are large. The mean air change efficiency was higher than 64 %-units for the three different experimental cases, and higher than 60%-units for all measurements, indicating the model has good displacement ventilation.

Temperature measurements show the east corner had a higher temperature compared to other parts of the open office landscape. The temperature gradient in the east corner was however lower than in the south corner. This indicate that less air enters the east corner, which has also been seen from the smoke visualization and tracer gas measurements. The temperatures increase with a higher occupancy, as does the temperature gradients. However, scaled to full size, the temperature gradients are well within the maximum recommended vertical temperature difference.

The model and prototype results does not correspond. The model show results for good displacement ventilation, while the prototype indicate mixing ventilation and stagnant zones. The differing results does not mean that model similarity has not been reached, but indicate the prototype has a possibility of achieving good displacement ventilation. However, as the model has not been validated, that could not be determined for certain. The main reason for the differing results in the model and prototype have been identified as the different supply temperatures. The understanding of results are still valuable, since they demonstrate measurements for a smaller building, similar to the prototype.

Sammendrag

Denne oppgaven undersøker ventilasjonseffektiviteten og det termiske klimaet til Powerhouse Kjørbo, lokalisert i Sandvika, Bærum. Powerhouse Kjørbo består av to bygninger i et byggekompleks på ni blokker. Blokk 4 og 5 har blitt renovert fra konvensjonelle bygg til nullutslipps kontorbygg, som produserte mer energi enn de forbruker i den operasjonelle levetiden, minus utstyrsbelastningen. Blokk 4 er undersøkt videre i denne oppgaven. Ventilasjonssystemet installert er fortregningsventilasjon. Få tilluftsdiffusorer leverer luft til det åpne kontorlandskapet. Flere tidligere studier har undersøkt inneklimaet til Powerhouse Kjørbo. Sporgasmålinger har vist at ventilasjonseffektiviteten var lavere enn forventet, at den fungerer mer som blandingsventilasjon enn fortregningsventilasjon. CO_2 konsentrasjonsmålinger viste at den gjennomsnittlige luftkvaliteten i det åpne kontor landskapet var god. Konsentrasjonsmålinger fra hjørnet i øst antyder imidlertid at det var en stillestående sone, da konsentrasjonen var lik i høyden, og var høyere avtrekkskonsentrasjonen. Hjørnet i øst er nesten helt innestengt av bokhyller plassert direkte på gulvet. De kan hindre fortrengningsstrømmen betydelig.

En småskala modell er bygd av halvparten av 2. etasje i Powerhouse Kjørbo for å undersøke ventilasjonseffektiviteten og temperaturfordeling. Lufthastighetsmålinger har blitt utført på en tilluftsdiffusor. Røykeksperimenter har blitt utført på flere steder i modellen, for å få en bedre oversikt over luftstrømningsmønstrene. Temperatur- og sporingsgassmålinger har blitt utført samtidig for tre forskjellige eksperimentelle tilfeller, hvor de interne varmelastene ble endret. Temperaturfordelingen og ventilasjonseffektiviteten for forskjellige forhold ble målt. Resultatene er sammenlignet med tilgjengelige verdier fra prototypen.

Lufthastigheten til en tilluftsdiffusor i modellen ble kartlagt. Resultatene ble sammenlignet med målinger fra den tilsvarende tilluftsdiffusoren i prototypen. Hastighetskartleggingen viser at luftfordelingen i modellen og prototypen er forskjellig. Modellresultatene viser den negative oppdriftseffekten som forventes for fortregningsventilasjon. Prototypens resultater indikerer at tilførselsluften kan være for varm. Røykvisualisering av luftstrømningsmønstrene i modellen viser generelt at luften oppfører seg som for fortregningsventilasjon. Noen røykeksperimenter viser at luftstrømningsmønstrene er ustabile. Det østlige hjørnet får en betydelig mindre luft tilførsel på gulvnivå, sammenlignet med hjørnet i sør. Dette bekreftes av sporgassmålingene gjort.

Den lokale luftvekslingsindikatoren i det østlige hjørnet er 95%-poeng til 159%-poeng mindre enn i det sørlige hjørnet, avhengig av den interne varmelasten og antall personer tilstede lokalt. Imidlertid viser både østre og sørlige sporgassmålinger verdier som er konsistente for god fortregningsventilasjon. Minste måling på gulvnivå var 161%-poeng (øst 25, sak II). Den lokale luftvekslingsindikatoren økte med økt tilstedeværelse. Det østre hjørnet var nesten helt innestengt av to store bokhyller. For å se om den lokale luftvekslingsindikatoren økte med en mindre bokhylle, ble den nordre bokhyllen halverte i størrelse. Sporgassmålinger viste en liten økning i den lokale luftforandringsindeksen (13%-poeng ved 25mm høyde), men målingens usikkerhet er stor. Den gjennomsnittlige luftvekslingseffektiviteten var høyere enn 64%-poeng for de tre forskjellige eksperimentelle tilfeller, og høyere enn 60%-poeng for alle målinger. Dette indikerer at modellen har god fortregningsventilasjon.

Temperaturmålinger viser at hjørnet i øst hadde en høyere temperatur sammenlignet med andre deler av det åpne kontorlandskapet. Temperaturgradienten i øst var imidlertid lavere enn i sør. Dette indikerer at mindre luft kommer inn mellom bokhyllene i det østre hjørnet. Dette har også blitt observert fra røykvisualiseringer og sporgassmålinger. Temperaturene og temperaturgradientene øker med en høyere varmelast. Skalert til full størrelse, så holder temperaturgradientene seg godt innenfor den maksimale anbefalte vertikale temperaturforskjellen.

Modellen og prototypens resultater samsvarer ikke. Modellen viser resultater for god fortregningsventilasjon, mens resultatene fra prototypen indikerer blandingsventilasjon og stillestående soner. De ulike resultatene betyr ikke at similaritet mellom modellen og prototypen ikke er oppnådd, men indikerer at prototypen har mulighet for å oppnå god fortregningsventilasjon. Ettersom modellen ikke er validert, kan det fra resultatene ikke konkluderes sikkert. Hovedårsaken til de ulike resultatene i modellen og prototypen er identifisert som de ulike tilluftstemperaturene. Resultatene som er funnet er likevel verdifulle, ettersom de uansett viser målinger for en mindre bygning, ganske lik prototypen.

Contents

Abbreviations

AHU	Air Handling Unit
BREEM	Building Research Establishment Environmental Assessment Method
BREEM-NOR	Norwegian adaptation of BREEM
BAS	Building Automation System
CAV	Constant Air Volume
CRE	Contaminant Removal Effectiveness
DCV	Demand Controlled Ventilation
FME ZEB	The Research Centre on Zero Emission Buildings
HVAC	Heating, Ventilation and Air Conditioning system
IAQ	Indoor Air Quality
NGBC	Norwegian Green Building Council
PK	Powerhouse Kjørbo
PMV	Predicted Mean Vote
PPD	Percentage People Dissatisfied
SD	Standard Deviation
SFP	Specific Fan Power
VAV	Variable Air Volume
ZEB	Zero Emission Building

Nomenclature

A	Area	[m^2]
Ar	Archimedes number	[-]
C	Concentration	[ppm]
C_p	Specific heat	[J/kgK]
d	Depth	[m]
g	Gravitational constant	[m/s^2]
h	Heat transfer coefficient	[W/m^2K]
	Height	[m]
H	Heat loss	[W]
k	Thermal conductivity	[W/mK]
	Amount of convective heat flux	[%]
L	Length	[m]
N	Number, amount	[-]
n	Air change rate	[h^{-1}]
p	Pressure	[Pa]
Pr	Prandtl number	[-]
q	Volumetric flow rate	[m^3/s]
Re	Reynolds number	[-]
S	Scaling number	[-]
t	Time	[s]
T	Temperature	[K], [ºC]
U	U-value	[W/m^2K]
u, v, w	Velocity	[m/s]
V	Volume	[m^3]
$\dot{V}_{tg}$	Tracer gas flow rate	[h^{-1}]
β	Thermal expansion coefficient	[K^{-1}]
λ	Scaling factor	[-]
ε^a	Air change efficiency	[%-units]
ε_p^a	Local air change index	[%-units]
ε^c	Contaminant removal effectiveness	[-]
ε_p^c	Local air quality index	[-]
μ	Viscosity	[kg/ms]

ν	Kinematic viscosity	[m2/s]
ρ	Density	[kg/m^3]
$\langle \bar{\tau} \rangle$	Room mean age of air	[h]
τ_n	Nominal time constant	[h]
$\bar{\tau}_P$	Local mean age of air	[h]
$\bar{\tau}_r$	Actual mean air change time	[h]
Φ	Convective heat flux	[W]

Subscript

0	Reference value
∞	Infinite time
a	Air
c	Convection
e	Exhaust
i, inf	Infiltration
M	Model
P	Prototype Point in Room
r	Radiation
s	Supply
t	Transmission
tg	Tracer gas
tot	Total
V	Ventilation

Superscript

^	Instantaneous value
–	Mean value

Chapter 1 Introduction

As part of the Zero Emission Building (FME ZEB) research programme, Powerhouse Kjørbo – Stage 1 was built in 2013-2014. It was planned and built as a pilot project, showing that it is possible to renovate an older building to a ZEB standard, as well as a plus energy building. Two old office buildings, of a larger park of five buildings from the 1980, were renovated as a part of stage 1. They are renovated to a high standard, fulfilling the criteria of a passive house. The heat demand is covered by a ground source heat pump, with district heating peak load coverage. Solar panels produce enough clean energy to compensate for the greenhouse gasses produced in the buildings operational lifetime. Renovation of a third building in the park, Powerhouse Kjørbo – Stage 2, started in 2016, and is ready for occupation in July 2017. The buildings are located at Kjørbo in Sandvika, Bærum, Norway. See Powerhouse (2016c) for more information on the buildings.

1.1 Background

Powerhouse Kjørbo has a displacement ventilation system, where the open office landscape and the meeting rooms have demand controlled (DCV), variable air volume (VAV) supply flow rates, and the cell offices have constant air volume (CAV) supply. The indoor climate is controlled by a Building Automation System (BAS), which collect information from temperature, CO_2 and motion sensors placed in the buildings. Temperature and CO_2 sensors control the ventilation airflow to a room. Previous studies have examined the heating, cooling and ventilation system of the buildings. Tracer gas measurements done on the displacement ventilation system indicate that the ventilation efficiency is lower than expected. The results suggest a short circuiting of the ventilation, and further investigation of the system has been recommended. CO_2 measurements show even vertical concentrations, suggesting the ventilation is closer to mixing than displacement. Some areas of interest have been pointed out, circled in red in Figure 1.1.

The dimensions of the building are quite large, and only a few diffusers supply fresh air to the open office landscape. This means the air must travel long distances to ventilate all parts of the room. The challenge with few supply diffusers in a large space is to deliver the air where it should go. The east corner is located far away from the nearest supply diffuser, and the air seems to be pulled toward the exhaust before it enters the east corner. In addition, the eastern corner is almost completely enclosed by surrounding bookshelves, as seen in Figure 1.2. This hinders the displacement supply air flow to this area. CO_2 measurements done in this corner

show a higher concentration than in the exhaust air. The air flow to the southern corner of the open office landscape is also restricted by bookshelves, and a wall is separating the office space from the area in the south (circled in green in in Figure 1.1). The concern is that fresh air is hindered and hot air is trapped in these areas, causing stagnant zones.

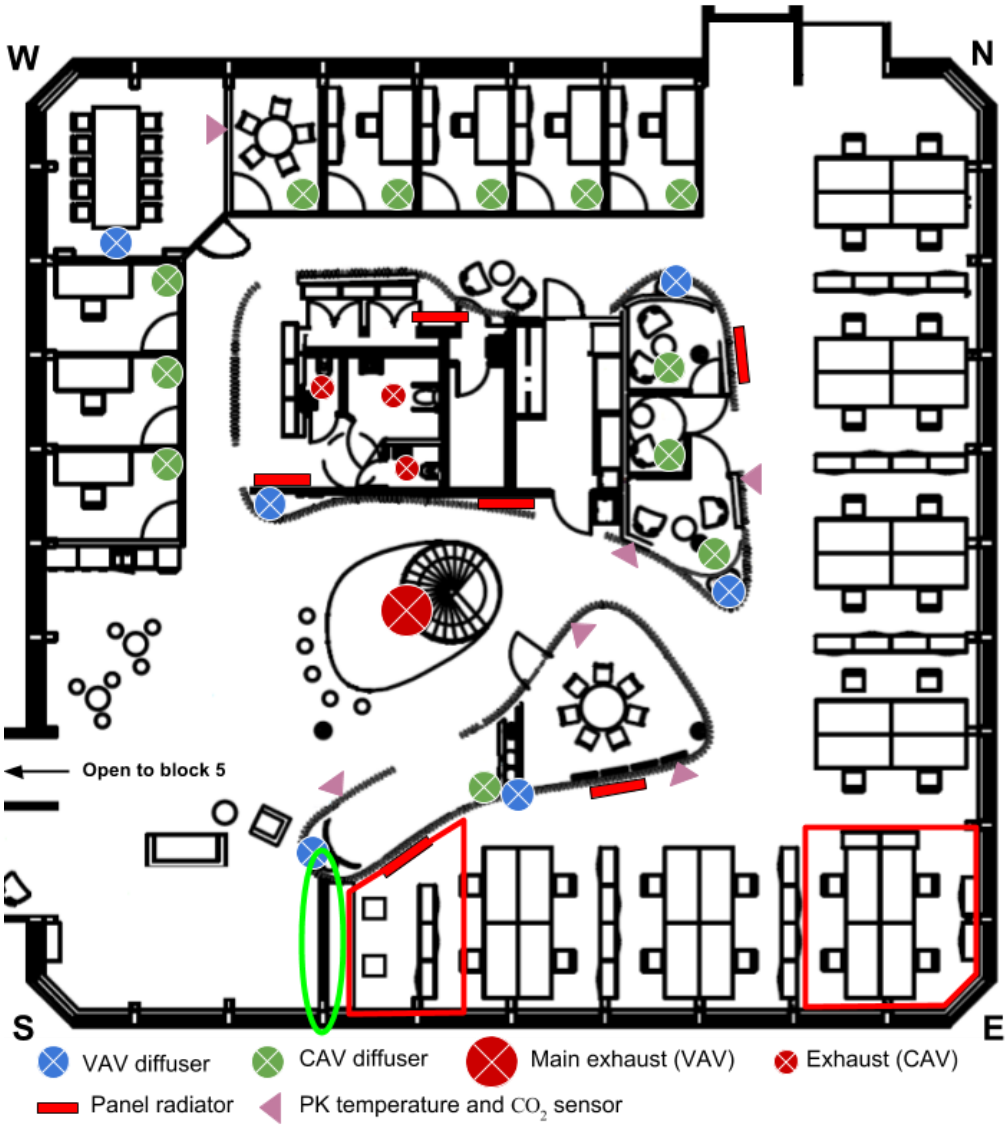

Figure 1.1 Areas of interest at Powerhouse Kjørbo, 2nd floor of building 4. Based on illustration by Søgnen (2015b) and Sangnes (2016)

Figure 1.2 East corner of office landscape at Powerhouse Kjørbo. (Sangnes, 2016)

A small scale model was built by Sangnes (2016) to investigate the air flow pattern and ventilation effectiveness of the building, though satisfactory similarity between the model and prototype was not reached. Additional improvements have been done during project work fall 2016, and for this master thesis spring 2017. Further investigation into the problem areas are planned for this thesis.

1.2 The Powerhouse, ZEB and BREEM/BREEM-NOR Concepts

1.2.1 The Powerhouse Alliance and Concept

The Powerhouse Alliance consists of six companies that cooperate on designing and building energy positive buildings. The members are the real estate company Entra, the entrepreneur Skanska, the architect office Snøhetta, the environmental organization ZERO, the aluminium solutions company Sapa and the consulting company Asplan Viak. The goal of the Powerhouse Alliance is to show that it is possible to build energy positive buildings in colder climates, such as Norway, not just in warmer southern climates. They want to show that these buildings can be profitable economically, as well as environmentally friendly (Powerhouse, 2016a).

The Powerhouse definition on an energy positive building is (Powerhouse, 2016b):

> *A Powerhouse shall during its lifetime produce more renewable energy than it uses for materials, production, operation, renovation and demolition.*

1.2.2 Zero Emission Buildings

A Zero Emission Building (ZEB) is a building that produces enough renewable energy to compensate for the greenhouse gas emissions during its lifetime. Powerhouse Kjørbo is a pilot project for the Research Centre on Zero Emission Buildings (FME ZEB). The ambition of Powerhouse Kjørbo is to be a ZEB-COM÷EQ building.

FME ZEB defines a ZEB-COM÷EQ as (FME ZEB, 2016):

> *The building's renewable energy production compensates for greenhouse gas emissions from operation of the building minus the energy use for equipment (pug loads).*

1.2.3 BREEM-NOR

BREEM (Building Research Establishment Environmental Assessment Method) is a worldwide method used to assess, rate and certify the sustainability of projects, infrastructure and buildings. It was created to help develop cost-effective means of bringing sustainable value to development (BRE, 2016). BREEM-NOR is the Norwegian adaptation of the BREEM concept, and the industry's tool to measure environmental performance of buildings. It has been developed by the Norwegian Green Building Council (NGBC), in cooperation with the Norwegian building industry.

The BREEM-NOR certification is issued in five levels; Pass, Good, Very Good, Excellent and Outstanding. It is based on nine categories; management, health- and indoor climate, energy, transport, water, materials, waste, area usage, and ecology and pollution (NGBC, 2016).

Powerhouse Kjørbo has been rewarded a BREEM-NOR Outstanding certification for the design-, and as built phase (Powerhouse, 2016c).

1.3 Objectives

The final goal of the work is to study whether the applied solutions for ventilation and cooling at Powerhouse Kjørbo can provide good thermal environment and indoor air quality. If the solution has weaknesses, improvements should be suggested. It should be discussed if the solutions in general are well suited for ZEB. The work is to be based on measurements in the scaled model of an open office landscape in the laboratory. The work is a continuation of the project thesis (Trydal, 2016).

The following tasks can be considered:

1. Conduct a literature study on the state of the art solutions for ventilation and indoor climate, relevant for super insulated buildings.
2. Study how to apply displacement ventilation in larger open office areas and compare with the current solution at Kjørbo.
3. Discuss the theoretical basis for scaled models and their limitations.
4. Calibrate the model against the prototype.
5. Perform measurements in the model for different conditions.
6. Make tests for possible alternative solutions.

1.4 Scope and Limitations

This thesis investigates displacement ventilation in a super insulated office building. As the building is located in a colder climate, when investigating theory on ventilation, heating and cooling, the focus is on displacement ventilation and heating and cooling of super insulated buildings in similar environments. The ventilation effectiveness and thermal climate in a scaled model of Powerhouse Kjørbo is examined. When investigating the theory of indoor climate, the theory on acoustic, actinic and mechanical environment have not been considered. The objective of the model experiments is to find whether the ventilation system provide a good thermal environment and indoor air quality.

More experiments were planned in the model, but due to delays and problems with the equipment, there was not time to do them. Some of the problems and delays were:

- Improvements were made to the model. It took time both to plan what changes should be made and implementing the changes.
- Other students and employees worked in the lab, using the same equipment as required to perform experiments in the model.
- The licence key for the tracer gas program, Innova 7620, disappeared. A new one was ordered, which arrived in the end of April.
- The compressor for the cooling circuit had a fatal breakdown in the start of May. A different solution was installed, ready for use some weeks later. As the cooling unit and other necessary equipment were reserved for use some weeks, experiments for this thesis could not start until the end of May.

A substantial time used for initial planning and building the improvements of the model was expected, though it took more time than anticipated. However, the problems with the licence key and the broken compressor could not be foreseen during planning. Combined with other

students and employees work in the lab, it lead to a significant delay in retrieving and processing results from the model. As the model experiments were delayed, the focus was on performing experiments to explore the ventilation effectiveness in the original model, not changing too many factors. However, some factors were changed, as the internal heat gain and the furniture in the east corner. There was no time to move or change the number of supply diffusers and exhausts, to see how that would impact the indoor climate.

The new cooling equipment did not have the same cooling capacity as the old one. Due to the delays stated above, the experiments were conducted during a period when the outside temperature was quite high. The cooling battery in the AHU was not able to keep the supply temperature stable and cool. The air temperature gradually increased during the day, and decreased in the evening. In addition, at times the supply temperature could suddenly increase by 0,5K, then drop 0,5K, causing bumps in the supply temperature. This unstable supply temperature affect the temperature measurements in the model. New measurements in the model with better control of both the supply temperature and the surrounding ambient room temperature was desired, but there was no time to implement improvements or perform the experiments again. However, the ventilation effectiveness measurements did not seem to be greatly impacted due to the unstable supply temperature.

If there had been enough time, and good results was achieved from the scale model, field work at Powerhouse Kjørbo was planned. Velocity mapping of different diffusers and tracer gas measurements for different loads were experiments thought interesting to perform. As the model experiments took longer than expected, this trip was cancelled. As the field work was not done, and a risk assessment on the field work was not performed.

The ventilation efficiency in the model is measured by conducting tracer gas experiments. However, as the air change efficiency in the model is very fast, the tracer gas equipment does not have time to perform many concentration measurements per step-up and step-down set. This reduces the robustness of the ventilation efficiency calculations, especially for the local air change index. However, even though the calculated values were not 100% accurate, they still give a good indication on the local air change. It was also noticed that the supply flow rate varied at times. This lead to curving logarithmic concentration curves and varying nominal time constants. The values not considered accurate were eliminated from the ventilation efficiency calculations.

1.5 Approach

This master thesis is a continuation of a project thesis fall 2016 (Trydal, 2016) and a previous master thesis (Sangnes, 2016). The scale model was built by Sangnes (2016), and further improved in the project work preceding this master thesis. The conclusion of the project thesis was that similarity of the model and prototype was not reached, so further improvements should be made. A list for further recommended work was stated, and some of the improvements suggested have been implemented:

- 16 lightbulbs have been added, increasing the total amount to 32 lightbulbs. 16 lightbulbs simulate people and 16 lightbulbs simulate computers.
- Grey painted cylinders have been fitted around the lightbulbs simulating people, to increase the similarity of the thermal plumes.
- The lightbulbs simulating computers have been fitted on steel plates, representing computer screens, increasing the similarity of the thermal plumes.
- All seals in the model have been tightened, minimizing the air leakage from the model. A thermal camera has been used to find remaining leakages.
- The supply diffusers have been properly balanced.
- A voltmeter has been used to find the actual delivered voltage from the Variacs.

This thesis is partially a literature research on ventilation and indoor climate of super insulated buildings, theory regarding indoor climate, displacement ventilation, ventilation effectiveness and scaled models, and ventilation experiments in the scald model in the lab at NTNU.

Improving the scaled model, performing experiments and analysing the results have been the main focus of this thesis. Velocity mapping was performed on the south-east diffuser, smoke experiments were conducted at several locations in the model, and the temperature and ventilation efficiency were measured for different internal loads and east corner setups. The results were compared to the prototype, to see if satisfactory similarity was reached.

1.6 Information Retrieval

A literature research has been conducted, finding information for both the theory chapter and “Ventilation and Indoor Climate of Super Insulated Buildings” chapter of this thesis. The literature research for this master thesis is mainly taken from the project thesis (Trydal, 2016). A new literature search has been done, but little new information was found. Specific theory on similarity principles regarding displacement ventilation have searched for, but no additional information was found.

Relevant literature has been searched for in several database, such as Scopus, Oria, Danish National Research Database, Science Direct and Google Scholar. Figure 1.3 shows an example of how a search is narrowed in the Scopus database

Figure 1.3 Example of narrowing a search in the Scopus database.

Other key words used was “super insulated building”, “highly insulated building”, “passive house”, “heating”, “cooling”, “chilled ceiling”, “heated ceiling”, “scaled model”, “reduced scale model”, “similarity theory”, “similitude”, etc. Search operators used are AND, OR, AND NOT, *, “ “, and W/n.

Chapter 2 Theory

2.1 Indoor Climate

Indoor climate is a concept that describes the state of an indoor environment. Factors influencing the indoor climate are thermal climate, indoor air quality, acoustic environment, actinic environment and mechanical environment, as well as aesthetic and psychosocial factors (Ingebrigtsen et al., 2015). For an office building, a good indoor climate is important for the personal comfort and health, as well as the productivity of the occupants of the building. Heating, cooling and ventilation of a building is three important aspects of achieving a good indoor climate (Commtech Group, 2003). This chapter will describe two of the main factors influencing the indoor climate that are of special interest concerning ventilation, indoor air quality and thermal climate. To ensure a good indoor environment, there are some requirements stated in different regulations, as can be seen in chapter 2.1.3.

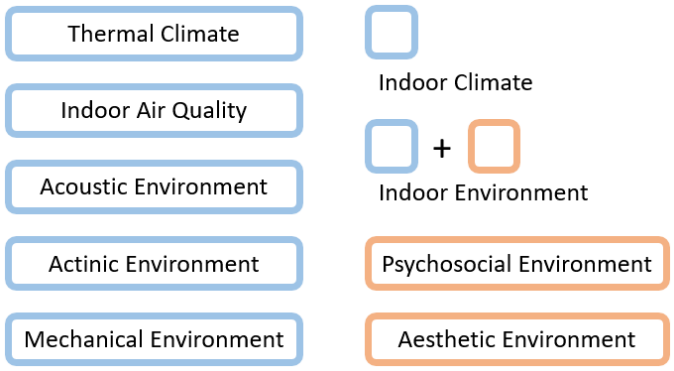

Figure 2.1 The factors of indoor climate and indoor environment. Based on illustration by Søgnen (2015a)

2.1.1 Indoor Air Quality

Indoor Air Quality is a measure of the cleanliness of the air in a room. The concept considers the perceived air quality of humans, the potential damaging effects the pollutants in the air might have on the human health, and what effect the pollutants in the air might have on items indoors. The indoor air quality is determined by the amount of gases, smells, chemical components and particles in the air. From a human perspective, the air quality is perceived as a combination of the air humidity, the air temperature and the age of the air. The indoor air quality is controlled by the ventilation effectiveness. The ventilation effectiveness of a system describes how fast and effective the air can be changed in, or contaminants can be removed from, a room. Theory on ventilation effectiveness is further described in Chapter 2.3.

2.1.2 Thermal Climate

The thermal climate in a building important to achieve thermal comfort for the occupants. The experience of thermal comfort is individual, and a person is said to be in thermal comfort with the surroundings when he or she expresses satisfaction with the thermal environment. The thermal climate is determined by several factors, as the air temperature, the surrounding surfaces radiative temperatures, and the air velocity and humidity level. In addition, the metabolic rate and clothing level of a person is important aspects that affects the thermal comfort of a person.

The operative temperature is often used to describe the thermal climate in a room. It describes the heat transfer due to convection and radiation of the air dry-bulb temperature and the radiative temperature.

$$T_0 = \frac{h_c T_a + h_r T_r}{h_c + h_r} \tag{2.1}$$

Where:

T_0 – operative temperature [^oC]

T_a – dry bulb temperature [^oC]

T_r – radiative temperature [^oC]

h_c – heat transfer coefficient for convection [W/m^2K]

h_r – heat transfer coefficient for radiation [W/m^2K]

If the air velocity is lower than 0,2 m/s and the difference between the air dry-bulb temperature and the mean radiative temperature is less than 4 K, the operative temperature can be calculated as the mean temperature of the air and mean radiant temperature:

$$T_0 = \frac{T_a + T_r}{2} \tag{2.2}$$

(SINTEF and NTNU, 2007)

2.1.2.1 Vertical Temperature Gradient

The vertical temperature gradient is a measure of the temperature difference between two different heights in a room. As the ankle and neck areas are especially sensitive to temperature difference, the vertical temperature gradient is measured as the difference at ankle height, 0,1 m, and seated neck height, 1,1 m. The recommended maximum vertical temperature gradient

is 3 K (Standard Norge, 2006), though a lower value of 2 K has proven better at preventing thermal discomfort (Ingebrigtsen et al., 2015). A gradient of more than 3-4 K can cause unacceptable discomfort (Arbeidstilsynet, 2016). The vertical temperature distribution can be estimated using the "50%-rule". The 50%-rule states that the air temperature at floor level will be half way between the supply and the exhaust temperature (Skistad et al., 2004).

2.1.2.2 Asymmetric Temperature Radiation

Even though the operative temperature may be acceptable, a to large difference in the radiation temperature from different surfaces can cause discomfort. To avoid a PPD index higher than 5%, the asymmetric temperature radiation to a warm ceiling should not be larger than 5 K, and toward a cold wall or window it should not be larger than 10 K (Ingebrigtsen et al., 2015).

2.1.2.3 Draft

The feeling of draft is a combination of the air velocity and temperature. For higher temperatures, a higher air velocity may be acceptable. The recommended maximum value of air velocity in the occupancy zone is 0,15 m/s for areas where physically light work is done (Arbeidstilsynet veiledning 444).

2.1.2.4 Metabolic Rate

The metabolic rate tells something about the activity level of a person, and is defined as the mechanical work performed and heat generated from a person. Different activity levels have different metabolic rates. For a relaxed, seated person the metabolic rate is 58 W/m^2, which is defined as 1 met. For an office worker, doing light work, the metabolic rate is 70 W/m^2, or 1,2 met. The mean surface area of an adult human body, the Du-Bois area, is approximately 1,75 m^2. Thus, an office worker doing light work emits approximately 122,5 W (Ingebrigtsen et al., 2015).

2.1.2.5 Clothing Level

The insulating ability of clothes, the clothing level, is an important aspect concerning the thermal comfort. The measuring unit for the insulation of clothes are clo, where 1 clo = 0,155 m^{2}K/W. In an office building the normal clothing level varies from 0,5-1,0 clo, depending on the season. (SINTEF and NTNU, 2007)

2.1.3 Requirements for Indoor Climate

A good indoor climate is important in an office building, as it effects both the health and productivity of its occupants. The human health is generally connected to the air quality in a room, though all the factors influencing the indoor climate also affect the human health. The

performance of an office worker is greatly affected by the thermal climate, acoustic level and air quality of a room. By changing the metabolism (the body's automatic thermostat) and removing or adding clothes, a person can be at thermal comfort for a larger temperature range. However, a too hot or too cold thermal environment can greatly impact the performance of an office worker. Reviewing available scientific findings, Seppänen et al. (2006) found that the performance of an office worker increased with temperatures up to 21-22 ºC and decreased with temperatures higher than 23-24 ºC. The optimal performance was found at temperatures around 22 ºC. Wargocki et al. (2000) found that the performance of an office worker increased on average by 1,7% for every doubling of the ventilation rate. A previous study also showed that the performance increased with a decreasing pollution load (Wargocki et al., 1999).

To prevent a poor indoor climate, some requirements are stated in laws and regulations. The Planning and Building Act (Plan- og Bygningsloven) states through chapter 13 of The Norwegian Regulations on Technical Requirements for Building (TEK10:2016) some requirements regarding the ventilation rate and the thermal climate in new buildings. The Working Environment Act (Arbeidsmiljøloven) states through The Norwegian Labour Inspection Authority's guidelines for Climate and Air Quality in the Workspace (Arbeidstilsynets veiledning 444) some criteria for the indoor thermal climate and ventilation.

The ventilation system should be dimensioned in proportion to the polluting load from persons and materials. The CO_2 level of the indoor air should not exceed the outdoor CO_2 level with more than 500 ppm at maximum occupancy level (TEK10:2016). The room air CO_2 concentration should be kept below 1000 ppm (Arbeidstilsynet, 2016). Table 2.1 some minimum requirements for the ventilation air flow rate in a building. The numbers should be added together to find the minimum required air flow rate.

Table 2.1 Minimum ventilation air supply rates in a building where light work is done

Air supply due to:	**TEK10:2016**	**Arbeidstilsynets veiledning 444**
Occupant pollution [pr. person]	26 m^3/h	7,0 l/s
Material pollution when in use [pr. m^2 floor area]	2,3 m^3/h	> 2,0 l/s
Material pollution when not in use [pr. m^2 floor area]	0,7 m^3/h	0,7 l/s

Both TEK10:2016 and the Working Environment Act set temperature limitations for different work activity levels, as can be seen in Table 2.2. They also recommend that the air temperature

should be kept below 22 °C when space heating is required. Regarding the vertical temperature gradient, they state that an air temperature difference of more than 3-4 °C between the head and the feet result in unacceptable discomfort.

Table 2.2 Recommendations on operative temperature at the workspace. (Arbeidstilsynet, 2016) (TEK10:2016)

Activity group	Light work	Medium hard work	Hard work
Temperature [°C]	19-26	16-26	10-26

2.2 Displacement Ventilation

Displacement ventilation is a ventilation strategy that utilizes the density differences of air at different temperatures to remove old, contaminated air from a room. The idea behind displacement ventilation is to create two zones in a room. An occupied zone, with clean, colder air, and a warmer, polluted zone located above the occupied zone. Air is supplied at low temperatures (2-3K lower than the ambient room temperature) and low velocities. It is generally supplied at floor height, and extracted at ceiling height. The driving force of displacement ventilation is the buoyancy effect.

As fresh air is supplied to a room, it will fall to the floor and distribute itself along the ground. The air is then heated by warmer surfaces, such as people, heat emitting equipment and warm radiators. Due to a density difference, the warmer air rises to the ceiling while the cold air remains at floor level. Pollutants, such as CO_2, is entrained in the rising air and brought out of the occupied zone. To ensure a proper removal of contaminants from the room, they should be warmer (and/or lighter) than the surrounding air. As the colder clean air is heated by persons, fresh air is brought into the breathing zone. Persons breath out contaminants, which are entrained in the rising air and brought out of the occupied zone, where it is extracted. A well-functioning displacement ventilation system will have a better air quality in the occupant zone than mixing ventilation, at the same air flow rates.

Due to the low supply velocity of the displacement ventilation and the larger dimensions of the ducts, there is less friction loss in the air supply system. Thus, less power is needed in the air handling unit to counter the pressure loss in the system. This low SFP makes displacement ventilation ideal for low energy buildings, such as a zero emission buildings.

See Chapter 3.2 for heating and cooling with displacement ventilation.

2.2.1 Convection flows

Convection flows are the driving force of displacement ventilation. As air flows along a hot or cold surface, the air will rise or fall, respectively. The hot air that rises above a warm surface, is called a thermal plume, as illustrated in Figure 2.3 and Figure 2.2. As the hotter air rises, it entrains more and more air, forming a cone shape. The centreline velocity and plume air flow rate can be calculated from the convective heat flux, Φ (Skistad et al., 2004). The convective heat loss from a human body is approximately 40% of the total heat loss (Etheridge and Sandberg, 1996), while a computer and monitor will have 70-80% convective heat loss (Hosni et al., 1999).

$$u_z = 0{,}128\Phi^{1/3} z^{-1/3} \tag{2.3}$$

$$q_{v,z} = 5\Phi^{1/3} z^{5/3} \tag{2.4}$$

Where:

u_z – centreline velocity, z meters above the source [m/s]

$q_{v,\,z}$ – air flow rate, z meters above the source [m^3/s]

$\Phi = k \cdot \Phi_{tot}$ = the convective heat flux [W]

Φ_{tot} – total heat flux [W]

k – convective part of the heat flux [%]

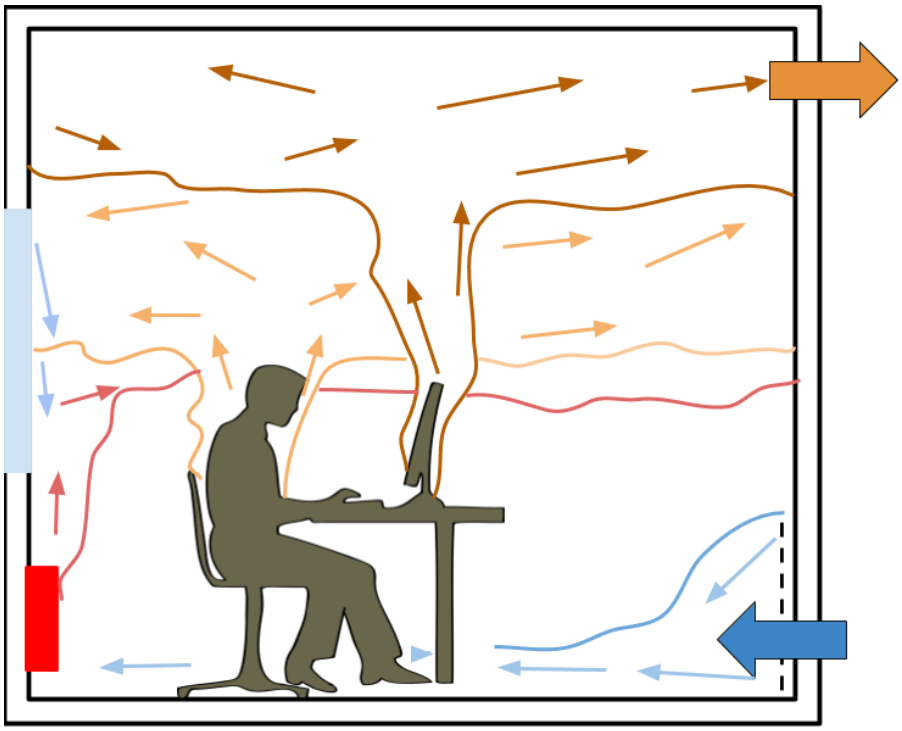

Figure 2.2 Convection air flows

Thermal plumes in practical ventilation are turbulent flows, and can be treated as fully developed turbulent flows. This also means that they follow the similarity rules of turbulent flows.

2.2.2 Air Distribution in Displacement Ventilated Rooms

The movement of air flows in displacement ventilated areas are highly dictated by the air density differences. The air will divide itself in thermally stratified layers, as illustrated in Figure 2.3. Keeping the air thermally stratified is essential to achieve a good air quality in a displacement ventilated room. The thermal stratification and distribution of contaminants are sensitive to moving objects, for example moving people or doors opening and closing (Yuan et al., 1998). In an open office landscape, there will be persons moving about in the room. This will cause a mixing of the stratified air, as well as occasionally higher air velocities than desired.

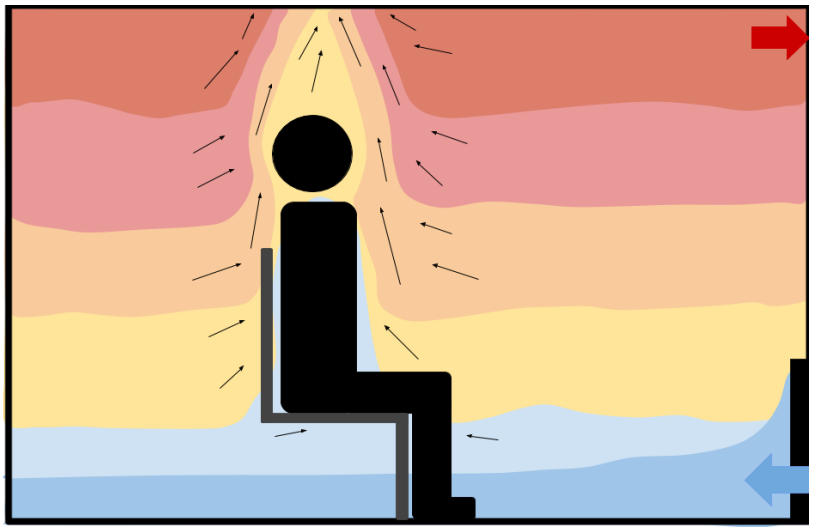

Figure 2.3 Thermal stratification and plume above a seated person. Based on illustration by Skistad et al. (2004)

As fluids move along the path of least resistance, barriers and obstructions may hinder the flow from moving correctly. This can cause stagnant zones areas with a suboptimal air quality. To prevent this, the desired path for the airflow should be kept clear of barriers. The maximum velocity of the flow is located close to the floor (1 to 4 cm above), so barriers placed directly on the floor will hinder the flow more than objects that allow air movement underneath (Nielsen, 1993). Figure 2.4 illustrates the air flow pattern in a room with different objects as obstructions.

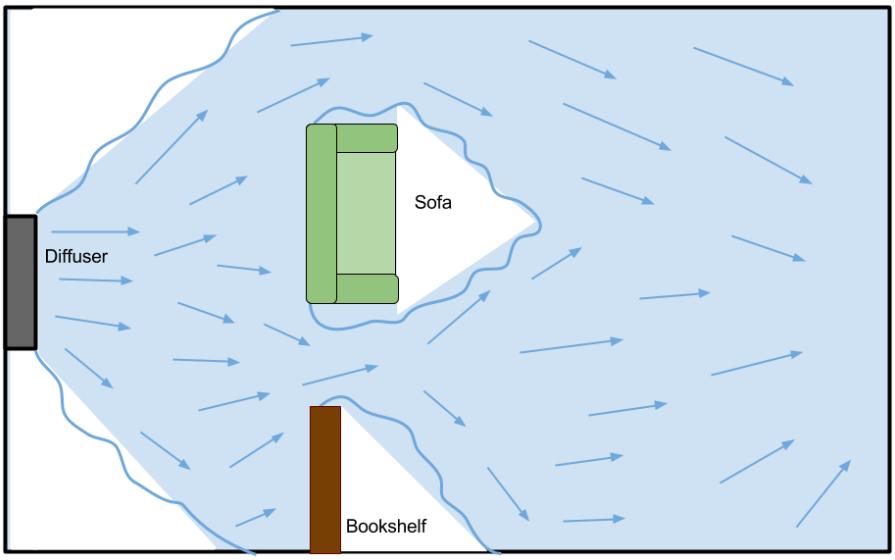

Figure 2.4 Air distribution around obstructions. Based on illustration by Price Industries (2016)

2.2.3 The Adjacent Zone of a Diffuser

The airflow from a wall mounted plane diffuser with a forward discharge will spread out in a radial distribution. Within a certain distance from the supply diffusers, the air velocities are higher than the recommended velocities. This area is called *the adjacent zone*, or *the near-zone*, of a diffuser. To avoid draft from the supplied air, the adjacent zone should not be a part of the occupant zone. No furniture should be placed in this zone, as this will hinder the air distribution. The discharge from the diffuser experience an initial downward acceleration, due to the negative buoyancy effect of the colder flow, before it deaccelerates along the floor. The adjacent zone of a diffuser ends when the air velocity has dropped below a certain limit, usually 0,2 m/s.

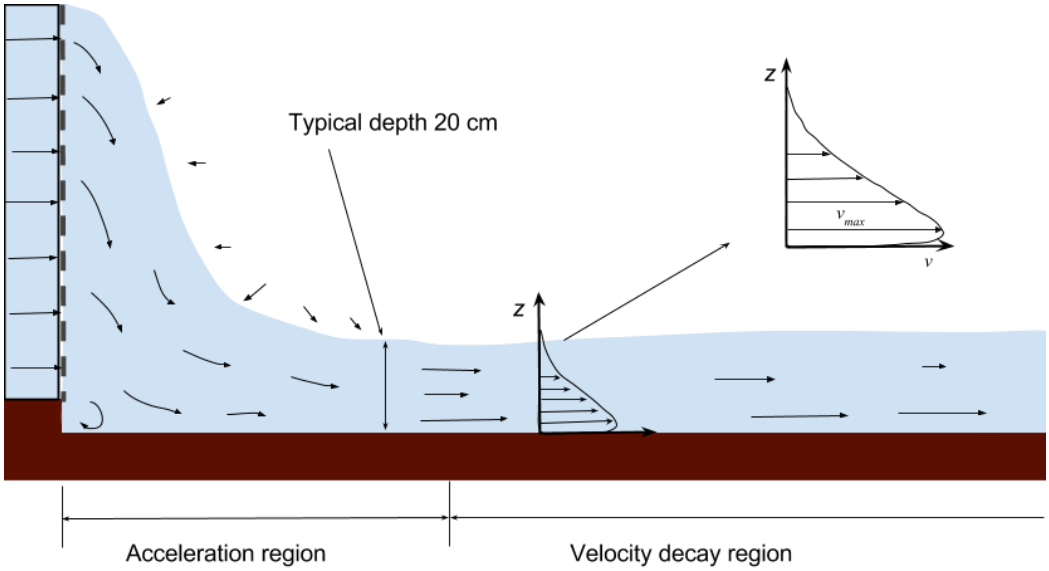

Figure 2.5 Depth of diffuser discharge flow. Based on illustration by Skistad et al. (2004)

A large supply diffuser can experience an instability in the discharge flow. This is especially prominent in low-velocity diffusers, used for displacement ventilation. This can lead to an unstable discharge flow from the diffuser.

(Skistad et al., 2004)

2.2.4 Displacement Ventilation in Larger Open Office Areas

Displacement ventilation has proven to work well in larger open areas, where the ceiling height is minimum 3 m. To avoid a short circuiting of the ventilation system, the supplied air should to be 2-3 K colder than the ambient room temperature. A larger temperature gradient is not recommended, due to concern regarding the thermal comfort. As mentioned in Chapter 2.2.2 and 2.2.3, no furniture should be placed in front of the diffusers or in the desired air flow path. This may hinder the air flow, and create stagnant zones with poor air quality. To achieve a good

distribution of the supply air, diffusers should be placed strategically to cover the whole area. Too few supply devices, or disadvantageous placing can also cause stagnant areas with bad air quality. (Skistad et al., 2004)

A challenge with few supply diffusers in a large area is to provide good air quality for the whole room. With few supply diffusers for a large area, the distances will be longer and the system will be less robust. Obstructions placed in the way of the air flow, or an area enclosing by objects placed at the floor can more easily cause stagnant zones. As the air is hindered, it may more easily be pulled toward the exhaust before it reaches the intended area. The air will be heated as it travels from the supply diffuser into the room. If the distance is too long it may rise to the ceiling before it reaches the intended destination.

With only one exhaust for a large area, the contaminated air has to travel long distances in the ceiling before it is extracted. Lighting fixtures, ducts and sound barriers are objects that often are placed in the ceiling. They will act as barriers, hindering the flow. This will cause more mixing of the fresh air in the occupancy zone and the contaminated upper layer. As the ducts often carry colder supply air, they can cool the surrounding air. This will also cause additional mixing. In addition, there will always be people moving in an open office area. The movement will cause mixing of the stratified layers.

2.2.5 Constant Air Volume and Variable Air Volume

There are two main strategies used for control of the air supply in a room in a mechanical ventilation system:

- Constant air volume (CAV)
- Variable air volume (VAV)

The CAV method supplies a constant volume of air to the room. The air is usually supplied at a suitable temperature, but additional heating of the air can be done ether by a heating coil upstream in the ventilation system, or by radiators in the relevant zone. The VAV method varies the air volume supplied in a room. The air supply has a constant temperature, but the air supply is often regulated according to the room temperature. (Commtech Group, 2003)

2.2.6 Demand Controlled Ventilation

Demand controlled ventilation (DCV) can be thought of as a method to regulate a VAV system. The amount of air supplied in a room can be controlled as needed, depending on different parameters. The regulating factors can be concentration of contaminants, room air temperature,

air humidity, or presence of people. Sensors measuring different parameters can be placed in the occupant zone, giving real time information to a control unit, regulating the ventilation air flow. The use of DCV in a building can reduce necessary supply air volume significantly. Consequently, the required fan speed is reduced which again lead to a lower the power usage.

2.3 Ventilation Effectiveness

This chapter contain theory on ventilation effectiveness, and describes how to find the air change efficiency using tracer gas measurements. All information was found in the handbook Ventilation Effectiveness by Mundt et al. (2004), unless stated otherwise.

The ventilation effectiveness of a system shows how fast a system can remove contaminants or change the air in a room, and can be defined in two ways:

- Contaminant removal efficiency; the system's ability to remove airborne contaminants.
- Air change efficiency; the system's ability to exchange the air in the room. The age of air concept is used to evaluate the air change efficiency.

The air change efficiency is generally higher in a displacement ventilated room, compared to a room with mixing ventilation. Tracer gas measurements can be used to measure the ventilation efficiency.

2.3.1 Age of Air

The age of air in a room is a measure of how long the air has been in the room. When air enters a room, the air molecules will travel different paths to different parts of the room, as shown in Figure 2.6. The air in a point in the room consists of air molecules that have been in the room for different lengths of time. The age of air in the point is an average of the age of all the molecules in the point, also called the local mean age of air, $\bar{\tau}_P$. The room mean age of air, $\langle \bar{\tau} \rangle$, can be found as a mean value of all the local mean ages of air.

The fresher, younger air can be found close to the supply diffusers, while the older air can generally be found close to the extract. If there is a short circuiting of the ventilation system, the age of the air in the stagnant part of the room will be high.

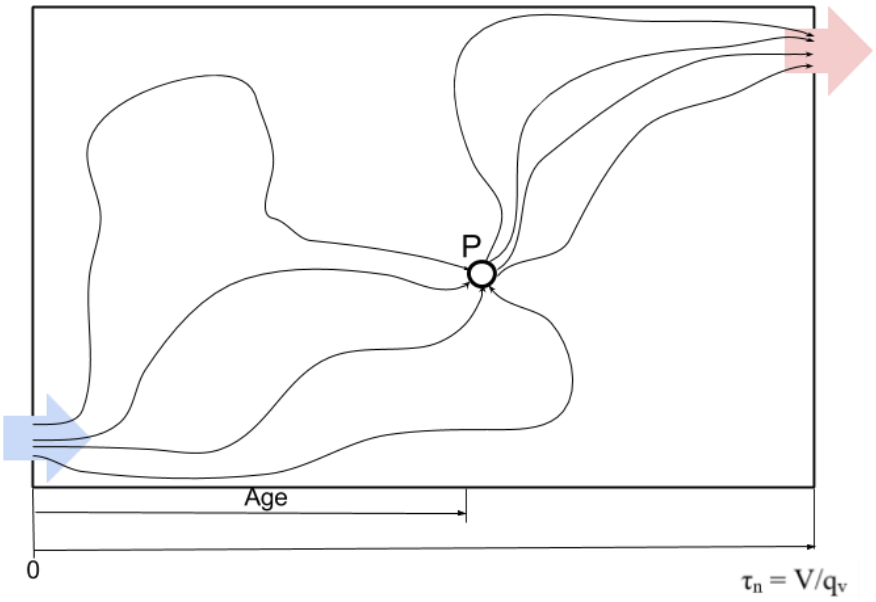

Figure 2.6 Age of air at a point P in a room. Based on illustration from Mundt et al. (2004).

The mean age of air in the exhaust, also called the nominal time constant τ_n, can be found from Equation (2.5). The local mean age of air in the exhaust is always equal to the nominal time constant.

$$\tau_n = \frac{V}{q_v} \qquad [h] \qquad (2.5)$$

Where:

τ_n – *nominal time constant [h]*

V – *room volume [m^3]*

q_v – *ventilation air flow [m^3/h]*

2.3.2 Air Change Rate

The nominal air change rate, n, can be found as the inverse of the nominal time constant. The air change rate number is used to express the ventilation performance, giving a ratio of the volume of air entering a room per hour and the effective volume of the room.

$$n = \frac{1}{\tau_n} = \frac{q_v}{V} \qquad [h^{-1}] \qquad (2.6)$$

The effectiveness of the ventilation cannot be found from the air change rate. If there is a high degree of short circuiting, a higher air change rate will not improve the local air qualities. The air change rate should not be used to describe the ventilation effectiveness, as it can give a wrong impression of the room air quality (Ingebrigtsen et al., 2015).

2.3.3 Air Change Efficiency

The air change efficiency is a measure of how fast the air volume in a room can be replaced with fresh air, compared to the theoretical fastest possible air change in the room. The lowest possible room average age of air can only be obtained for a piston flow, and is equal to the local mean age of air in the exhaust. The actual mean air change time $\bar{\tau}_r$, is twice the room mean age of air $\langle \bar{\tau} \rangle$. The air change efficiency can be calculated from Equation (2.7):

$$\varepsilon^a = \frac{\tau_n}{\bar{\tau}_r} \cdot 100 = \frac{\tau_n}{2\langle \bar{\tau} \rangle} \cdot 100 \qquad \text{[\%-units]} \tag{2.7}$$

Where:

ε^a *– air change efficiency [%-units]*

$\overline{\tau_r}$ *– actual mean air change time [h]*

$\langle \bar{\tau} \rangle$ *- room mean age of air [h]*

The maximum air change efficiency, $\varepsilon^a = 100$, is obtained from an ideal piston flow. The air change efficiency for different flow patterns can be found in Table 2.3.

Table 2.3 Room mean age of air and air change efficiency for different flow patterns.

Air flow pattern	**Room mean age of air, $\langle \bar{\tau} \rangle$**	**Air change efficiency, ε^a**
Ideal piston	$\langle \bar{\tau} \rangle = \frac{\tau_n}{2}$	$\varepsilon^a = 100\%$
Displacement ventilation	$\frac{\tau_n}{2} < \langle \bar{\tau} \rangle > \tau_n$	$50\% \leq \varepsilon^a \geq 100\%$
Fully mixed	$\langle \bar{\tau} \rangle = \tau_n$	$\varepsilon^a = 50\%$
Short-circuit	$\langle \bar{\tau} \rangle > \tau_n$	$\varepsilon^a \leq 50\%$

Usually the air change efficiency for a displacement ventilation system is around 55-60%. With an efficiency above 60%, the ventilation system works very well. (Mathisen, 2017)

The local air change index, $\varepsilon^a{}_P$, describe the conditions at a specific point in the room. It is defined as the ratio between the nominal time constant and the local mean age of air at that point.

$$\varepsilon_P^a = \frac{\tau_n}{\bar{\tau}_P} \qquad \text{[\%-units]} \tag{2.8}$$

Where:

ε_P^a – *local air change index [%-units]*

$\bar{\tau}_P$ – *local mean age of air [h]*

The local air change index can be very large or very small, depending on where in the room the measurements are taken, and the air flow pattern at that position. In the case of a short circuiting the local air change index will be low in the stagnant zone, and high in the shortcut. In a room where there is full mixing the local mean age of air is the same at all points in the room, and is equal to the nominal time constant. This gives a local air change index $\varepsilon_P^a = 100\%$ in the whole room. The air change efficiency and local mean ages of air can be found by performing tracer gas experiments.

2.3.4 Contaminant Removal Effectiveness (CRE)

The contaminant removal effectiveness is a measure of the ventilation system ability of removing contaminants by supplying fresh air to a room. It compares the concentration of contaminants in the room air and the concentration of contaminants in the exhaust air, and tells us how quickly the ventilation system can remove air-borne contaminants from the room air.

$$\varepsilon^c = \frac{C_e - C_s}{C_{mean} - C_s} \qquad [-] \qquad (2.9)$$

Where:

ε^c – *contaminant removal effectiveness [-]*

C_e – *the concentration of contaminants in the exhaust air*

C_s – *the concentration of contaminants in the supply air*

C_{mean} – *the average concentration of contaminants in the room air*

If the room air is fully mixed, the exhaust air concentration of contaminants will be equal to the room air concentration, $\varepsilon^c = 1$. However, a room is seldom fully mixed. The mean room air concentration depends on the ventilation strategy and the location of the contaminant sources in the room, and can vary from small to large values. If the mean concentration in the room is low compared to the exhaust concentration, the ventilation is satisfactory.

As the room air is seldom fully mixed, the local air quality index, $\varepsilon^c{}_P$, may give a better description of the room air quality. It is defined as the ratio between the concentration of

contaminants at the exhaust, C_e, and the concentration of contaminants at the point P in the room C_P.

$$\varepsilon_P^c = \frac{C_e}{C_P} \qquad [-] \qquad (2.10)$$

Where:

ε_P^c *– local air quality index [-]*

C_P *– the concentration of contaminants at point P*

2.3.5 Tracer Gas Measurements

The ventilation effectiveness can be calculated from tracer gas experiments. The nominal time constant, mean age of air and local age of air can be calculated from the measured concentrations in the room, from which the air change efficiency and local air change index can be calculated from.

There are some conditions when selecting a tracer gas for use in experiments. The gas should not be toxic or explosive and should not already be present in the environment. It should be chemically stable and inert, environmentally friendly, and the gas density should be as close as possible to the density of air at atmospheric conditions. It is also important that the gas is easily detected and measured, even at small concentrations. Common tracer gases used are sulphur hexafluoride (SF_6), carbon dioxide (CO_2) and nitrous oxide (N_2O, more commonly known as laughter gas). If CO_2 is used as a tracer gas, the background CO_2 concentration must be constant.

Tracer gas experiments can be performed by the means of different methods:

- ***Constant concentration;*** Tracer gas is injected into the room at controlled, varying flow rates, to keep a constant concentration in the room. This method requires a larger amount of tracer gas.
- ***Step-up;*** At t_0 a constant, continuous stream of tracer gas is supplied to the room, which has an initial concentration $C_0 = 0$. The time it takes to reach a certain concentration level in the exhaust air is measured.
- ***Step-down;*** A constant, known concentration of tracer gas had been added to the room air prior to the experiment start. At t_0 the tracer gas dosage is stopped, and the time it takes for the concentration to reach zero is measured.

- ***Pulse;*** Pulses of tracer gas is added at certain times and known concentrations. The amount of gas present at a point is measured over time. This method uses a low amount of tracer gas, but precise measurement equipment is required.

2.3.5.1 Tracer step-up method

In the tracer gas step-up method, also called the constant injection method, the tracer gas is injected into a room at a constant flow rate. The step-up concentration in the room is then recorded over time. The concentration of gas in the room at the start of the sampling period is zero, or a known constant concentration (e.g. for CO_2). Measurements are logged until the room air achieve a uniform steady state concentration. The tracer gas is usually injected into the ventilation system, to ensure complete mixing of the tracer gas and supply air. Figure 2.7 illustrate a typical development of the gas concentration in the exhaust air for a step-up experiment.

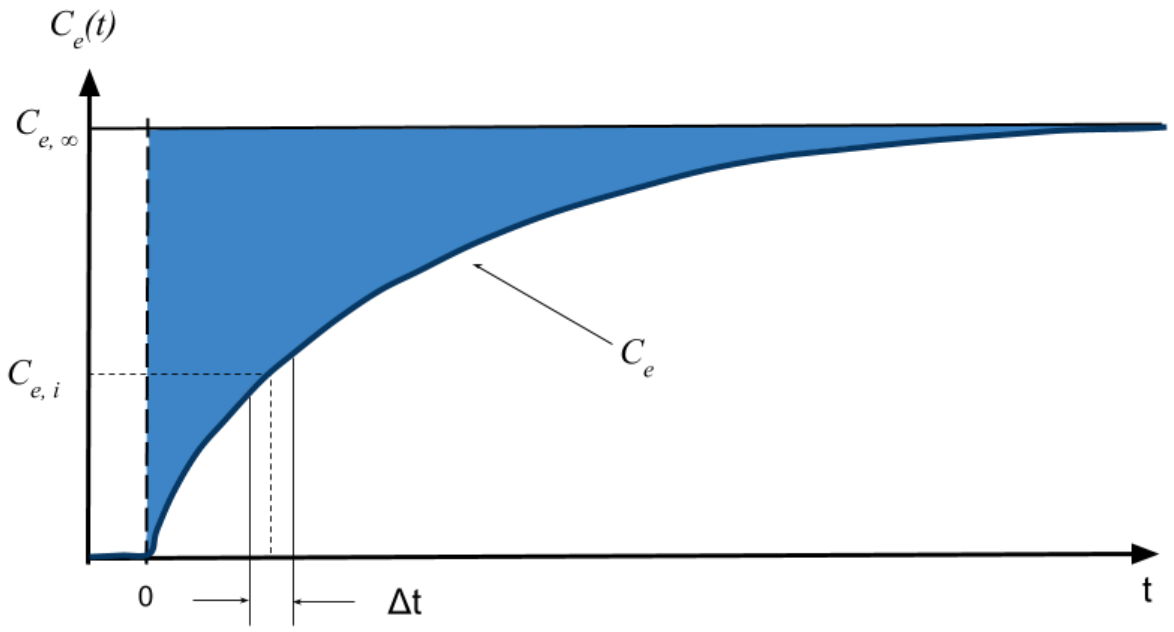

Figure 2.7 Tracer gas concentration step-up curve. Based on illustration by Mundt et al. (2004).

2.3.5.2 Tracer step-down method

In a tracer gas step-down test gas is injected into a room until it reaches an even concentration. The gas injection is then stopped, and the decay concentration of tracer gas is logged until it has decreased a specific concentration, usually zero. The tracer gas is usually injected into the room via the ventilation system. This is to ensure good mixing of the gas. Mixing fans can also be placed in the room, to achieve an even concentration throughout. A typical decay of tracer gas concentration for a step-down test can be seen in Figure 2.8. The green line illustrates the

exhaust concentration, while the dotted line illustrates the concentration decay at a point P in the room.

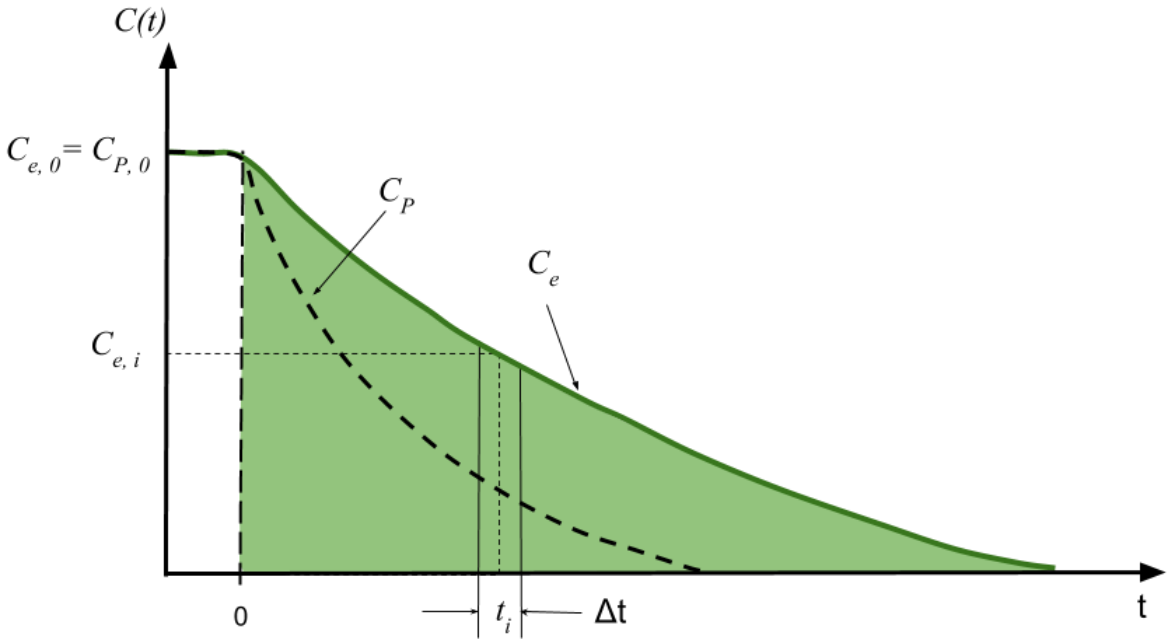

Figure 2.8 Tracer gas concentration decay (step-down) curve. Based on illustration by Mundt et al. (2004).

The step change response methods, step-up and step-down can be performed in one experiment. First a constant stream of tracer gas is injected into the room, and the step-up response is measured. When the tracer gas concentration in the room reaches a certain level, the gas injection is stopped. The step-down response is then measured and logged. The concentration increase and decay for a step change response experiment is illustrated in Figure 2.9.

Both the step-up and the step-down concentrations can be plotted as logarithmic curves. It is important to investigate the experimental results in both a linear and logarithmic diagram, as they will provide different information. The inverted step-up and normal step-down concentrations curves will appear as straight lines in a logarithmic diagram, with a negative slope. Instabilities and irregularities are easily spotted here, as they will deviate from the straight logarithmic line.

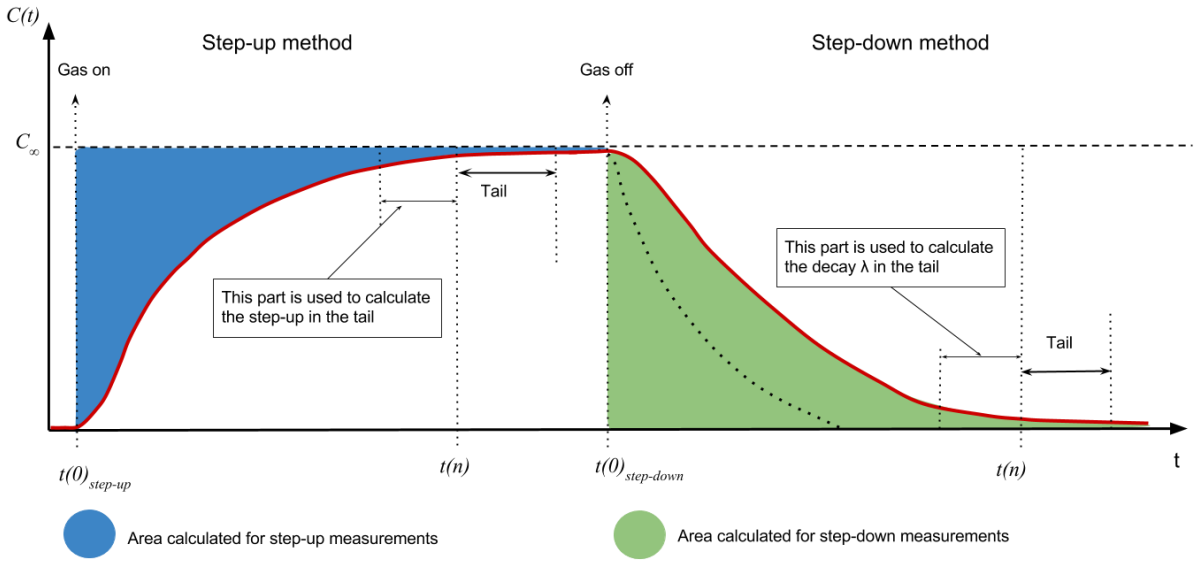

Figure 2.9 Tracer gas step change response method. Based on illustrations by Mundt et al. (2004) and Søgnen (2015b).

Table 2.4 Mean age of air equations for the step response methods (Mundt et al., 2004).

	Local mean age of air $\bar{\tau}_P$	**Room mean age of air $\langle \bar{\tau} \rangle$**
Step-down method	$\bar{\tau}_P = \int_0^\infty \frac{c_p(t)}{c_e(o)} \cdot dt$	$\langle \bar{\tau} \rangle = \frac{1}{\tau_n} \int_0^\infty t \cdot \frac{c_e(t)}{c_e(0)} dt$
Step-up method	$\bar{\tau}_P = \int_0^\infty \left(1 - \frac{c_p(t)}{c_e(\infty)}\right) \cdot dt$	$\langle \bar{\tau} \rangle = \frac{1}{\tau_n} \int_0^\infty t \cdot \left(1 - \frac{c_e(t)}{c_e(\infty)}\right) dt$

2.3.5.3 Analysis of the Tracer Gas Measurements

The mean age of the air, the nominal time constant and the air change efficiency can be calculated from the tracer gas measurements using a computer spread-sheet program (e.g. Excel). Mundt et al. (2004) present a process for calculating these values, which can be used both for the step-up and the step-down method. This process applies for both the air change efficiency and the local air change index;

1. Set a precise point t(0) for when the tracer gas is turned on/off.
2. Plot the measured concentrations as a function of time in a logarithmic diagram. The measurements should appear as a straight line, with an initial elapse. Due to low concentration at the end and signal noise from the analysers, the curve often become irregular at the end. These irregularities should be removed from the analysis. Denote the last usable concentration c_n at time t = n.

3. Calculate the slope from the straight part of the logarithmic curve. This will be used to extrapolate the tail concentrations from t = n to infinity.
4. Calculate the mean age of air, nominal time constant and air change efficiency using Equation (2.11), (2.12) and (2.7) for the step-down measurements, and Equation (2.14), (2.15) and (2.7), for the step-up measurements.

Step-down

For a step-down experiment the area under the concentration curve is used to calculate the ventilation efficiency, as can be seen in the right part of Figure 2.9. The mean age of air is calculated from the weighted area below the curve, using Equation (2.11). Part I and III of the equation represent part of the concentration curve from the start to the last usable concentration c_n. Part II and IV represent the tail of the curve.

$$\langle \bar{\tau} \rangle = \frac{\sum_{i=1}^{n} \left[\frac{c_{e,i} + c_{e,i-1}}{2} \cdot (t_i - t_{i-1}) \cdot \frac{t_i + t_{i-1}}{2} \right] + \frac{c_n}{\lambda} \cdot \left[\frac{1}{\lambda} + t_n \right]}{\sum_{i=1}^{n} \left[\frac{c_{e,i} + c_{e,i-1}}{2} \cdot (t_i - t_{i-1}) \right] + \frac{c_n}{\lambda}} = \frac{I + II}{III + IV} \quad (2.11)$$

Where:

c_e – the tracer gas concentration in the exhaust air

t – the time

λ – the slope for the extrapolated trend of the tail area in absolute value

The nominal time constant can be calculated from Equation (2.12):

$$\tau_n = \frac{\sum_{i=1}^{n} \left[\frac{c_{e,i} + c_{e,i-1}}{2} \cdot (t_i - t_{i-1}) \right] + \frac{c_n}{\lambda}}{c_0} = \frac{III + IV}{c_0} \quad (2.12)$$

Where:

c_0 – constant concentration at infinite time

The local mean age of air at point P in the room can be calculated from Equation (2.13):

$$\bar{\tau}_P = \frac{\sum_{i=1}^{n} \left[\frac{c_{P,i} + c_{P,i-1}}{2} \cdot (t_i - t_{i-1}) \right] + \frac{c_{P,n}}{\lambda}}{c_0} \quad (2.13)$$

Note that the equation for the nominal time constant is the same as the equation for calculating the local mean age of air. As mentioned in Chapter 2.3.1, the nominal time constant is always equal to the local mean age of air in the exhaust.

The air change efficiency can be calculated from Equation (2.7) and the local air change index can be calculated from Equation (2.8) in Chapter 2.3.3.

Step-up

If the step-up curve is inverted, it is similar to the step-down curve. This is done by subtracting the steady state concentration at infinite time with the actual concentration. The new concentration is defined as $C' = C_\infty - C$. Thus, the same method can be used to calculate the ventilation efficiency for the step-up measurements. The area calculated is located above the curve, as illustrated in the left part of Figure 2.9. The equations for calculating the mean age of air, the nominal time constant and the local mean age of air become as following:

$$\langle \bar{\tau} \rangle = \frac{\sum_{i=1}^{n} \left[\frac{c_i' + c_{i-1}'}{2} \cdot (t_i - t_{i-1}) \cdot \frac{t_i + t_{i-1}}{2} \right] + \frac{c_n'}{\lambda} \cdot \left[\frac{1}{\lambda} + t_n \right]}{\sum_{i=1}^{n} \left[\frac{c_i' + c_{i-1}'}{2} \cdot (t_i - t_{i-1}) \right] + \frac{c_n'}{\lambda}} \tag{2.14}$$

$$\tau_n = \frac{\sum_{i=1}^{n} \left[\frac{c_i' + c_{i-1}'}{2} \cdot (t_i - t_{i-1}) \right] + \frac{c_n'}{\lambda}}{c_\infty} \tag{2.15}$$

$$\bar{\tau}_P = \frac{\sum_{i=1}^{n} \left[\frac{c_{e,i}' + c_{e,i-1}'}{2} \cdot (t_i - t_{i-1}) \right] + \frac{c_{P,n}'}{\lambda}}{c_\infty} \tag{2.16}$$

Where:

C_∞ – constant concentration at infinite time

It can take a long time for the room concentration to reach the supply concentration, especially for large rooms. As a simplification, the concentration at infinite time, C_∞, is set as the last usable concentration measured, C_n. If the experiment is run for a long enough time and there is good mixing of tracer gas in the room air, this value should be good enough, even though it may not be correct.

2.4 Scaled Models

Investigating a full-size ventilation system in a small scale physical model can give good insight into the air movements and ventilation efficiency of the building ventilation. A properly conducted model and model experiments can give information on the necessary amount of ventilation air needed, the optimal supply air velocity and temperature, the air flow pattern and

velocities in the room, the temperature in the occupancy zone, the turbulence intensities and the distribution of contaminants in the rooms (Awbi, 2003). This chapter will explain the similarity principles and theory on scaled models. The term "prototype" refers to the full-scale building modelled, while "model" refers to the small-scale representation of the building modelled.

2.4.1 Similitude

The similarity principles are the base of the scale model experiments, and when they are achieved the experimental results from the model will be applicable in the prototype. There are some similarity principles that must be realized for the results in the model to be transferable to the prototype. The dimensionless numbers describe how the physical elements in the model behave, and can be found either by the Buckingham Pi theorem, or be deducted from the governing equations. They set the conditions for similar behaviour in the prototype and the model. To achieve complete similarity between model and prototype, they have to have geometric similarity, kinematic similarity and dynamic similarity (Zohuri, 2015).

2.4.1.1 Geometric similarity

Geometric similarity is achieved for a prototype and a model when all parts of the model are equal to the corresponding parts of the prototype, at a different scale. The scaling factor (λ) in room air modelling is usually $\lambda \leq 1$. All parts of the model should be reduced by the same scaling factor. When modelling a ventilation system, special attention should be focused on the scaling of the supply and extract air terminals, as these greatly dictate the air movement in the model (Awbi, 2003).

The ratio of the dimensions of the prototype and the model can be found:

$$\frac{L_P}{L_M} = \lambda \Rightarrow L_M = \frac{1}{\lambda} L_P \tag{2.17}$$

$$\frac{A_P}{A_M} = \frac{L_P^2}{L_M^2} = \lambda^2 \Rightarrow A_M = \frac{1}{\lambda^2} A_P \tag{2.18}$$

$$\frac{V_P}{V_M} = \frac{L_P^3}{L_M^3} = \lambda^3 \Rightarrow V_M = \frac{1}{\lambda^3} V_P \tag{2.19}$$

Geometric similarity is achieved when the ratio and angles of all the dimensions of the model and prototype are equal.

2.4.1.2 Kinematic similarity

Kinematic similarity refers to quantities related to motion. Motion is the related to distance and time, thus the kinematic similarity refers to similarities of lengths (geometric similarity) and time. The fluid flow of both the prototype and the scaled model must go through similar time rates of change. This means that the air streamlines in both the prototype and the model must be geometrically similar at corresponding times. To achieve kinematic similarity, there must be geometric similarity.

2.4.1.3 Dynamic similarity

Dynamic similarity is reached when the ratio of the forces acting on a point in the prototype and on the corresponding point in the model are constant. This must be true for all the corresponding points in the prototype and the model. To achieve dynamic similarity, both geometric and kinematic similarity must be realized. Reaching dynamic similarity can be challenging.

2.4.1.4 The Governing Equations

Some parameters are required to describe both the prototype and the model air movements. Developing the governing equations in dimensionless form will provide dimensionless numbers that can describe the systems for similarity analysis.

Continuity equation:

$$\frac{\partial \hat{u}}{\partial x} + \frac{\partial \hat{v}}{\partial y} + \frac{\partial \hat{w}}{\partial z} = 0 \tag{2.20}$$

Where $\hat{u}, \hat{v}, \text{and } \hat{w}$ are the instantaneous velocities in the three directions x, y, and z, respectively.

Navier-Stokes equation, in y-direction (gravitational direction):

$$\rho\left(\frac{\partial \hat{v}}{\partial t} + \hat{u}\frac{\partial \hat{v}}{\partial x} + \hat{v}\frac{\partial \hat{v}}{\partial y} + \hat{w}\frac{\partial \hat{v}}{\partial z}\right) = -\rho\beta g\left(\hat{T} - T_0\right) - \frac{\partial \hat{p}}{\partial y} + \mu\left(\frac{\partial^2 \hat{v}}{\partial x^2} + \frac{\partial^2 \hat{v}}{\partial y^2} + \frac{\partial^2 \hat{v}}{\partial z^2}\right) \tag{2.21}$$

Where $\hat{p}, \hat{T}, \text{and } t$ are the instantaneous pressure, temperature and time. T_0 is reference temperature (supply temperature), and ρ, β, μ and g are density, thermal expansion coefficient, viscosity and gravitational constant, respectively.

Energy equation:

$$\rho c_p \left(\frac{\partial \hat{T}}{\partial t} + \hat{u} \frac{\partial \hat{T}}{\partial x} + \hat{v} \frac{\partial \hat{T}}{\partial y} + \hat{w} \frac{\partial \hat{T}}{\partial z} \right) = k \left(\frac{\partial^2 \hat{T}}{\partial x^2} + \frac{\partial^2 \hat{T}}{\partial y^2} + \frac{\partial^2 \hat{T}}{\partial z^2} \right) \tag{2.22}$$

Where c_p is the specific heat and k is the thermal conductivity.

By formulating Equation (2.20), (2.21) and (2.22) in dimensionless form, the dimensionless numbers; Reynolds number (Re), Archimedes number (Ar) and Prandtl number (Pr), can be found.

$$\text{Ar} = \frac{\beta g L \Delta T}{u_0^2} \tag{2.23}$$

$$\text{Pr} = \frac{\mu c_p}{k} \tag{2.24}$$

$$\text{Re} = \frac{\rho L u_0}{\mu} \tag{2.25}$$

The length L is a characteristic length of interest in the problem. In ventilation problems, it is often the height of the supply diffuser. The reference velocity u_0 is the supply velocity (Tahti and Goodfellow, 2001, Chapter 12).

2.4.2 Similarity Requirements

To achieve complete dynamic similarity, the dimensionless numbers of the model and the prototype must be equal at all points in the model and prototype. The Archimedes number can be considered the ratio of thermal buoyancy and inertial force, and describes the motion of fluids related to buoyancy forces. When the characteristic length has been chosen, the variable parameters are the velocity *u*, and the temperature difference ΔT. The thermal expansion factor β, for air is considered constant, as it varies little with different temperatures. Equality between the Archimedes numbers of the model and prototype is required, thus the equations can be rearranged:

$$Ar_M = Ar_P \tag{2.26}$$

$$\frac{\beta g L_M \Delta T_M}{u_M^2} = \frac{\beta g L_P \Delta T_P}{u_P^2} \tag{2.27}$$

$$u_M = u_P \sqrt{\frac{\Delta T_M}{\Delta T_P} \frac{L_M}{L_P}} = u_P \sqrt{\frac{\Delta T_M}{\Delta T_P} \frac{1}{\lambda}} \tag{2.28}$$

$$\Delta T_M = \Delta T_P \frac{u_M^2}{u_P^2}\frac{L_P}{L_M} = \Delta T_P \frac{u_M^2}{u_P^2}\lambda \tag{2.29}$$

The Prandtl number may be looked upon as the ratio of momentum diffusivity to thermal diffusivity. When the medium used in the model is the same as the medium in the prototype, the Prandtl numbers are equal.

$$Pr_M = Pr_P \tag{2.30}$$

The Reynolds number may be considered as the ratio of inertial force to viscous force. When the characteristic length is set, there are no variables in the equation. The equality of the Reynolds numbers gives a ratio of the model and prototype velocities.

$$Re_M = Re_P \tag{2.31}$$

$$\frac{\rho_M L_M u_M}{\mu_M} = \frac{\rho_P L_P u_P}{\mu_P} \tag{2.32}$$

$$u_M = u_P \frac{L_P}{L_M} = u_P \lambda \tag{2.33}$$

Combining Equation (2.28) and (2.33) gives a ratio of the temperature differences, no longer dependent on the velocity:

$$u_{M,Re} = u_{M,Ar} \tag{2.34}$$

$$u_P \lambda = u_P \sqrt{\frac{\Delta T_M}{\Delta T_P}\frac{1}{\lambda}} \tag{2.35}$$

$$\Delta T_M = \Delta T_P \lambda^3 \tag{2.36}$$

To satisfy both the Reynolds number and the Archimedes number, the velocity and temperature difference ratios must satisfy Equation (2.37) and (2.38).

$$\frac{u_M}{u_P} = \lambda \tag{2.37}$$

$$\frac{\Delta T_M}{\Delta T_P} = \lambda^3 \tag{2.38}$$

It is impossible to match all the dimensionless parameters, achieving complete similarity. There will always be some deviations between the model and the prototype, both in geometry and operating conditions. The Prandtl number is easy to match. As air can be considered an incompressible gas in the relevant temperatures and velocities for model experiments on ventilation, the Prandtl number is automatically fulfilled. To satisfy both the Archimedes number and the Reynolds number for $\Delta T_P = 2$ K, then $\Delta T_M = 128$ K. This is not realistically achievable. Thus, the results apprehended from the model will not correspond perfectly to the prototype. A reduced scale model can still give valid and valuable information, even if the similarity is not perfect. If a streamline is fully developed turbulent, it is independent of the Reynolds number. If all the streamlines in the prototype and model are in the turbulent regime, the flow patterns will be similar. Thus, it is important that all the flows are fully developed turbulent. If the velocities close to the wall are of little concern in the simulations, then $Re_c > 2{,}4 \cdot 10^3$, or perhaps less (Etheridge and Sandberg, 1996). It is generally agreed that if the flow is fully within the turbulent region and the same working medias is used, the Archimedes number is the most important number to match between the prototype and the model (Etheridge and Sandberg, 1996, Awbi, 2003). However, achieving a higher temperature difference in the model lead to higher velocities used. This causes a higher Reynolds number and better similarity.

The same similarity principles must be realized for displacement ventilation, as for other mechanical ventilation principles. The Archimedes number is the most important to match, as long as the air flows are in the turbulent region. If the air movements were purely convection driven (no mechanical supply air flow), the Grashof number would be the critical dimensionless number to evaluate (Etheridge and Sandberg, 1996).

2.4.3 Thermal Loss

There must be a balance between the supplied and extracted heat in the model to achieve the desired temperature difference. The heat extracted from the ventilation and the heat lost through facades must be supplied as heat in the model to achieve thermal balance. The total heat loss from a building can be calculated as:

$$H = H_t + H_V + H_i \tag{2.39}$$

Where:

H – overall heat loss [W]

H_t – heat loss due to transmission through the building envelope [W]

H_V – heat loss due to ventilation [W]

H_i – heat loss caused by infiltration [W]

The transmission heat losses are due to heat conduction through the walls, windows, doors, roof, floor to the ground and through thermal bridges. Transmission to unheated rooms are also included here. The heat transfer through a building construction depends on the insulating ability and thickness of the building materials, and the temperature difference on each side of the construction. The transmission heat losses can be calculated as:

$$H_t = \frac{k}{d} A\Delta T = UA\Delta T \tag{2.40}$$

Where:

$U = \frac{k}{d}$ – heat transfer coefficient [W/m^{2}K]

A – area of the surface [m^2]

ΔT – temperature difference on each side of the surface [K]

k – thermal conductivity of the material [W/mK]

d – thickness of the material [m]

The heat losses due to ventilation and infiltration can be calculated as:

$$\mathrm{H}_V = c_p \rho q_v \Delta T \tag{2.41}$$

$$\mathrm{H}_i = c_p \rho n_{inf} \mathrm{V} \Delta T \tag{2.42}$$

Where:

c_p – the specific heat of air [J/kgK]

ρ – the air density [kg/m^3]

q_v – the volumetric air flow rate [m^3/s]

n_{inf} – the air change for infiltration [h^{-1}]

V – volume of building [m^3]

ΔT – temperature difference between supplied and extracted air [K]

(SINTEF and NTNU, 2007)

If the building of the scaled model has been done properly, the boundary conditions should be correct and the heat losses of the model should already be addressed by the model laws. Providing the correct heat load through internal heat gains should maintain the desired temperature difference.

2.4.4 Scaling factors/Scaling laws

The scaling factors S, are an orderly way to present the ratios between the prototype and model system parameters. Equality of the dimensionless numbers can be expressed as following:

$$S_{Ar} = \frac{Ar_M}{Ar_P} = S_u^2 \cdot S_\beta^{-1} \cdot S_{\Delta T}^{-1} \cdot S_g^{-1} \cdot S_L^{-1} = 1 \tag{2.43}$$

$$S_{Re} = \frac{Re_M}{Re_P} = S_\rho \cdot S_L \cdot S_u \cdot S_\mu^{-1} = 1 \tag{2.44}$$

$$S_{Pr} = \frac{Pr_M}{Pr_P} = S_\mu \cdot S_{c_p} \cdot S_k^{-1} = 1 \tag{2.45}$$

As the gravitational constant is equal for the prototype and model, and β, ρ, μ and C_p are substance constant at the relevant temperatures, S_g, S_β, S_ρ S_μ and S_{Cp} can all be excluded from the scaling factors.

The length scale is chosen, and can be expressed as:

$$S_L = \frac{L_M}{L_P} = \lambda \tag{2.46}$$

Rearranging Equation (2.43) provide the temperature scale and the velocity scale:

$$S_{\Delta T} = S_u^2 \cdot S_L^{-1} \tag{2.47}$$

$$S_\mathrm{u} = S_L^{0.5} \cdot S_{\Delta T}^{0.5} \tag{2.48}$$

Volume flow scale can be expressed as:

$$S_\mathrm{q} = S_u \cdot S_L^2 \tag{2.49}$$

As the velocity is defined as distance per time, the time scale can be found as:

$$S_\mathrm{t} = S_L \cdot S_u^{-1} \tag{2.50}$$

And finally, using Equation (2.41) the effect scale can be calculated as:

$$S_\mathrm{E} = \frac{E_M}{E_P} = S_q \cdot S_{\Delta T} = S_u \cdot S_L^2 \cdot S_{\Delta T} \tag{2.51}$$

Chapter 3 Ventilation and Indoor Climate of Super Insulated Buildings

By super insulated building, it is understood that it refers to buildings which are highly insulated and generally very air tight. It is generally taken as a house where the building envelope fulfil the passive house criteria.

Super insulated buildings are built with the intention that they trap heat (or cold) within the building envelope, reducing the need for heating (or cooling). They are also good at trapping air, making the air change to the surroundings minimal. This airtightness reduces the thermal loss in the building due to exfiltration and infiltration. The goal of a super insulated building is to minimize the need for heating, cooling and ventilation, and accordingly minimize the energy budget. To achieve a good indoor climate it must have a properly designed system for controlling the thermal environment and air distribution. The heating, ventilation and air conditioning system (HVAC) is key to this control, and properly designed (and maintained) it can provide a good indoor climate at a low energy expense. Net energy, heating, cooling and ventilation requirements, as well as some building specifications for non-residential passive houses can be seen in Table 3.1.

As mentioned in Chapter 2.1, a good indoor climate is highly dependent on the indoor air quality and thermal climate. There is a danger that if too much focus is on achieving a low energy use, and too little attention is on the design of the HVAC system, it can lead to poor indoor air quality and suboptimal temperatures. As the performance of office workers increase or decrease depending on a good or poor indoor environment, providing a sufficient ventilation air flow and keeping a comfortable thermal environment is paramount. A good HVAC system can regulate the air flow rate, temperature, humidity and cleanliness. Strategically placed temperature and CO_2 sensors can provide good control of the thermal and atmospheric environment. In addition, the interior design and solar control are important issues in the design to achieve a good indoor climate.

Thomsen and Berge (2012) conducted a literature research on the indoor climate in several residential passive houses and low energy houses located in Europe. Most of the findings are also relevant for non-residential passive houses. The indoor climate in the passive houses were found to be just as good, or even better than the indoor climate in conventional buildings. They found that the indoor air quality depended on the ventilation strategy chosen. The best air quality was found in buildings with balanced mechanical ventilation. Highly insulated buildings

with mechanical ventilation showed a lower occurrence of mould than in buildings with natural ventilation. The biggest factor for mould growth in passive houses was found to be moisture trapped in the building materials during construction. They also found that natural ventilated buildings achieved too few air changes to uphold the requirements, appearing too air tight. Low air changes lead to higher relative humidity, increasing the risk of moisture damage and occurrence of dust mites.

3.1 Ventilation

For an airtight building, a well-functioning ventilation system is necessary to provide a good indoor air quality. Chapter 2.2 explain the theory on displacement ventilation, while Chapter 2.2.5 and 2.2.6. explained the concepts on regulation of air flow; constant air ventilation (CAV), variable air volume (VAV) and demand controlled ventilation (DCV). A short description of natural, hybrid and mixing ventilation is presented in Chapter 3.1.1 below.

3.1.1 Natural, Hybrid and Mixing Ventilation

Natural ventilation use the wind and the buoyancy forces of air to ventilate a building. The ventilation effectiveness is dependent on the placement of the supply and extract openings, and the pressure difference between these. Natural ventilation is beneficial in that it uses little energy, requires low maintenance, and give the user a sense of influence on the indoor climate. However, there are several drawbacks regarding this type of ventilation. There is no possibility of heat recovery from the extract air, the performance efficiency is uncertain, and draft may be a problem. If there are no wind, and the temperature on the outside and the inside is equal, there will be no ventilation.

Hybrid ventilation, often called mixed mode ventilation, utilizes both natural and mechanical ventilation. It is a quite energy efficient system, as the ventilation fans only run when the pressure difference between the inlet and outlet is too small to supply air through natural ventilation. Disadvantages with this system is that it is expensive to install and maintain, it requires extensive planning in the design phase, and there is no possibility for heat recovery of the natural ventilated air.

Apart from natural ventilation, mixing ventilation is probably the most common type of ventilation. The principle of mixing ventilation is to supply air at a high enough flow rate and velocity, so that the room air is completely mixed. The goal is to achieve a uniform temperature and contamination level in the room air. Mixing ventilation requires relative high air flow rates

to achieve a satisfactory indoor air quality, thus requiring higher fan power (SFP) than displacement ventilation (Commtech Group, 2003).

The passive house building standard require a minimum ventilation heat recovery of 80% (NS3701). As both natural and hybrid ventilation cannot recover heat from the naturally displaced air, a building with these ventilation systems cannot fulfil the passive house requirements.

Both mixing and displacement ventilation can deliver good indoor air quality, though a well-functioning displacement ventilation system will achieve a better air quality at lower ventilation rates. Mixing ventilation requires relative high air flow rates to achieve a satisfactory indoor air quality, thus requiring higher fan power (SFP) than displacement ventilation. The low SFP makes displacement ventilation ideal for low energy houses such as ZEB.

3.1.2 Ventilation heating and cooling

The primary method for heating and cooling of a ventilated building, is to regulate the ventilation air temperature and flow rate. A heat exchanger in the AHU recycles the heat (or cold) from the extract air, heating the supply air to an appropriate temperature. To achieve passive house standard, the heat recovery rate has to be ≥ 80 % (NS 3701). If the heat exchanger is not able to heat the supply air to the desired air temperature, a heating circuit can warm the air further. The same is valid for cooling of air, where a cooling circuit acts as a cooling battery. The air temperature should not exceed 22 ºC in the heating season, as recommended by Arbeidstilsynet (2016).

Field work performed by Cable et al. (2014) showed that for a highly insulated building with a low heating demand, ventilation heating for mixing ventilation can cover the heating demand. The thermal climate and ventilation efficiency in an office were measured. The thermal climate was found very good for several different supply rates, with little risk of draught with 0,15m/s air velocities in the occupied zone. When the office was unoccupied, a short circuiting could occur when supplying warm air ($\varepsilon_c = 89\%$). However, full mixing occurred when the office was occupied. Installing a presence sensor could limit the energy loss due to heating of an unoccupied room.

Hybrid window ventilation can be used as a cooling method for a super insulated building. Allowing venting of surplus heat through a window can greatly reduce the energy required for cooling. If the temperature on inside a building is higher than on the outside, an opening in the ceiling will vent the hot air. If there is wind, a pressure difference between different openings

will cause cross-ventilation. A simulation done by Alonso et al. (2015) showed that mixed mode ventilation provided fairly good cooling for a highly insulated kindergarten located in Larvik, Norway. However, at the hottest days it was necessary with additional cooling.

3.2 Heating and Cooling with Displacement Ventilation

As displacement ventilation is dependent on the buoyancy forces of the air, there must be a temperature difference between the supply and ambient room air. If the supply air is too hot, the air will rise straight to the ceiling, short circuiting the ventilation system. Ventilation heating is therefore not a suitable option for a displacement ventilation system. Radiators and convectors are good options for room heating, and should generally be placed under cold surfaces to avoid downward draft. In super insulated buildings the building envelope has little heat loss. This require fewer heating panels, and they may be placed centrally to distribute the heat evenly. Heated ceiling panels work well with displacement ventilation, as it stabilizes the thermal stratification of the room. However, the head and neck area are sensitive to heat, so a too large temperature gradient between the head and ankle may lead to discomfort. Floor heating can work well with displacement ventilation, at moderate temperature levels. It will heat the supplied air, leading it towards the ceiling. If the floor heating has a too high temperature, the fresh air can be overly heated. The hot air will rise, causing mixing of the fresh and the contaminated air, lowering ventilation effectiveness. (Skistad et al., 2004). Causone et al. (2010) found that floor heating worked well with displacement ventilation, as long as the supply temperature was not excessively heated before it reached the intended area.

The two-zone model displacement ventilation is based on, lead to a lower required cooling load compared to mixing ventilation. It is suitable for moderately cold supply air temperatures, but too low it may cause an increased sensation of draft. High air supply rates, and thus higher air speeds, can also cause unwanted draft. If a higher air flow rate is required for cooling, the diffusers must be sized and designed to avoid too high air velocities outside the adjacent zone. Chilled ceilings are effective at providing cooling to a building, but in displacement ventilated rooms there is a danger of disrupting the thermal stratification. A cool ceiling may cause a downward draft, mixing the air of the contaminated upper zone with the fresh air in the occupant zone (Novoselac and Srebric, 2002). Chilled floors in displacement ventilated rooms can cause a high vertical temperature difference and increase the risk of draft at ankle height, causing discomfort. Causone et al. (2010) performed measurements for a chilled floor in a displacement ventilated room. He did not find an increased risk for draft at ankle height, though it increased the vertical temperature gradient.

3.3 Space Heating

A super insulated building is designed so that is reduces the required amount of space heating needed, or in the best case eliminate it entirely. If located in a colder climate, the building will require some heating in the winter to maintain a satisfactory thermal environment. To keep an acceptable thermal climate all year-round, the building should have access to a sufficiently high heating load. The recommended minimum operative temperature in a building where light work is performed is 19 ºC (Arbeidstilsynet, 2016).

Passive heat sources can be exploited to reduce the energy required for heating. The design and orientation of the building could maximize the solar heat gain, and reduce the heat loss due to external sources, such as wind exposure. A compact design of the building envelope reduces the surface area, and thus the thermal transfer through the structure. An even, low energy solution for heating is thermal mass. Materials with the proper abilities can absorb heat from the sun during the day and release it when the sun sets, keeping a stable interior temperature (Wing, 2008). Solar collectors can also be used to trap heat from the sun. Solar radiation heat the water in the collectors, which can be stored in accumulator tanks for use at a later time. It can deliver heat to the indoor heating system, or be used in the domestic hot water production (Commtech Group, 2003).

3.4 Space Cooling

A disadvantage of super insulated building is that they are susceptible to overheating in the summer. They do not necessarily require a higher cooling load, but the cooling season for super insulated buildings start earlier and lasts longer than for other buildings. The higher solar radiation of the season and lower thermal exchange with the surroundings lead to excess heat that needs to be removed. The maximum operative temperature recommended in a building where light work is performed is 26 ºC (Arbeidstilsynet, 2016). To minimize the energy needed for cooling, passive methods for shading and cooling is the first step to look at. If the passive methods are not enough to provide a satisfactory thermal environment, mechanical cooling must be provided. Methods to minimize the necessary cooling should be explored in the design phase.

Passive methods for cooling can be landscape architecture and orientation. Trees that shade most in the summer and less in the winter, when the foliage has disappeared can be planted at advantageous positions. Shading from nearby buildings or landscape orientation can be utilized, and shading of glazed areas due to building design or installed blinders or curtains. Other

solutions for cooling can be chilled ceilings and radiators, thermal mass, and ventilation cooling. Thermal mass, like an exposed concrete ceiling can keep the temperature comfortably cool in the day. In combination with night cooling, it can reduce the number of hours with need for additional cooling in the summer (Søgnen, 2015a). Heat pumps installed for heating may also have the possibility to deliver free cooling, at low energy cost.

3.5 The system at Powerhouse Kjørbo

Powerhouse Kjørbo is designed to minimize the necessary heating and cooling of the buildings. The compact, airtight and highly insulated building envelope, and a thoroughly designed HVAC system enables a low energy use. The required net energy use for heating and cooling is quite a bit lower than the requirement set for a passive house, as can be seen in Table 3.1.

A balanced displacement ventilation system is installed in the buildings. The general location and type of air diffusers is explained in Chapter 4.1.1. As the workstations are separated by bookshelves that are placed directly at the floor, there is a concern that this will obstruct the airflow to certain areas. Both temperature and CO_2 sensors are placed around in the office landscape and selected meeting rooms. The air supply flow rate is controlled by these sensors, whose locations can be seen in Figure 3.1. The minimum air flow requirements and the average air flow rate at powerhouse Kjørbo can be seen in Table 3.1.

A geothermal heat pump is installed to cover 95% of the heat load in the buildings, and district heating covers the peak load. The heating system delivers hot water to the buildings, via a low-temperature hydronic distribution system. Between 6 and 8 waterborne panel radiators are placed around the centre at each floor, as see in Figure 3.1. The thermal environment in the cell offices are therefore dependent on the supply air and the air flow through open doors. Additional electrical heaters have been installed in the western corner meeting room (room 4106) and in one adjacent office (room 4104) on the ground floor. Due to restricted access to these rooms, the doors were generally closed, limiting the heat transferred via the movement of heated air. (Søgnen, 2015b)

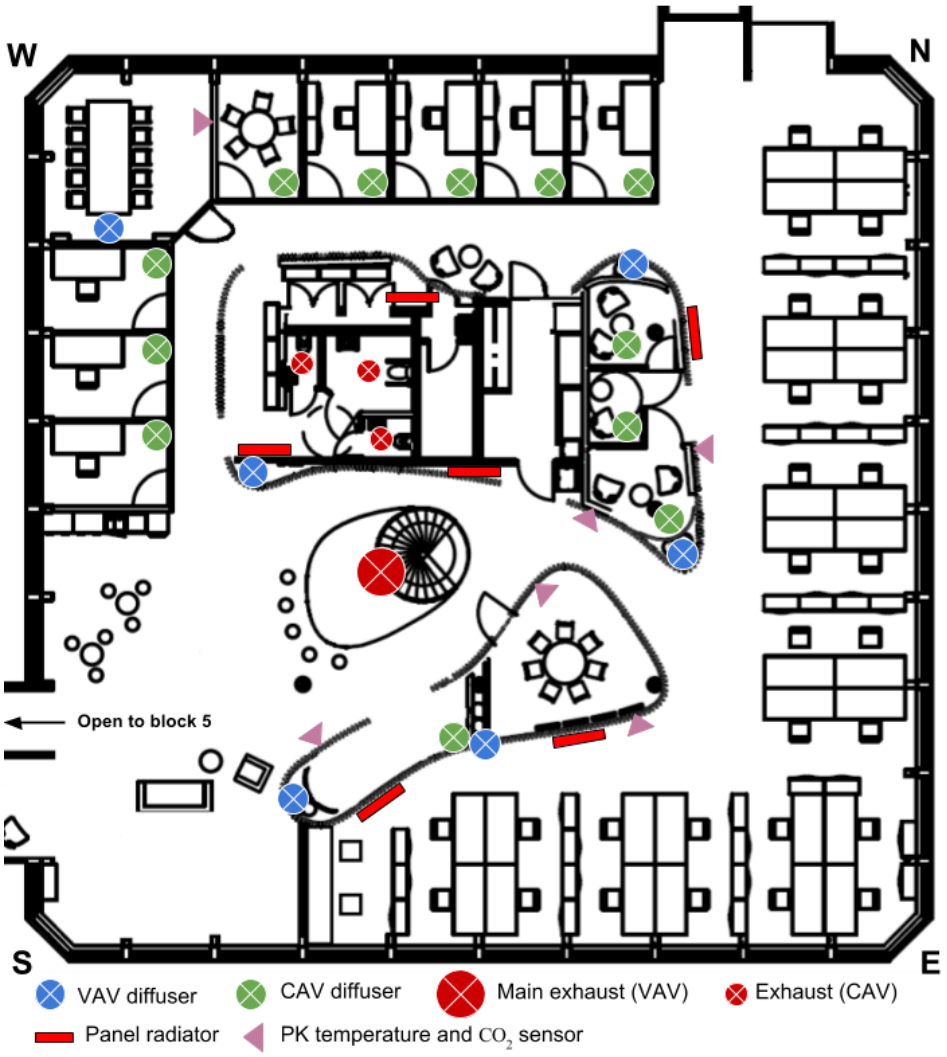

Figure 3.1 Floor plan of Powerhouse Kjørbo building 4, 2nd floor (Søgnen, 2015b)

As Powerhouse Kjørbo is designed to avoid high temperatures, there are no mechanical cooling installed in the buildings. Instead ventilation cooling, external shading and window venting is used to keep the temperature satisfactory (Midtbust, 2014). The windows at the workstations can be opened, so there is an option of some user controlled ventilation. There is a possibility of venting excess heat through a window in the ceiling of the stairwell, that can be opened. In the summer the heat pump can deliver free cooling, which is used to cool the air in the ventilation system. Free cooling for the ventilation cooling is allowed when the outside temperature is above 12 ºC (Rådstoga, 2014). Average values for the building specifications of block 4 and 5 of Powerhouse Kjørbo can be seen in Table 3.1.

Table 3.1 Average values for Powerhouse Kjørbo (Thyholt, 2014), and technical requirements for passive house buildings (NS3701) and new buildings (TEK10:2012). Values from 2012 is used in the TEK10 comparison, as that was the requirements for Powerhouse Kjørbo when built. Numbers in parenthesis are form TEK10:2016.

	Powerhouse Kjørbo	**NS3701**	**TEK10**
Total net energy use [kWh/m^{2}year]	59,3	≤ 95	≤ 150 (115)
Net energy demand for heating [kWh/m^{2}year]	15	≤ 20,1	-
Net energy demand for cooling [kWh/m^{2}year]	3,9	≤ 9,4	-
U-values			
External walls [W/m^{2}K]	0,13	≤ 0,10 – 0,12	≤ 0,18 (0,22)
Roof [W/m^{2}K]	0,08	≤ 0,08 – 0,09	≤ 0,13 (0,18)
Floor [W/m^{2}K]	0,20	≤ 0,08	≤ 0,15 (0,18)
Windows and doors [W/m^{2}K]	0,80	≤ 0,80	≤ 1,20 (1,20)
Normalized thermal bridge, Ψ" [W/m^{2}K]	0,025	≤ 0,03	≤ 0,06
Technical equipment			
Specific fan power (SFP) [kW/m^3/s]	0,70	≤ 1,5	≤ 2,0
Efficiency for heat exchanger	87 %	≥ 80 %	≥ 80 %
Leakage number, n_{50} [h^{-1}]	0,24	≤ 0,60	≤ 1,5 (1,5)
Minimum airflow during operating hours [m^3/h]	7 per m^2	≥ 6 per m^2	≥ 2,5 per m^2 + 26,0 per person
Minimum airflow outside operating hours [m^3/m^{2}h]	2 / 0	≥ 1	≥ 0,7
Power demand for lighting during operation hours [W/m^2]	3,11	≥ 4	≥ 8[2]

Chapter 4 The Scaled Model

This chapter will describe the scale model and the prototype it is based on, as well as the experimental setup. The scale model was built as part of Sangnes' (2016) master thesis spring 2016, and improved as part of this master thesis and Trydals (2016) project thesis autumn 2016.

4.1 The Prototype

The prototype building is located in the Kjørbo park in Sandvika, Norway. It is a four story office building, where the second level was chosen for modelling by Sangnes (2016). The building envelope fulfils the criteria of a passive house, meaning the heat loss through the walls and windows are relatively small. The building also has a low air leakage number (50 Pa), of 0,24 h^{-1} (Thyholt, 2014). Other specifications for the buildings can be seen in Table 3.1.

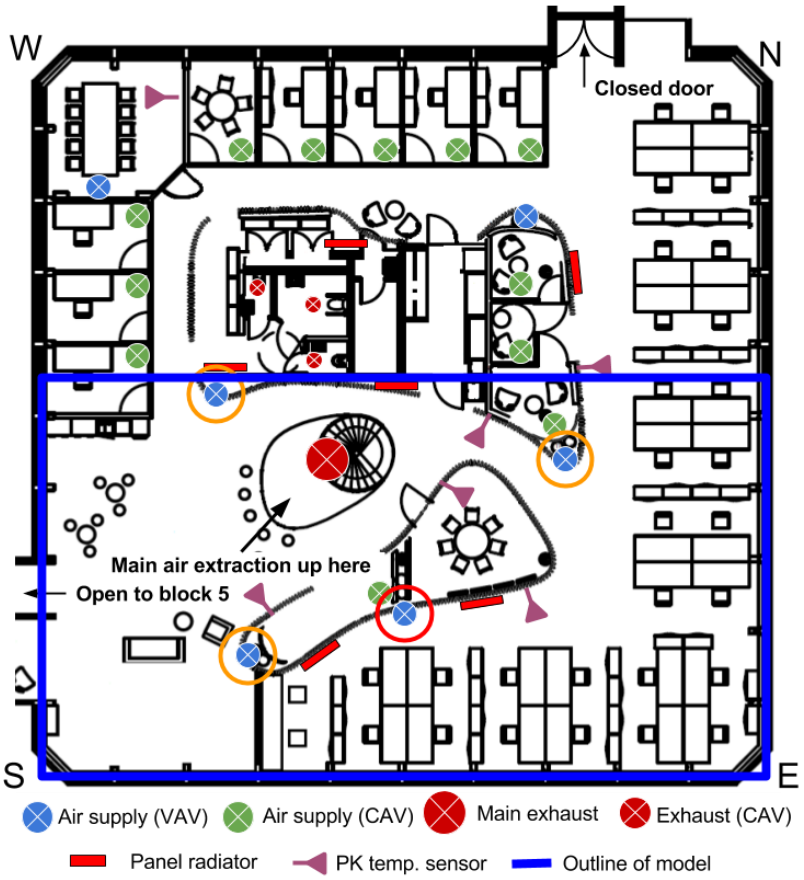

Figure 4.1 Floor plan of Powerhouse Kjørbo, 2nd floor in building 4, with outline of modelled part. Based on illustration by Søgnen (2015b)

The floor plan of the 2nd level of Powerhouse Kjørbo can be seen in Figure 4.1. It consists of cell offices, meeting rooms and an open office landscape, with room for approximately 40 employees. The open office landscape consists of several workstations separated by bookshelves, and has room for 30 employees. The workstations are made up of two or four

desks grouped together, each with one laptop and an extra computer screen. The blue outline in Figure 4.1 illustrate what is physically built at a reduced scale model, which covers approximately 304 m^2. The north-west part of the floor not built is simulated as air supplied by two large cross-section diffusers. This is further explained in Chapter 4.2.

Tracer gas measurements were done at Kjørbo by (Søgnen and Sangnes, 2016) March 9 and 10, as well as air velocity mapping and smoke experiments. The results from these measurements will be used to validate the model.

4.1.1 The Ventilation System

The ventilation at Powerhouse Kjørbo is a demand controlled displacement ventilation system. There are twelve CAV diffusers located at the 2nd floor, one in each of the small cell offices and study rooms. One VAV diffuser is placed in the larger, west facing meeting room, and the remaining five VAV diffusers are spread out in the open office landscape, four of which is located inside the modelled part of the prototype. The main exhaust is through the stairwell located at the centre of the building, though each of the toilets have small CAV exhausts installed. None of the cell offices or meeting rooms have extract vents installed, instead the air overflows into the hallway. Panel radiators are distributed centrally in the open office landscape, as shown in Figure 4.1. The diffuser used for air velocity mapping (see Chapter 4.4.3) can be seen in Figure 4.1, circled in red. It is 2000 mm long and 550 mm high.

Table 4.1 Ventilation air flow rates in prototype. Values from Sangnes (2016)

Source of air	**# of diffusers**	**Air flow rate [m^3/h]**	**Total air flow rate [m^3/h]**
VAV wall diffuser	5	696,68	3 483,40
CAV diffuser office	8	60,00	480,00
CAV diffuser large meeting room	1	450,00	450,00
CAV diffuser small meeting room	4	60,00	240,00
Total	**18**		**4 653,40**

4.1.2 Internal Heat Gains

According to presence of people inspection done by Sangnes (2016), there was an average of roughly 20 persons on the 2nd floor during the workday. The average heat emitted from a seated person doing sedentary work is 122,5 W, as mentioned in Chapter 2.1.2.4. The heat emitted from a laptop with an extra screen in use is estimated to be 80 W (Mathisen, 2016). The light installed in the prototype contributes with 3,11 W/m^2 heat gain (Thyholt, 2014). The solar

radiation on March 9 and 10 was quite low, as the days were cloudy. Thus, it is assumed the heat gain from the sun is neglectable. Table 4.2 summarizes the internal heat gains in the prototype.

Table 4.2 Internal heat gains in the modelled part of the prototype

Internal heat gain	#	Output [W]	Heat gain [W/m^2]
Radiators	6	-	2,00*
Persons	20	122,5	-
Workstations	20	80	-
Light	-	-	3,11
Solar radiation	-	-	-

* Number found by Sangnes (2016)

4.2 The Scaled Model

A 1:4 scaled model of the 2nd floor of the prototype was built by Sangnes (2016), and further improved by Trydal (2016). The area chosen for modelling is made up of roughly half of the 2nd floor of Powerhouse Kjørbo. The floor plan of the reduced scale model can be seen in Figure 4.2, covering an area of 21,5 m^2. The area of interest is 19 m^2, which is made up of the lounging area, the staircase and part of the open office landscape. The open office area seats 22 employees. The working fluid for the experiments is air, supplied at low temperatures by an external air handling unit (AHU).

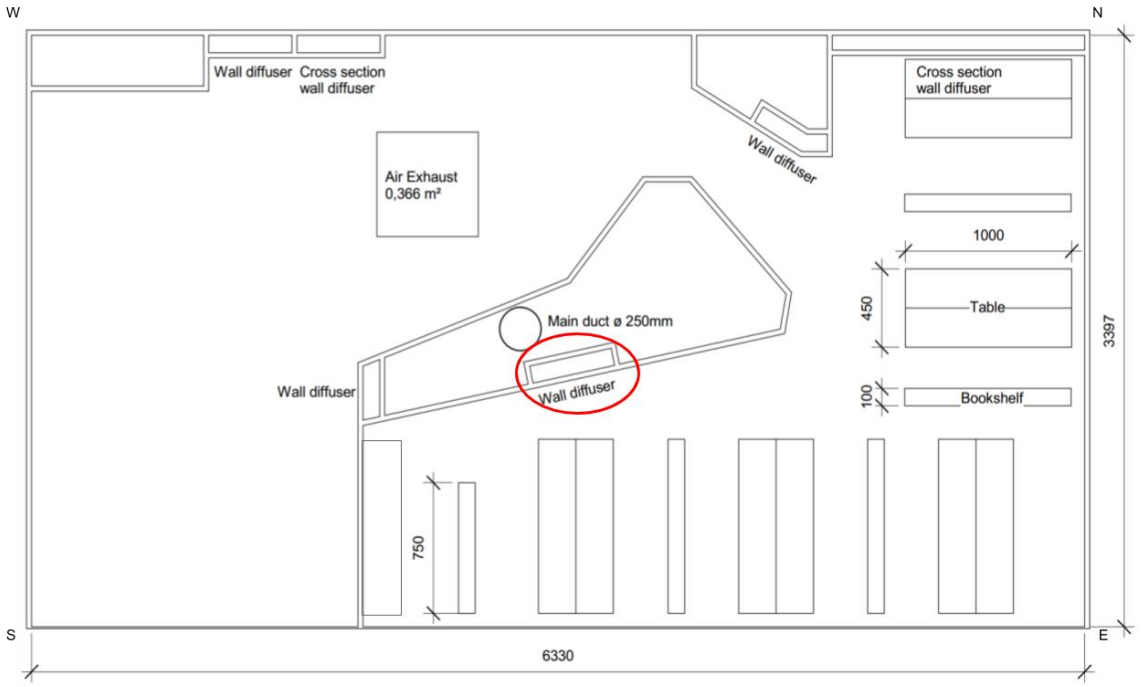

Figure 4.2 Floor plan of reduced scale model of Powerhouse Kjørbo. Circled diffuser used for air velocity mapping. Based on illustration by Sangnes (2016)

4.2.1 The Building Materials

The internal walls and the ceiling of the model is built with extruded polystyrene foam (Styrofoam), which has good insulating abilities. The areas of the ceiling experiencing the highest temperatures are covered with an extra layer of Styrofoam. This is done to prevent cooling of the top layer of air and thus avoid mixing of new and old air. The south-eastern wall is made up of wood and Plexiglas, to permit experiments that contains smoke visualization. To prevent downward draft during the temperature measurements and tracer gas experiments, the plexiglass wall has been covered in Styrofoam. It can easily be removed for insight during smoke experiments. The remaining walls of the model are the walls of the climate room. They are insulated with varying thickness of Rockwool, in addition to covering of plaster, wood or metal. The floor consists of wood and insulation. The U-values for the climate room walls and floor is found in a previous master thesis (Forn, 2008). The scaffolding of the model is wooden poles at the walls, and metal strips in the ceiling. The furniture is built to scale in Styrofoam and wood, and consists of five large and one small workstation, and five bookshelves. Lightbulbs are placed at the workstations to simulate the heat output from people and computers, and electric floor heating are installed to simulate light-, radiator- and solar heat gain in the building.

Table 4.3 Estimation of thermal abilities of the model building materials.

Facade	Material	Area [m^2]	U-value [W/m^2K]
Ceiling	Styrofoam	19	1,13
Floor	Wood, insulation	19	0,30
Wall (N-W)	Rockwool (10 cm), plaster	4,75	0,41
Wall (N-E)	Rockwool (5 cm), plaster	2,32	0,53
Wall (S-W)	Rockwool (5 cm), plaster	2,32	0,53
Wall (S-E)	Plexiglas	2,37	40

4.2.2 The Ventilation System

In reduced scale model ventilation experiments the supply diffusers are particularly important to achieve similarity to the prototype, as mentioned in Chapter 2.4.1.1. The model supply diffusers are made geometrically similar at a reduced scale, though some dissimilarities are found. The ventilation system in the model consists of four CAV diffusers, that corresponds to the four VAV diffusers seen within the outline of the model in Figure 4.1. The rest of the air is supplied from two large CAV cross section wall diffusers, which also simulates the half of the

building model not built. The placement of the supply diffusers and the exhaust can be seen in Figure 4.2.

The four wall supply diffusers are connected to the air handling unit (AHU) via four flexible ducts, that are connected to a vertical duct in the middle of the model. The vertical duct is connected to the original air duct system in the ceiling of the room. The diffusers are balanced by Iris-dampers. The supply air flow rate can be found from the pressure drop over the dampers. See Appendix G for more information on the dampers. The vertical duct is fitted with a separate branching with an Iris-damper, that vent excess air before it reaches the model. This permits a higher air flow rate from the AHU and a lower heat transfer per volume flow, letting colder air to reach the model. The two wall diffusers are connected to a channel fan, supplying the model with air at ambient temperature. The cross-section diffusers are designed to blow air evenly into the model, to simulate the air movement towards the exhaust in the prototype. The air exhaust is through a hole in the ceiling, fitted with a TSI Accubalance Air Capture Hood simulating the stairwell. This make it possible to measure the exhaust flow rate, and thus the leakage of the model. Table 4.9 list the dimensions of the diffusers and the scaled air flow rates for a chosen temperature scale, $S_{\Delta T} = 5{,}0$.

4.2.3 Internal Heat Gains

There are 32 lightbulbs placed in the model, divided in two circuits. Sixteen lightbulbs of 60 W simulate people and sixteen lightbulbs of 25 W simulate workstations. Both circuits are fitted with a Variac, making it possible to adjust the output power. As derived in Chapter 2.4.4, the power scaling factor depend on the chosen temperature scale. The lightbulbs may be removed, changing the number of people present. This enables experiments in the model with varying presence of people. The average presence of people in the modelled part of the prototype building during the tracer gas experiments conducted by Sangnes (2016) was 10 people.

To improve the thermal plumes from the lightbulbs, some improvements have been made. The lightbulbs simulating people are fitted with grey painted cylinders. These cylinders have an area of a 1:4 scaled down du Bois-area, and can be thought of as simplified thermal mannequins. They are 0,25 m tall, and have a diameter of 0,10 m. To imitate the emissivity of a clothed person, the cylinders have been painted grey. (Zukowska et al., 2012) Tubular lightbulbs are chosen to simulate the workstations. They have been fitted horizontally to 130mmX80mm aluminium plates, standing at a slight angle, simulating a computer screen.

Table 4.4 Internal heat gains in the model. Output at 230V

Internal heat gain	#	Area [m²]	Output [W/#]	Output [W/m²]
Light bulbs	16	19	60	
Light bulbs	16	19	25	
Electrical floor heating		12,48		125

The heat gain solar radiation is simulated in the heated floor mats. The output from the floor mats is also controlled by a Variac. The location of the lightbulbs and electrical floor mats can be found in Figure 4.3.

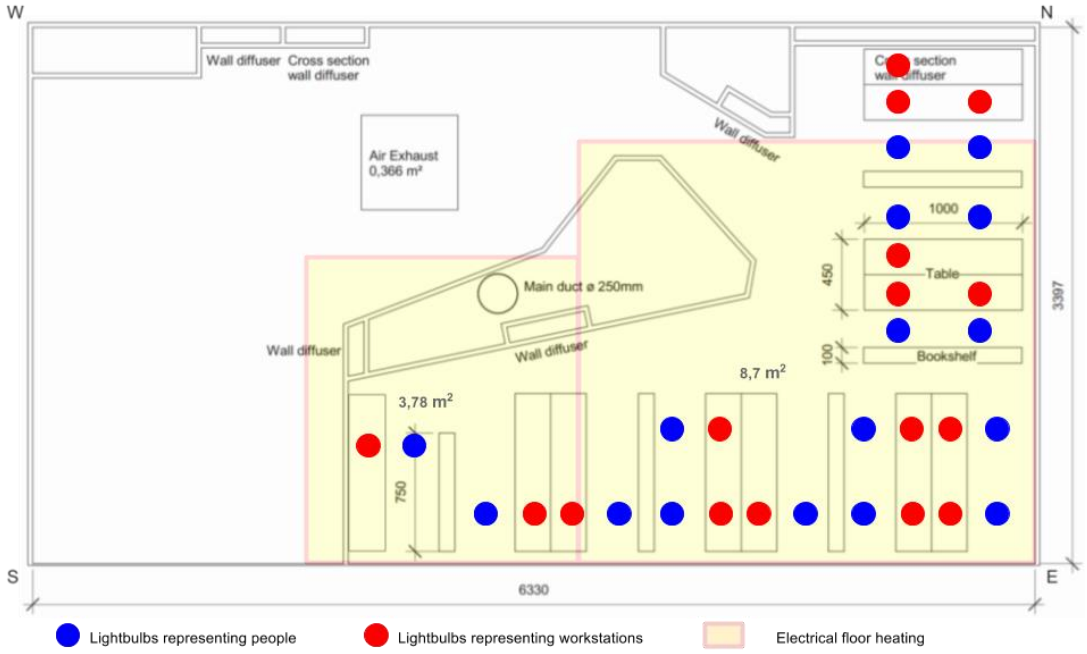

Figure 4.3 Location of internal heat gains in the model. Based on illustration by Sangnes (2016)

4.3 Model characteristics

As mentioned in Chapter 4.2.2, it is impossible to match all the dimensionless numbers between the prototype and the model. To satisfy both the Archimedes number and the Reynolds number for $\Delta T_P = 2$ K, then $\Delta T_M = 128$ K. This very a high and not realistically achievable temperature difference. The critical similarity requirement to match is the Archimedes number, and at the same time the streamlines should be in the turbulent region, $Re > 2{,}3 \cdot 10^3$. A temperature scaling factor $S_{\Delta T} = 5{,}0$ is chosen, making it possible to derive the remaining scaling factors. The scaling factors can be seen in Table 4.5. Properties used for the calculations can be seen in Table 4.6, and parameters for the prototype and model can be seen in Table 4.7.

Table 4.5 Model scaling factors for chosen $S_{\Delta T}$ = 5,0

S_L	0,25
$S_{\Delta T}$	5,00
S_t	0,22
S_u	1,12
S_q	0,07
S_E	0,35

Table 4.6 Gravitational constant and properties of air

g	9,81	m/s^2
β	0,00341	K^{-1}
ρ	1,2041	kg/m^3
μ	$1{,}819 \cdot 10^{-5}$	*kg/ms*
ν	$1{,}51 \cdot 10^{-5}$	m^2/s
k	0,0257	*W/mK*
C_p	1005	*J/kgK*

Table 4.7 Prototype and model parameters.

	Prototype	**Model**	
Scale	1	4	
A_{floor}	304	19	m^2
H	3	0,75	*m*
$A_{diffuser}$	1,1	0,069	m^2
$h_{floor\ to\ diffuser\ top}$	0,7	0,175	*m*
ΔT	2	10	*K*
q_{total}	4653,4	325,2	m^3/h
$u_{diffuser}$	0,176	0,197	*m/s*
Pr	0,713	0,713	
$Re_{diffuser}$	8,15E+03	2,28E+03	
$Ar_{diffuser}$	1,51	1,51	

The calculated Reynolds number for the air leaving the diffuser is not completely turbulent, as shown in Table 4.7. However, due to the internal roughness of the supply duct (flexi duct), the perforated metal grill covering the supply diffuser and the negative buoyant effect of the air, the air flow will be fully developed turbulent. The Archimedes numbers for the model and prototype diffusers match. The thermal plumes in the model are fully developed turbulent, as can be seen in Table 4.8. Note that the Archimedes number for the thermal plumes in the prototype and model are equal, as required by the scaling laws.

Table 4.8 Thermal plume characteristics for prototype and scaled model. Centreline velocity calculated from Equation (2.3).

	Prototype		**Model**	
	Person	*Computer*	*Person*	*Computer*
k	0,4	0,75	0,4	0,75
Φ [W]	100	40	34,9	14,0
u centreline max [m/s]	0,304	0,282	0,339	0,315
Re thermal plume	6,03E+04	5,59E+04	1,68E+04	1,56E+04
Ar thermal plume	2,18	2,53	2,18	2,53

The scaled air supply can be found in Table 4.9. The air supplied through the cross-section diffusers simulate the part of the 2nd floor of the prototype not built as a model. The air is therefore supplied at exhaust air temperature, simulating old air.

Table 4.9 Dimension of diffusers in model, and scaled air flow rates for ΔT=10K, $S_{\Delta T}$ = 5,0.

Source of air	**Dimension [mm]**	**# of diffusers**	**Air flow rate [m^3/h]**	**Total air flow rate [m^3/h]**
CAV wall diffusers	137,5 x 500	4	48,68	194,73
West cross section diffuser	750 x 500	1	32,6	32,6
South cross section diffuser	750 x 1500	1	97,8	97,8
Total		**6**		**325,17**

The average presence of people in the prototype was 10 people during the tracer gas experiments (Sangnes, 2016). For the initial experiments used to validate the model, the same presence must be simulated. Table 4.10 give a summary of the internal heat gains in the prototype, and the scaled internal heat gains for the validation experiments.

Table 4.10 Internal heat gains in prototype, and scaled for model validation experiments. S_E = 0,35

Internal heat gains in prototype					**Internal heat gains scaled to model**				
	#	*m^2*	*W/m^2*	*Effect [W]*		*#*	*m^2*	*W/m^2*	*Effect [W]*
P person	10			1000	**P person**	10			349,40
P PC	10			400	**P PC**	10			139,80
P lighting		304	3,11	945,44	**P lighting**		19	17,39	330,32
P radiator		304	2,00	608,00	**P radiator**		19	11,18	212,43
P sun		304	0,00	0,00	**P sun**		19	0,00	0,00
P tot				**2953,44**	**P tot**				**1031,95**

The ventilation heat losses can be calculated from Equation (2.41). The air supplied by the four CAV diffusers is used as the volume flow in the ventilation heat loss calculation. As the air supplied through the cross-section diffusers are at exhaust air temperatures, it has no heat loss connected to the ventilation. The transmission and infiltration heat loss in the model is calculated as the difference between the internal heat gains and the ventilation heat loss.

Table 4.11 Ventilation and transmission heat loss in the model

ΔT_M [K]	q CAV diffusers [m^3/h]	H_V [W]	$H_{T, inf}$ [W]
10	194,73	654,57	377,38

4.4 Experimental Setup

The model is set up with equipment to measure temperatures, air velocities, tracer gas, and conduct smoke experiments. This chapter will explain the experimental setup and methodology. The results of the experiments are presented in Chapter 5.

4.4.1 Temperature Measurements

The thermocouples are placed at areas of interest, the location can be seen Figure 4.4, with corresponding vertical heights in Table 4.12. The thermocouples measure the temperature continuously, and the results are logged using Lab View. See Appendix E for more information on the thermocouples and the logging software.

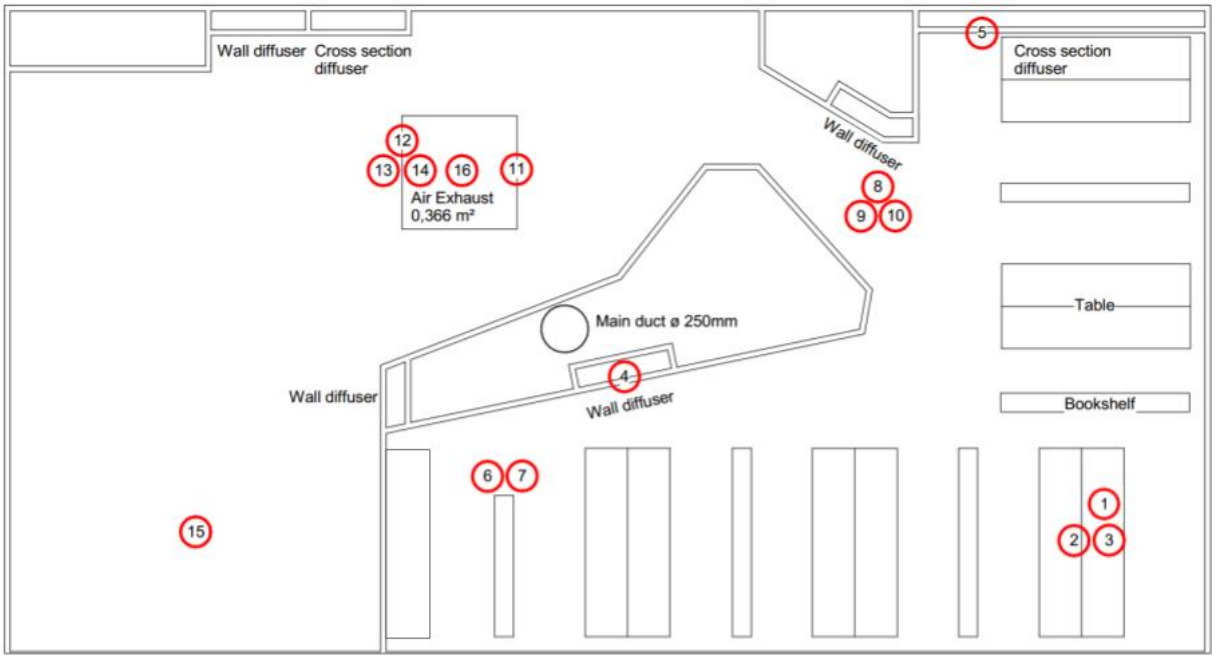

Figure 4.4 Location of thermocouples in model (Sangnes, 2016)

Table 4.12 Thermocouple height

Thermocouple	Height [mm]	Thermocouple	Height [mm]
1	25	**9**	375
2	375	**10**	725
3	725	**11**	725
4	Supply	**12**	375
5	Cross-section	**13**	725
6	25	**14**	25
7	725	**15**	725
8	25	**16**	Exhaust

4.4.2 Tracer Gas Measurements

There are several principles of tracer gas experiments, as described in Chapter 0. For the model experiments, tracer gas measurement sets were chosen. These consist of a step-up experiment to a consent concentration, followed by a step-down experiment to zero concentration. Performing a step-up and step-down set consecutively is time effective, and provide a larger amount of data, generating more secure results. Tracer gas measurements were performed at different locations in the model, measuring the ventilation efficiency and local air change indexes. Three different measurement sets were conducted, see Table 4.13. The tracer gas concentration is measured by a sampler and monitor system by Brüel & Kjær. Nitrous Oxide was chosen as the tracer gas. Further description of the measurement equipment and properties of the tracer gas can be found in Appendix E.

4.4.2.1 Method

Pressurized Nitrous Oxide (N_2O) is supplied trough a plastic tube into the supply duct, creating a uniform mix of air and tracer gas. The amount of gas supplied is controlled by a flow rotameter. The necessary gas flow rate, $\dot{V}_{tg}$, required to maintain a predetermined tracer gas concentration, C_{tg}, can be calculated from Equation (4.1). The desired tracer gas concentration was set to 25 ppm. With a total supply air flow of 325,2 m^3/h, the required tracer gas flow rate is 8,13 L/h.

$$\dot{V}_{tg} = C_{tg} \cdot 10^{-6} \cdot q_v \cdot 1000 \frac{l}{m^3} \tag{4.1}$$

Where:

$\dot{V}_{tg}$ *– tracer gas flow rate [l/h]*

C_{tg} – desired tracer gas concentration [ppm]

q_v – ventilation air flow rate [m^3/h]

Plastic tubes are stretched from the tracer gas sampling equipment, to several locations in the model. See Table 4.13 and Figure 4.5 for the exact sampling location. The 375mm measuring points are at a height just higher than the desks and bookshelves. To measure the fully mixed air and tracer gas, the sampling point in the supply duct is located some distance from the tracer gas insertion point. The exhaust concentration is measured in the top of the Air Capture Hood.

Table 4.13 Location of tracer gas sampling points for the different measurement sets.

Set 1 – All 375			**Set 2 – South Corner**			**Set 3 – East Corner**		
Location		**Height [mm]**	**Location**		**Height [mm]**	**Location**		**Height [mm]**
1	South	375	1a	South	25	3a	East	25
2	South-East	375	1b	South	275	3b	East	275
3	East	375	1c	South	500	3c	East	500
4	North	375	1d	South	725	3d	East	725
5	Supply	-	5	Supply	-	5	Supply	-
6	Exhaust	-	6	Exhaust	-	6	Exhaust	-

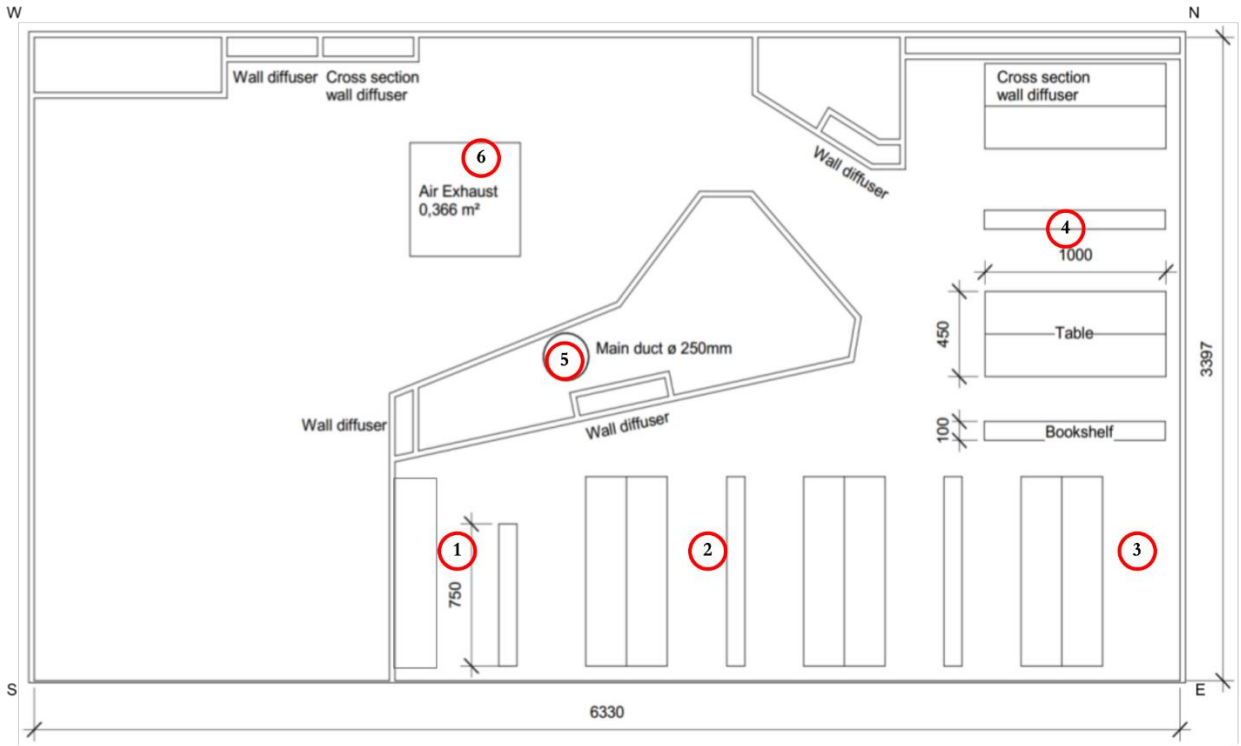

Figure 4.5 Tracer gas measuring locations. Based on illustration by Sangnes (2016)

The monitoring equipment start logging the concentration in the room, and then at time t_0 the tracer gas insertion is started. The concentration is measured continuously, till it reaches a constant concentration throughout the room. Then, at time t_n, the supply of tracer gas is shut off. The room concentration is measured until it reaches approximately zero concentration. The data files are exported, and analysed further using the method described by Mundt et al. (2004).

4.4.3 Air Velocity Mapping

The air velocity mapping of the model diffuser was done in the same way the prototype diffuser had been mapped by Sangnes (2016) in order to have a correspondence between the prototype and model velocities. The diffuser mapped in the model is the corresponding diffuser to the one mapped in the prototype, circled in red in Figure 4.1. The air probes were placed at four different heights (see Table 4.14 and Figure 4.6), that correspond to the heights in the prototype. The anemometers were moved between certain grid points, shown in Figure 4.7. The probes measured the velocity at one location for 120 seconds, before being moved to a new location in the grid. This was done for all points in the grid, A1 to F4. The measurements are logged in LabVIEW. The results are then exported to excel, where the measured velocities are averaged. The ventilation air flow rate was kept constant for the duration of the velocity mapping. See Appendix E for more information on anemometers and the logging software.

Table 4.14 Anemometer probe height

Anemometer	**Height [mm]**
Probe 1	7,5
Probe 2	25
Probe 3	100
Probe 4	175

Figure 4.6 Air velocity mapping in model

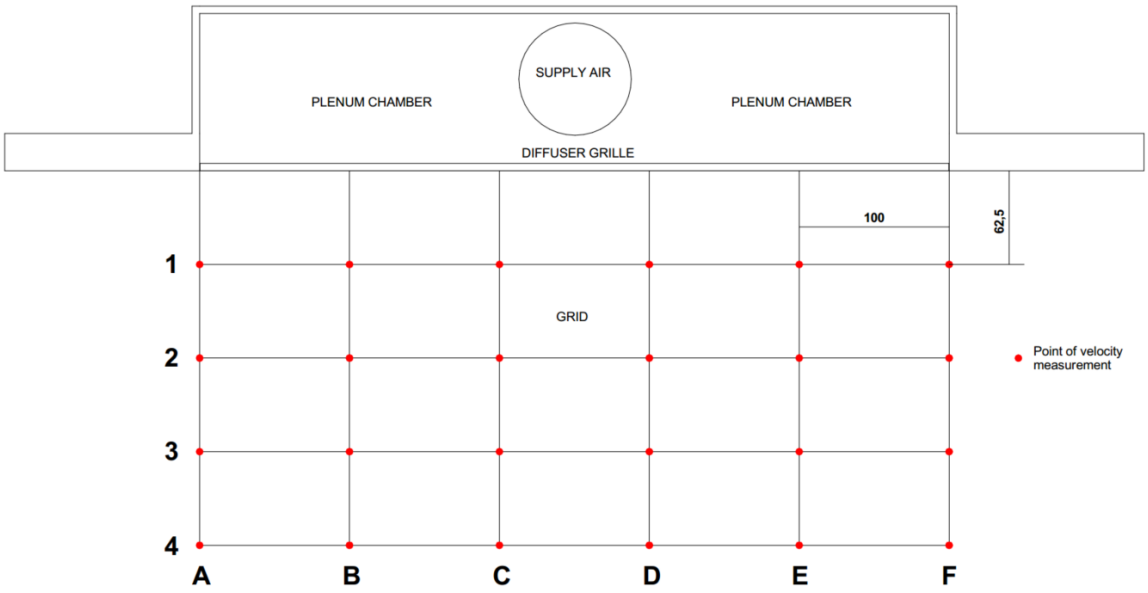

Figure 4.7 Velocity mapping grid (Sangnes, 2016)

4.4.4 Smoke Visualization

Smoke have been injected into several areas of the model open office landscape, using a smoke ampoule. The smoke will move along the streamlines, providing a visualization of the air movements. This will provide a better understanding of the air distributions in the room. As the smoke from the ampoule can be harmful in larger doses, it was connected to a plastic tube that can be accessed from outside the model.

4.5 Discussion of the Scaled Model

4.5.1 The Prototype

The east corner of the open office landscape is pointed out as an area of interest, as the bookshelves enclose the workstations. As they are placed directly on the floor, they can significantly hinder the airflow to this corner. Note the difference in the drawing of the east corner of the open office landscape in the prototype building in Figure 4.1 and the model floor plan in Figure 4.2. The book shelf facing the north is not built as illustrated in Figure 4.1, but is built as a larger book shelf as illustrated in Figure 4.2. This may have an impact on the air supply to the workstations in the east corner. Measurements show the local CO_2 concentration is higher than the exhaust air concentration. This indicate a stagnant zone in this area.

The open office landscape at Powerhouse Kjørbo is a large area, ventilated by few diffusers. As discussed in Chapter 2.2.4, supplying air to a large area with few diffusers can be challenging. The east corner is located the furthest away from a supply diffuser, and has the additional challenge of being enclosed by bookshelves. The entrance to the east corner is located about 7m from the nearest diffusers, and there is an additional 4-5m to the innermost corner.

4.5.2 Simplifications of the Scaled Model

If the building of the scaled model has been done properly, the boundary conditions should be fulfilled and the heat losses of the model should already be addressed by the model laws. As mentioned in Chapter 2.4, similarity requires that the boundary conditions are scaled correctly. However, quite a few simplifications have been made when building the scaled model. As the model simulate half of one floor in a four-storey building, the boundaries do not have the correct conditions. The floor, ceiling and north-west wall should have no heat losses, as they border areas with at equal conditions in the prototype. In the model, these areas border the ambient air outside the model. The exterior walls (south-west, south east and north east walls) should have the same heat transfer as in the prototype. Depending on the ambient air surrounding the model, the heat transfer through the model envelope can be higher (or lower) than expected. This can cause undesired air movements at the boundaries, and influence the temperature differences in the model.

In the ceiling of the prototype building, there are different objects that may disturb the air flow pattern. Pipes that may be cold, sound muffling panels, light fixtures, et cetera. In addition, people will be moving in the office. These obstructions and movements can cause additional

mixing of the air, decreasing the air change efficiency. The model ceiling is flat, without such obstructions, and the heat sources are stationary. The airflow in the model will therefor experience less mixing of the air, and possibly a higher air change efficiency.

The supply diffusers are important to scale correctly for model ventilation experiments. Nevertheless, there are some deviations between the model and prototype diffusers, which can cause deviations in the air flow pattern. Due to lacking information on the exact build of the VAV supply diffusers in the prototype, there may be some dissimilarities in the model design. The area of concern is where the supply duct enters the plenum chamber. The perforated metal grill covering is 35% open area, which slightly larger than in the prototype. This can cause a slightly more laminar flow compared to the prototype. Due to the roughness of the flexi duct interior and the negative buoyant effect of the cold air, the airflow is fully developed turbulent, fulfilling the similarity criteria.

The cross-section diffusers supply air to simulate the openings between the part built and the part not built. The air volume supplied in each diffuser is scaled due to the size of the opening between the built and not built part. However, the exact air flow through the west or north passages are not known. The cross-section diffusers supply air with a uniform temperature, with no vertical temperature gradient. In the prototype, the air is divided into thermal layers. The air at the corresponding places in the prototype is not uniform. This can cause problems with the similarity of the model. In addition, the lack of air volume for the part not built will cause problems for the tracer gas step up experiments. For the step-up experiments, the lack of volume will cause the tracer gas to enter the modelled volume too fast. For the step-down experiments, the lack of volume will cause the tracer gas to leave the modelled volume too fast. Thus, the cross-section diffusers cannot be used for the tracer gas experiments.

The heat gain from the from the lighting and radiator are not simulated, halving the total heat load calculated in Table 4.10. Initially the heat gain was thought to be supplied through the electric floor heating, but as displacement ventilation is very sensitive on the heat distribution, this would not give a correct picture of the air movement in the model. It is thought that not simulating the heat gain from the lighting and radiators will give a mode correct picture than simulating it through the electric floor heating. Ideally there should have been separate heat sources simulating the radiators and lighting. The electric heating mats has an area of 12,48 m^2, where about 1,5 m^2 reside outside the relevant area of the scaled model. See Figure 4.3 for the location of the floor mats. Only 11 m^2 of the 19 m^2 of the model is covered with floor heating, which simulate passive solar gain. This correspond to 176 m^2 of 304 m^2 receiving solar heat in

the prototype. Ideally, the electric floor heating should cover the whole 19 m^2. To achieve the calculated temperature difference between the supply and exhaust air, the entire heat load needs to be supplied in the model. As the electric floor heating, does not cover the whole 19 m^2 of the model, and the heat gain from the radiators and lighting is left out, the temperature difference between the supply and exhaust air will not reach the expected 10K. Rather, as the input effect is close to halved, the temperature difference is expected to be closer to 5K for the validation experiments. Consequently, the south corner of the model (with no heating) will experience significantly lower temperatures than desired, and the open office landscape (with floor heating and occupancy load) will experience some lower temperatures than desired. It is still thought that the south-east part open office landscape will give valuable results.

The thermal losses in the model are dependent on the temperature difference between the surrounding ambient air and the model temperature. The temperature differences, and thus the heat losses, vary due to different supply and ambient room air temperatures. As there is no control on the ambient room air temperature, and the supply temperature vary depending on the available cooling load, the thermal loss will be different from experiment to experiment. This will impact the temperature difference in the model. Ideally there should be a way to control the temperature of the ambient air.

The thermal cylinders are spray painted grey to simulate the emissivity of a clothed person. According to Herman (2016), the emissivity of a clothed human body is 0,95. The grey lacquer used to paint the cylinders has an emissivity of 0,90 (ThermoWorks, 2017). This difference is neglectable, according to Georges (2017).

To many simplifications in the model building compared to the prototype building will prevent the experimental results from being transferable to the prototype building. However, as the model scaled up to normal size can be thought of as a building similar to the prototype, one can draw some conclusions regarding the air movements and ventilation efficiency in a larger open office landscape with few supply diffusers and only one exhaust.

4.5.3 Air Flow Measurements

The air flow measured by the manometer and the air capture hood suggest a rather large air leakage. Tracer gas measurements performed suggest the opposite. As the TSI Accubalance Air Capture Hood has not been calibrated for over two decades, these numbers are not trusted. The manometer was calibrated a little over year ago, and showed little or no change since the

previous calibration. However, it has a measurement error of ±1 Pa which can impact the calculated air flow rate.

As the equipment used for tracer gas experiments is quite slow, to high air change rates is undesirable. Too high air changes in the model will cause poor results, as not enough measurements can be taken for the step-up or step-down sets. To avoid too high air change rates in the model, the temperature scaling factor was chosen to be no higher than $S_{\Delta T} = 5,0$.

Chapter 5 Results

Several experimental cases have been performed in the model, with different input values. A brief description of the different cases is presented in Chapter 5.1. Temperature and tracer gas measurements have been performed simultaneously for the different experiments. The air velocity mapping is presented in Chapter 5.2, the smoke visualization in Chapter 5.3, the temperature results in Chapter 5.4, and the tracer gas results in Chapter 5.5. The scaling factors and general model characteristics for the experiments can be found in Chapter 4.3. Simplifications have been made for all the experiments, which will be defined in Chapter 5.1. The presented results from the model are from several experiments performed in May and June 2017. The results presented from prototype was found by Sangnes (2016) and Alonso et al. (in preparation) in March 2016. The prototype results are presented after the model results, in Chapter 5.6.

5.1 Experimental Cases

All the experiments are performed with the same scaling factors, found in Chapter 4.3.

5.1.1 Air Velocity Mapping

Velocity mapping of the model diffuser was done to compare the supply air flow patterns in the prototype and model. The velocity mapping also show how the is air distributed into the model. The method described in Chapter 4.4.3 was used for measuring the diffuser air velocities. Air velocity mapping was performed with the same scaled air flow volume as for the temperature and tracer gas experiments. The air velocity scale is S_u = 1,12. The prototype and model characteristics can be found in Chapter 4.3. The measurements in the model were done May 29 2017. The air velocity mapping performed by Sangnes (2016) in the prototype March 9 2016 is used for comparison. The air velocity mapping results can be found in Chapter 5.2.

5.1.2 Smoke Visualization

To get a better understanding of the air flow pattern in the model, smoke visualization was performed. Normal occupancy was used as presence for the experiments, tried both with and without passive solar heat gain (floor heating). The smoke visualization was done June 1, June 2 and June 3. The smoke visualization findings are presented in Chapter 5.3.

5.1.3 Case I – Normal Occupancy

In order to validate the model to the prototype, the same conditions, at scaled values, must be applied. As the average presence of people in the prototype during tracer gas experiments was

10 people (Sangnes, 2016), the same amount of internal heat gains has to be used in the model for the validation experiments. See Figure 5.1 for the specific locations of the heat loads. The cross-section diffusers, simulating the part of the floor not built, are not used. As discussed in section 4.5.2, they will give the wrong results for the tracer gas measurements as the step-up and step-down decay curves will be wrong. The results will not be completely transferable to the prototype, but will give results of a similar, smaller building with an open office landscape. The air movements in the south and east part of the open office landscape is expected to be similar to the movements in the prototype. The measurements were done June 2 and June 8, and both temperature and tracer gas measurements were performed. In addition, an experiment was done in the east corner with the divider underneath the desk removed. Smoke experiments suggested that the divider underneath the desk hindered the airflow. The divider is located in the middle of the workstation, dividing the desks facing each other. A 6cm gap is measured from the floor to the bottom of the desk divider. Without it, the distance from the floor to the bottom of the desk is 20cm. It is expected that the local air change index in the east corner will be without this divider, compared to the original desk. This experiment was performed June 11.

With a temperature scale $S_{\Delta T} = 5{,}0$ and a temperature difference of $\Delta T_P = 2K$ in the prototype, the expected theoretical temperature difference between the exhaust and supply air is $\Delta T_M = 10K$. However, as the input power is close to halved compared to the scaled internal heat gains found in Chapter 4.3, the temperature difference between the exhaust and supply air will not reach 10K. New calculations show an expected temperature difference of 7,5K if there are no heat loss through the building envelope. However, as there will be transmission heat losses through the building envelope, the temperature difference is expected to be closer to 5K. The transmission heat losses are dependent on the relative temperature difference of the ambient air surrounding the model and the temperatures in the model. There is no control on the ambient air surrounding the model, so the transmission heat losses are dependent on the difference between the model air temperature and the ambient room temperature of the day. The temperature measurements for Case I are presented in Chapter 5.4.1, and the tracer gas results are presented in Chapter 5.5.1.

Table 5.1 Air flow volume in model. Normal occupancy.

q supply	194,7	m^3/h
q cross sectional diffuser	0,0	m^3/h
q tot	**194,7**	***m^3/h***

Table 5.2 Actual supplied effect to model. Values scaled prototype. Normal occupancy.

Model				Prototype
	#	m^2	Effect [W]	Effect scaled to Prototype [W]
P person	10		349,4	1000,0
P PC	10		139,8	400,0
P floor heating		11	0,0	0,0
P tot			**489,2**	**1400,0**

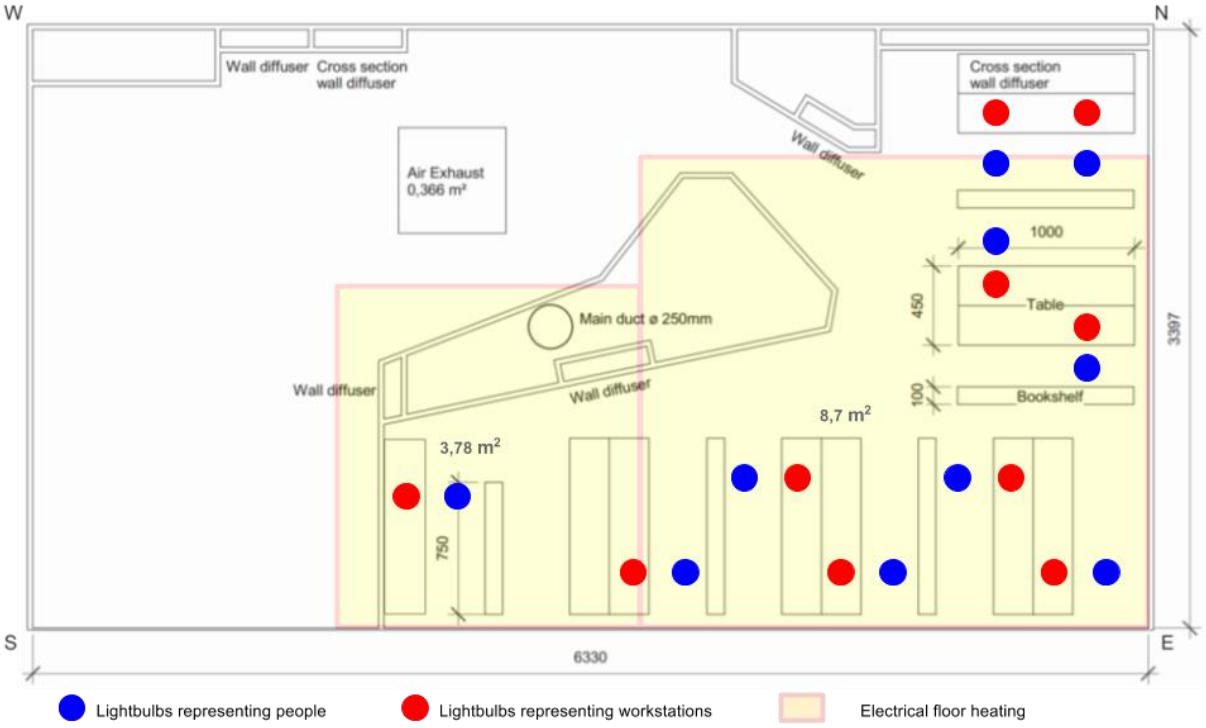

Figure 5.1 Location of internal heat gains for Case I and Case II.

5.1.4 Case II – Normal Occupancy and Solar Gain

This case simulates the presence of 10 people, 10 computers and floor heating simulating passive solar gain. The floor heating in the model correspond to 5 W/m^2 solar gain in the prototype. Temperature and tracer gas experiments are performed. The cross-section diffusers are not used for this case, as the step-up and step-down decay curves will be wrong for the tracer gas measurements. The tracer gas concentration is measured at All 375 height, in the south corner and in the east corner. Two different setups are used in the measurements in the east corner, where the north facing bookshelf is changed. The first experiment uses the regular (as built) bookshelf in the east corner, which is then changed for a smaller bookshelf, as drawn in the architect drawings. Figure 5.2 Show the different bookshelves in the east corner, circled in red. With the bookshelf change it is expected that the local air change index in the east corner

is higher. It is also expected that the temperatures decrease, and that the east corner temperature gradient decrease. With the chosen input values, a temperature difference of 12,3K between the exhaust and supply air is expected. However, as the model has heat loss through the envelope, it is not expected to reach 12,3K. The measurements were performed May 30 and May 31. The temperature measurements for Case II are presented in Chapter 5.4.2, and the tracer gas results are presented in Chapter 5.5.2.

Table 5.3 Air flow volume in model. Normal occupancy and solar heat gain.

q supply	194,7	m^3/h
q cross sectional diffuser	0,0	m^3/h
q tot	**194,7**	***m^3/h***

Table 5.4 Actual supplied effect to model. Values scaled prototype. Normal occupancy and solar heat gain.

	Model				**Prototype**			
	#	m^2	Effect [W]	W/m^2	#	m^2	Effect scaled to Prototype [W]	W/m^2
P person	10		349,4		10		1000,0	
P PC	10		139,8		10		400,0	
P floor heating		11	314,2	28,5		176	899,3	5,1
P tot			**803,4**				**2299,3**	

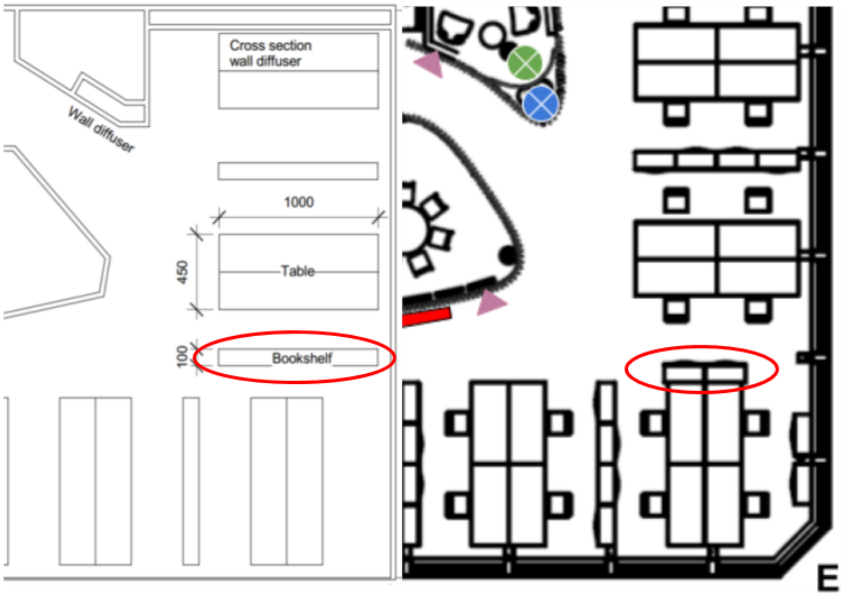

Figure 5.2 East corner bookshelf in model floor plan, as built (left picture) and architectural drawings (right picture).

5.1.5 Case III – High Occupancy

In this case a higher heat load was used for the experiments. The heat from 16 persons, 16 computers and floor heating simulating a small amount of passive solar heat gain was supplied to the model. The measurements were done June 4 and June 5. After one measurement in the south corner (June 5), the lightbulbs in the model were moved closer to the south, increasing the local presence. This was to see if a higher local heat load in the south will change the local air change index. As the lightbulbs simulating computers are fastened to the desks, they were not moved. It is expected that the local air change index in the south corner will be higher. See Figure 4.3 for exact location for the first measurements. Figure 5.3 show the locations after the heat sources were moved. The cross-section diffusers are not used, as they will give wrong results for the tracer gas experiments. With the chosen input values, a temperature difference of 12,9K between the exhaust and supply air is expected. However, with heat loss through the model envelope, it is expected to be quite a bit lower. The temperature measurements for Case III are presented in Chapter 5.4.3, and the tracer gas results are presented in Chapter 5.5.3.

Table 5.5 Air flow volume in model. High occupancy.

q supply	194,7	m^3/h
q cross sectional diffuser	0,0	m^3/h
q tot	**194,7**	***m^3/h***

Table 5.6 Actual supplied effect to model. Values scaled prototype. High occupancy.

	Model				**Prototype**			
	#	m^2	Effect [W]	W/m^2	#	m^2	Effect scaled to Prototype [W]	W/m^2
P person	16		559,0		16		1600,0	
P PC	16		223,6		16		640,0	
P floor heating		11	61,5	5,6		176	176,0	1,0
P tot			**844,1**				**2416,0**	

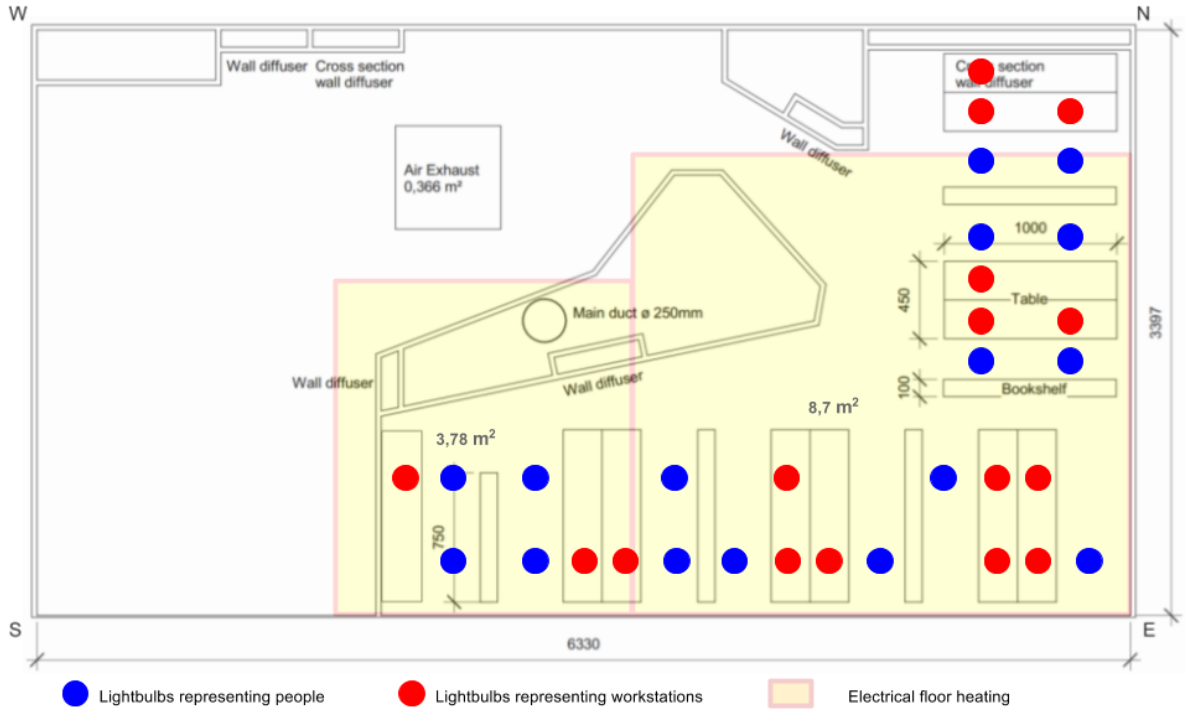

Figure 5.3 Internal heat gains for second half of experiments June 5 2017.

5.2 Air Velocity Mapping

Figure 4.7 illustrates the velocity mapping grid, seen from above. The measured velocities have been interpolated, and are presented as velocity profiles divided into six vertical planes A to F. The velocity profiles are located along the lines A to F. They show the velocities at fixed heights and distances from the diffuser. All the diffuser velocity profiles for the model and prototype can be found in Appendix A.

5.2.1 Results from Model

Figure 5.4 show the air velocity profile of vertical plane D, in the centre of the supply diffuser. The rest of the velocity profiles can be found in Appendix A. Figure 5.4 show the expected velocity profile for a displacement ventilation supply air flow. As the supply air is colder than the ambient room air, it experiences the initial downward acceleration due to the buoyant effect of the colder supply air. The highest velocities in Figure 5.4 can be found close to the floor, indicating this has happened. There is some instability in the discharge, the velocities do not distribute evenly and radial from the diffuser. Most of the air appear to be supplied in the centre of the diffuser, at low heights close to the floor. The velocity mapping show the highest velocities are in the middle of the diffuser (C and D), and slightly higher toward the east side (D). This turn toward the east is probably a result of the office geography. As the south corner

is completely walled in, there is nowhere for the air to flow in that direction. The path of least resistance for the air flow is therefore toward the east, causing a larger airflow this way.

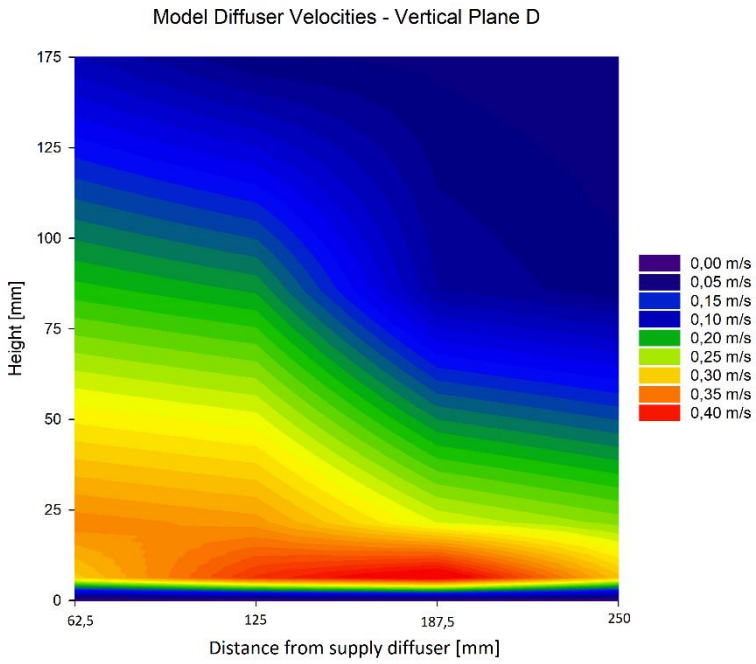

Figure 5.4 Air velocities at vertical plane D of model diffuser. Airflow direction from left to right.

5.2.2 Results from Prototype

The prototype diffuser velocities were measured in March 2016 by Sangnes (2016). Figure 5.5 show the velocity profile of vertical plane F of the prototype diffuser. The rest of the velocity profiles can be found in Appendix A. The velocity mapping indicates diffuser instability. There are large areas of the diffuser where little or no air is supplied. As mentioned in Chapter 2.2.3, a large diffuser is prone to instability in the discharge flow. The prototype diffuser is quite large at 55cm high, and 200cm wide. The velocity profiles also suggest that the supply air may be too hot. There is no downward acceleration of the air, instead it looks like the air rises toward the ceiling. As displacement ventilation require colder air to distribute itself along the floor, too hot supply air can cause a short circuiting of the ventilation, and stagnant zones with suboptimal air quality. The diffusers in the south-east part of the model has to travel a long distance from the main supply duct to the supply diffusers. As the ducts are uninsulated and located in the ceiling, it is possible that the air is excessively heated by the warm air in the upper zone.

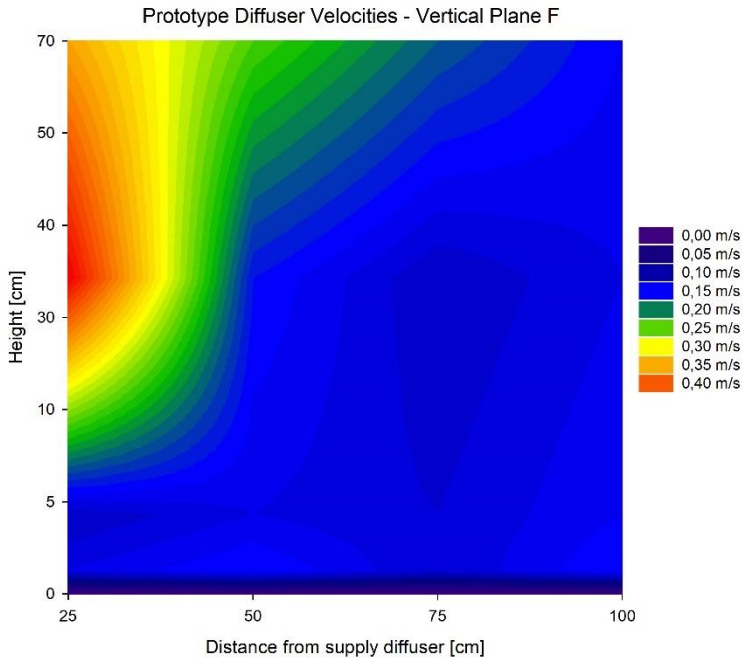

Figure 5.5 Air velocities at vertical plane F of prototype diffuser. Airflow direction from left to right.

5.2.3 Comparison of Model and Prototype Results

The velocity mapping from the model and prototype diffuser clearly show that the supply air flow patterns are different. The model supply air behaves similar to what is expected for a displacement ventilation supply flow. It has a downward acceleration, caused by temperatures colder than ambient air. The prototype supply air flow does not behave as expected for displacement ventilation. The air seems to rise toward the ceiling instead of falling to the floor. This suggests that the supply air is too hot, which can cause a short circuiting of the ventilation. This difference in supply air flow pattern can cause large differences in the air distribution in the prototype and model.

Scaling the model results to prototype velocities, all the grid points A4 to F4 has a velocity higher than 0,2m/s at 3cm height (7,5mm in model). The grid points in the centre of the diffuser, B4 to E4, has a velocity higher than 0,2m/s at 10cm height (25mm in model). Sangnes (2016) found the near zone to be no more than 1m from the diffuser. With the model results scaled to prototype size, the near zone of the diffuser is larger than 1m. Too high velocities can cause a sensation of draft. However, as there is more than 40 cm to the dearest desk (10cm in the model), the air velocity is assumed to drop below 0,2m/s before it enters a zone of occupancy.

5.3 Smoke Visualization

To provide a better understanding of the air movements in the model, smoke was injected at several locations.

The smoke visualization of the supply air diffuser (circled in red in Figure 4.2) showed that the air moved mostly toward the south-east workstations and in an eastern direction. There was an airflow toward the south corner, but it was notably smaller than in the opposite direction. As mentioned in Chapter 5.2.1, this is probably due to the geography of the office landscape, where the south corner is walled in. The maximum velocity looks to be located 2-5 cm height above the floor. When the floor heating is turned on, e.g. when the sun heats the floor in the prototype, the smoke rises higher, more quickly.

Figure 5.6 show smoke visualization of the supply air toward the east. After approximately 40cm the smoke is near 20 cm high. This corresponds to reaching 80cm height in the model, after 1,6m distance in a scaled-up prototype. This is a bit more mixing than expected. However, the smoke experiments show that the streamlines are not constant. Sometimes the smoke move along the floor as expected for the supply flow, mixing only about 10cm in height. See left picture in Figure 5.7. Sometimes the flow move along the wall seen in Figure 5.6, and other times the flow moves into the workstations in the south-east part of the office landscape (toward and behind the camera), as seen in the right picture in Figure 5.7. These different flow patterns suggest the air flow patterns in the room are unstable. As the driving forces of displacement ventilation are small, a small change in the supply air temperature or volume flow can have large consequences for the air flow pattern in the model. As the experiments were performed at three different dates, the model conditions varied some.

Figure 5.6 Smoke visualization of supply air diffuser. Smoke in eastern direction. No floor heating. The diffuser in the picture is the one used for velocity mapping, circled in red in Figure 4.2.

(a) *(b)*

Figure 5.7 Smoke visualization from supply diffuser. No floor heating. (a) Smoke move close to floor, along the back internal wall. (b) Smoke move toward the south-east work stations, mixing more in height.

The thermal plumes from the simulated persons and computers can easily be spotted with smoke. Figure 5.8 Show the thermal plumes above a simulated person and computer in the model. Smoke visualization in the north of the model show that the northern diffuser supply air move along the floor to the workstations close by. Smoke injected close to the ceiling show the air moving toward the narrow passage and exhaust, as expected.

Figure 5.8 Smoke visualization of thermal plume from simulated person (left) and computer (right).

The east corner has been suggested as a problem area, and therefore several smoke experiments was performed here. The visualization showed that air entered the east corner, though less than other areas. The smoke entering the east corner was heated quickly by the person close to the entrance. Some smoke moved past at floor level, but much of the smoke was heated, causing it to rise above floor level. This lead to the smoke being hindered by the divider beneath the desk, which decreased the amount of air supplied to the innermost corner. The gap between the floor and the divider is 6cm. If it is removed, the gap between the floor and the desk is 20cm.

Figure 5.9 Smoke hindered by the desk divider in the east corner. The desk divider can be seen both underneath and above the desk.

5.4 Temperature Measurements

Sixteen thermocouples are placed in the model, measuring the temperature at various locations. The specific location of the thermocouples can be found in Section 4.4.1. The temperature measurements in the model were done on seven different dates, measured for the three different cases mentioned in Section 5.1. The temperatures presented below are from when the temperatures have stabilized. Both the actual temperature and the temperature difference is shown. The supply temperature is used as reference temperature for the temperature differences. Due to an unstable supply temperature and varying ambient room temperature, the model temperatures varied both from date to date, and within one measurement.

5.4.1 Case I – Normal Occupancy

This case has the same occupancy load as the prototype, measuring the temperature distribution in the model for when 10 people are present, each using a computer. No solar gain is simulated. The experiments have been conducted without the use of the cross-section diffusers. This Case have been run on three different dates, as different tracer gas experiments were performed. Temperatures from a stable period June 2 are presented below in Figure 5.10 and Table 5.7. 78 measured values are used for the calculation of the mean, median and standard deviation. The temperature gradients for the east corner can be found for all the measurements in Figure 5.13. All the temperature measurements from June 8 and June 11 can be found in Appendix B1.

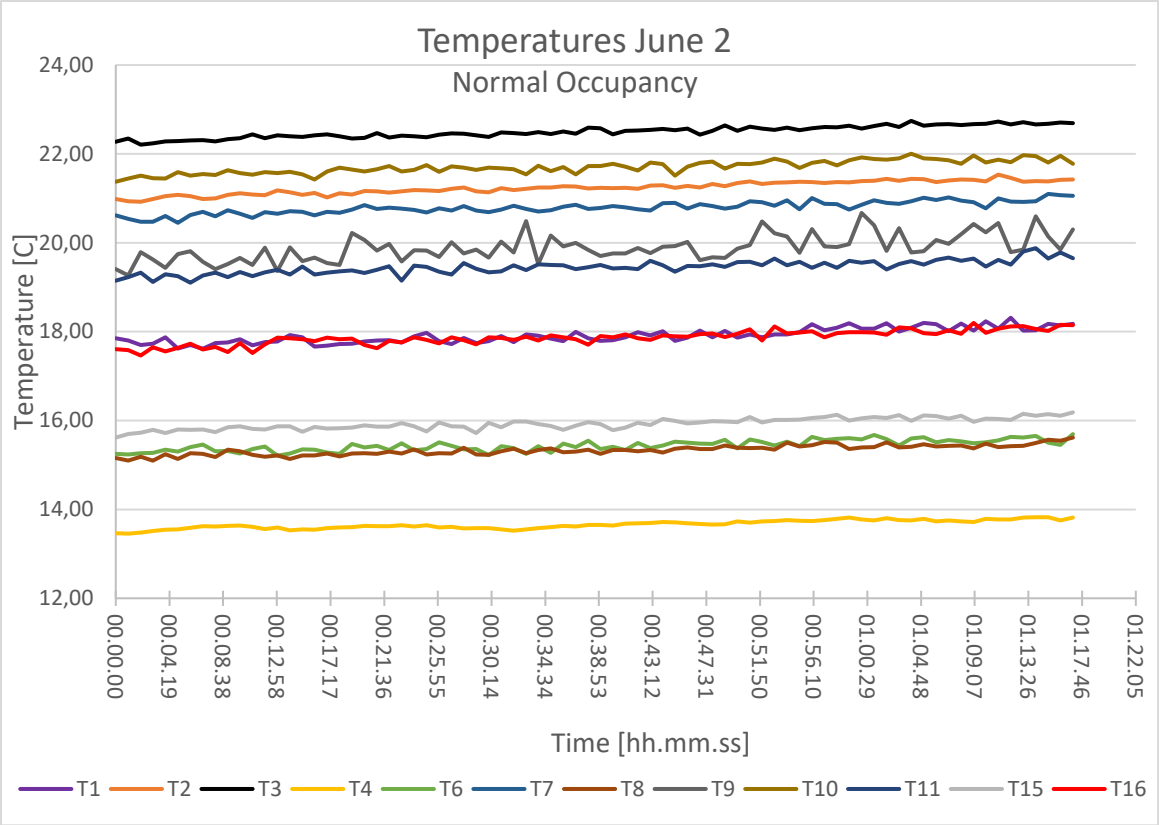

Figure 5.10 Temperatures in the model June 2 2017. Normal occupancy.

Table 5.7 Summary of temperatures in the model June 2 2017. Normal occupancy. N=78 for all temperature measurements.

Time	Minimum	Maximum	Mean	Median	Standard deviation
T1	17,61	18,31	17,91	17,87	0,16
T2	20,92	21,53	21,24	21,24	0,14
T3	22,21	22,74	22,50	22,50	0,13
T4	13,45	13,82	13,66	13,65	0,09
T6	15,21	15,69	15,44	15,43	0,12
T7	20,45	21,10	20,79	20,77	0,14
T8	15,10	15,62	15,33	15,34	0,11
T9	19,27	20,67	19,88	19,84	0,30
T10	21,37	22,00	21,71	21,71	0,15
T11	19,10	19,88	19,45	19,46	0,15
T12	15,69	16,23	15,98	15,97	0,12
T13	17,29	17,90	17,59	17,60	0,15
T14	15,11	15,61	15,41	15,40	0,12
T15	15,62	16,18	15,93	15,94	0,13
T16	17,46	18,20	17,86	17,87	0,16

The temperatures in the model are quite stable for the chosen period, but do still increase some. Looking at the mean and median values of the temperatures, they are quite similar. The temperature that varies the most is T9, located at 375mm height in the narrow passage. The choppy temperature measurement is a result of mixing from cold air from below and warm air from above. A diffuser is located just below, supplying cold air to the model, and the warm air moves toward the exhaust in the ceiling of the narrow passage. However, the temperatures in the model are not so important as long as the temperature differences are stable.

The temperature differences from June 2 are presented as a plot in Figure 5.11, with the supply temperature T4 used as reference. The linear trend functions of the temperature differences show they are quite stable, with a slightly positive slope. A summary of the minimum, maximum, mean and median temperatures can be found in Table 5.8. The mean and median values are either equal or close to equal for all the temperature differences in Table 5.8. This suggest that the temperature differences in the model seems not to be outliers in one direction. The standard deviations are small, indicating that the measured temperatures are relatively stable, close to the mean value.

The exhaust and supply air temperature difference June 2 reached a mean of 4,20K. On June 8 and June 11, the temperature difference between the exhaust and supply air reaches a mean of approximately 2,80K. The main reason for the low temperature difference June 8 and June 11 is thought to be heat loss through the building envelope. The relative temperature difference of the ambient temperature outside the model and the temperature inside the model was twice as high on June 8 and June 11, compared to June 2. This allowed higher temperature differences in the model June 2, as the heat loss through the envelope was smaller. This can also be observed in Figure 5.13, which show the east corner temperature gradients for the different measurements. The temperature in the east corner June 2 was 1K higher in the ceiling, compared to the temperatures June 8 and June 11. The heat loss on June 8 is calculated to be 214W. For both June 8 and June 11, the heat loss was slightly higher than 300W.

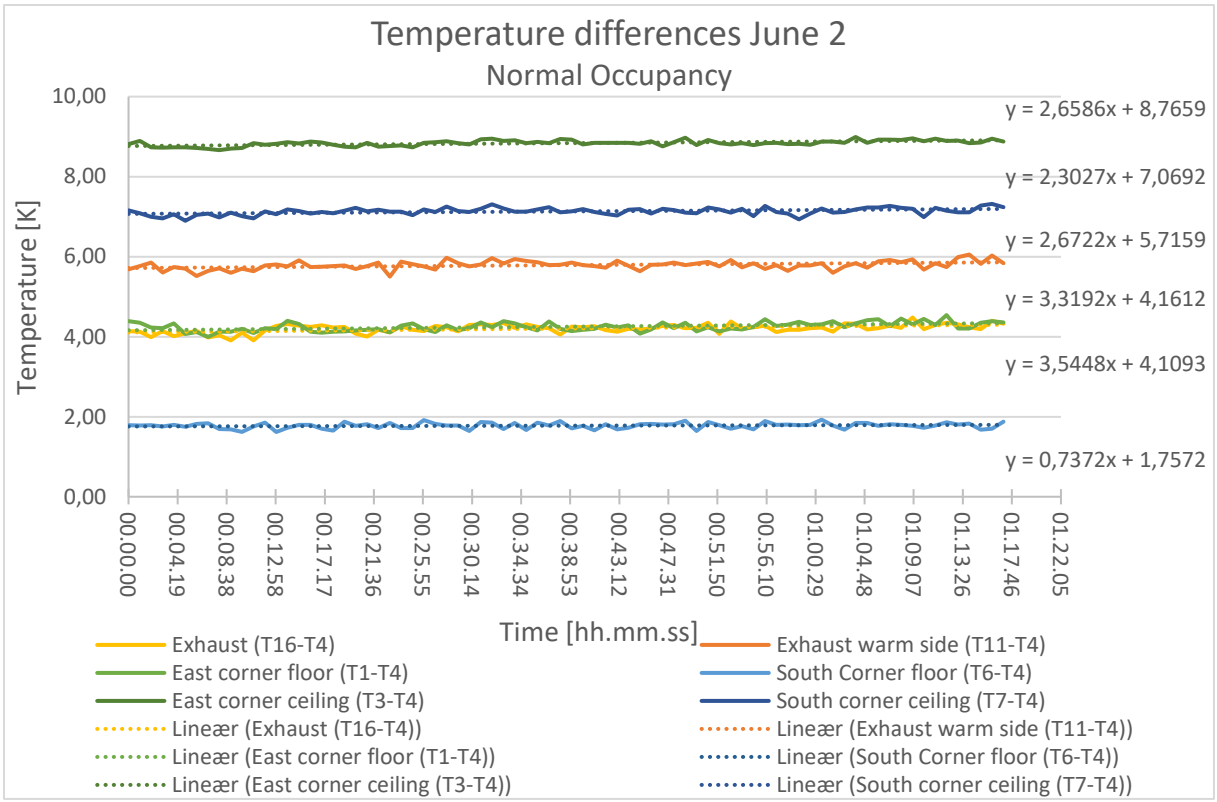

Figure 5.11 Temperature differences in the model June 2 2017. Normal occupancy. Supply air temperature (T4) used as reference.

The increase of temperature by time is shown by the slope of the regression analysis (Figure 5.11).

Table 5.8 Temperature differences in model June 2 2017. Normal occupancy. Supply temperature (T4) used as reference temperature. N=78 for all measurements.

Measurement		Minimum	Maximum	Mean	Median	Standard deviation
T3-T1	East Corner Gradient	4,35	4,78	4,59	4,59	0,10
T7-T6	South Corner Gradient	5,14	5,61	5,35	5,35	0,10
T10-T8	Narrow Passage Gradient	6,15	6,59	6,37	6,37	0,10
T1-T4	East corner floor	3,99	4,54	4,25	4,25	0,11
T3-T4	East corner ceiling	8,66	8,99	8,84	8,84	0,07
T6-T4	South Corner floor	1,62	1,93	1,78	1,78	0,07
T7-T4	South corner ceiling	6,90	7,32	7,13	7,13	0,09
T16-T4	Exhaust	3,91	4,48	4,20	4,20	0,11
T11-T4	Exhaust warm side	5,50	6,05	5,79	5,79	0,11

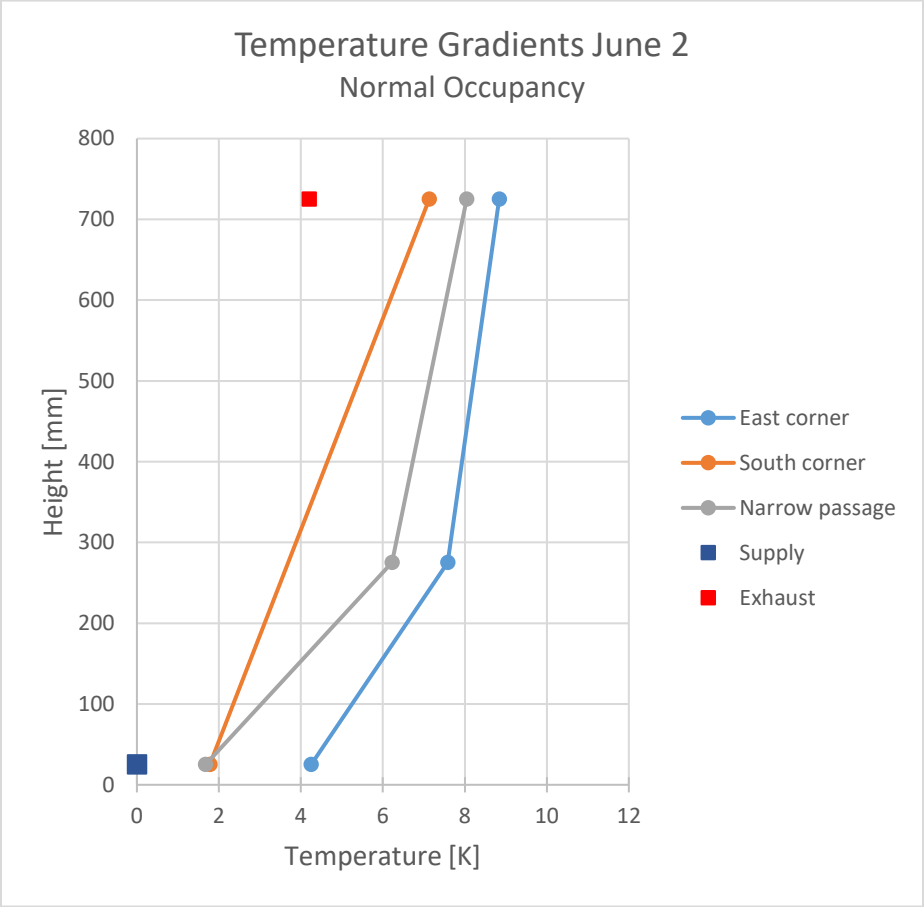

Figure 5.12 Temperature Gradients in the model June 2 2017. Mean temperatures presented. Normal occupancy. Each mean temperature calculated from 78 measured temperatures. Supply temperature used as reference.

In displacement ventilated rooms, the air will stratify itself in thermal layers. The temperature gradients shown in Figure 5.12 show a clear increase from the floor to the ceiling, indicating the air is stratified in the thermal layers. The temperatures in the east corner is clearly higher than in the south corner and in the narrow passage. The warmer floor temperature in the east corner suggests less (cold) supply enters here, compared to the south corner and narrow passage. The difference in temperature from floor to ceiling is also lower. The higher and more uniform temperatures from floor to ceiling in the east corner suggest a smaller local air change. With smaller temperature gradients, the relative buoyancy will be smaller.

The divider underneath the desk was removed to see if it would allow more air to enter the innermost part of the east corner. Figure 5.13 show the temperature gradients in the east corner June 2, June 8 and June 11. The measurements where the desk divider was removed was performed June 11. The temperature gradients in the east corner June 8 (with desk divider) and

June 11 (without desk divider) overlap almost perfectly. The temperature in the east corner is not visibly impacted by the removal of the desk divider. However, no conclusion can be made regarding the air quality in the east corner from these temperature measurements. As mentioned previously, the measurements done June 8 and June 11 had a higher, more similar thermal loss compared to June 2, which is why they are compared.

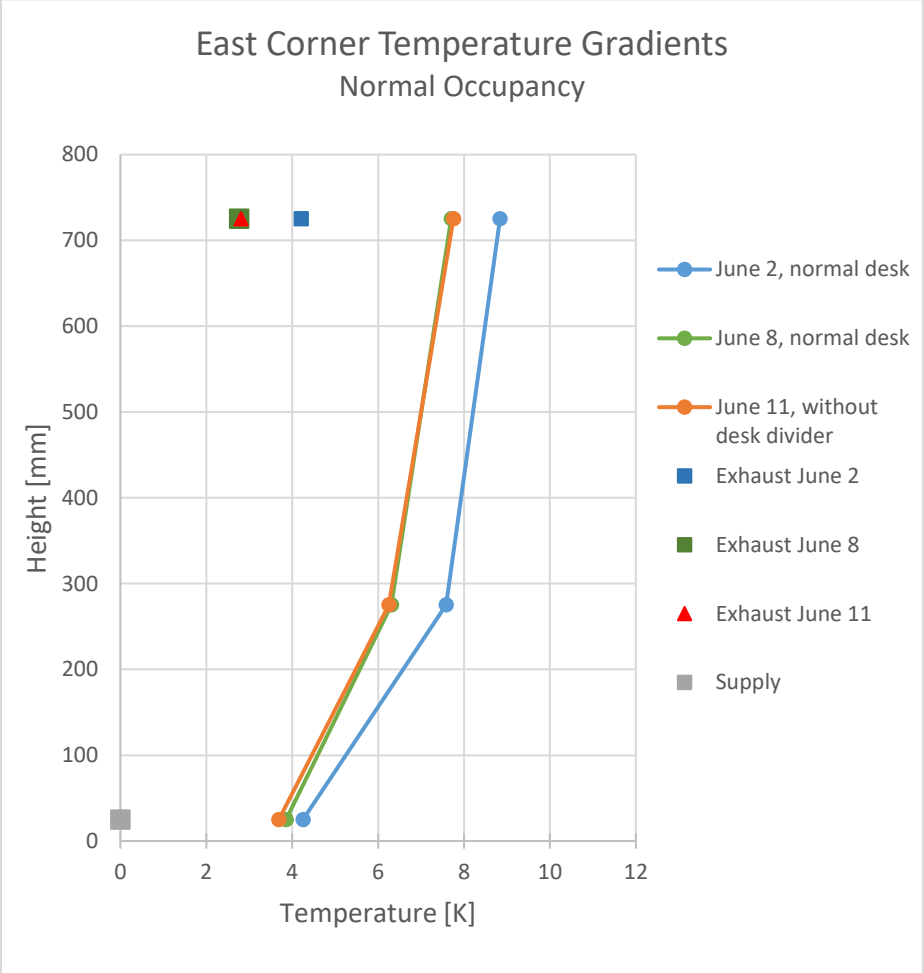

Figure 5.13 East corner temperature gradients. Mean values presented, calculated from 76 to 79 measured temperatures. June 2 and June 8 with normal desk, June 11 without desk divider underneath desk. Normal occupancy. Supply temperature used as reference.

5.4.2 Case II – Normal Occupancy and Solar Heat Gain

For this experimental case the person and computer heat load was the same as previous (10 people and 10 computers), but in addition floor heating was added to simulate solar heat gain. The bookshelf in the east corner was also changed from the regular large one to a smaller one half the size. This was done to see if the air quality in the east corner could be improved. The experiments for this case was performed on two different dates, the results from May 30 is presented below. The temperature measurements from May 31 can be found in Appendix B2.

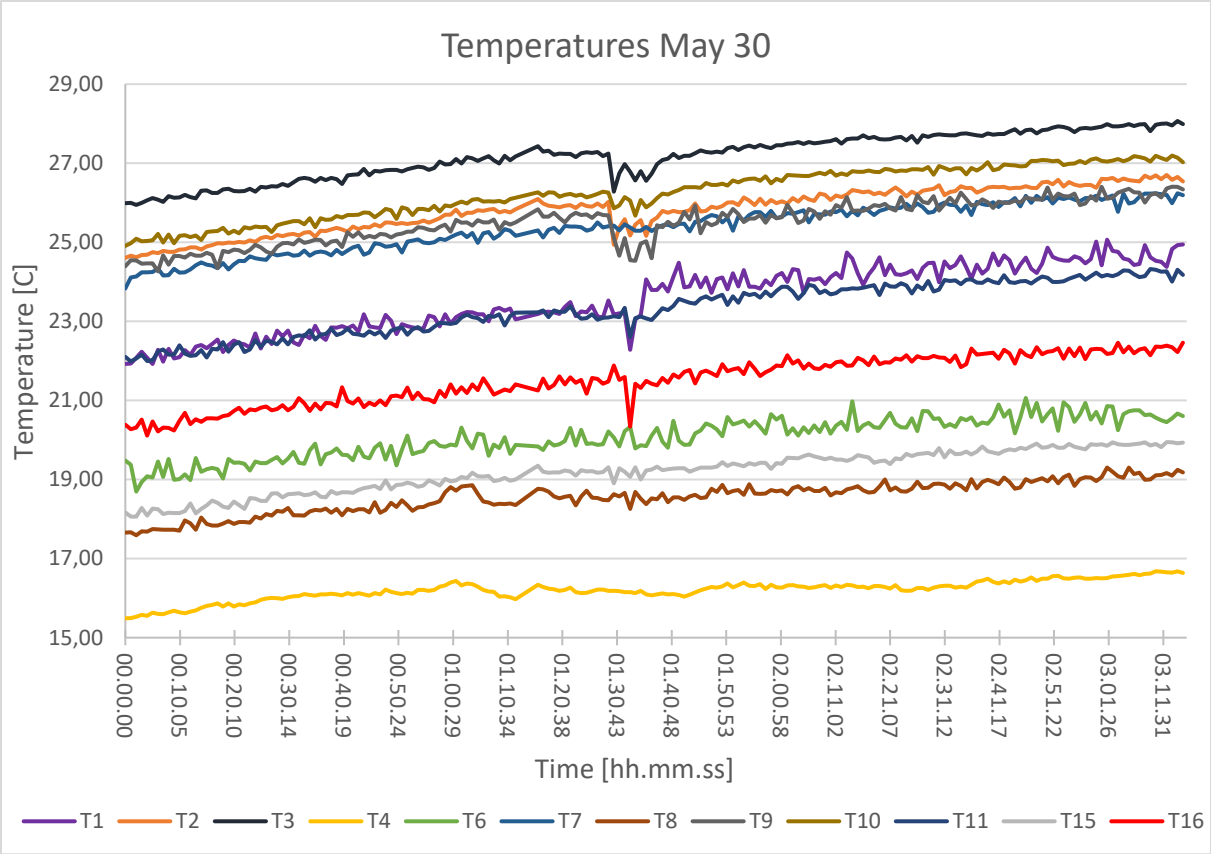

Figure 5.14 Temperatures in model, May 30 2017. Normal occupancy and solar heat gain.

The drop in temperature after 01:30 hours is caused by the opening of the model. At the start of the measurements the bookshelf in the east corner was the regular bookshelf, and halfway through the measurements the bookshelf was changed to the smaller one. One can clearly see from the temperature measurements that the temperature on the floor in the east corner (T1) increase after the bookshelf is changed. The temperature in the middle (T2) and in the ceiling (T3) of the east corner decrease slightly.

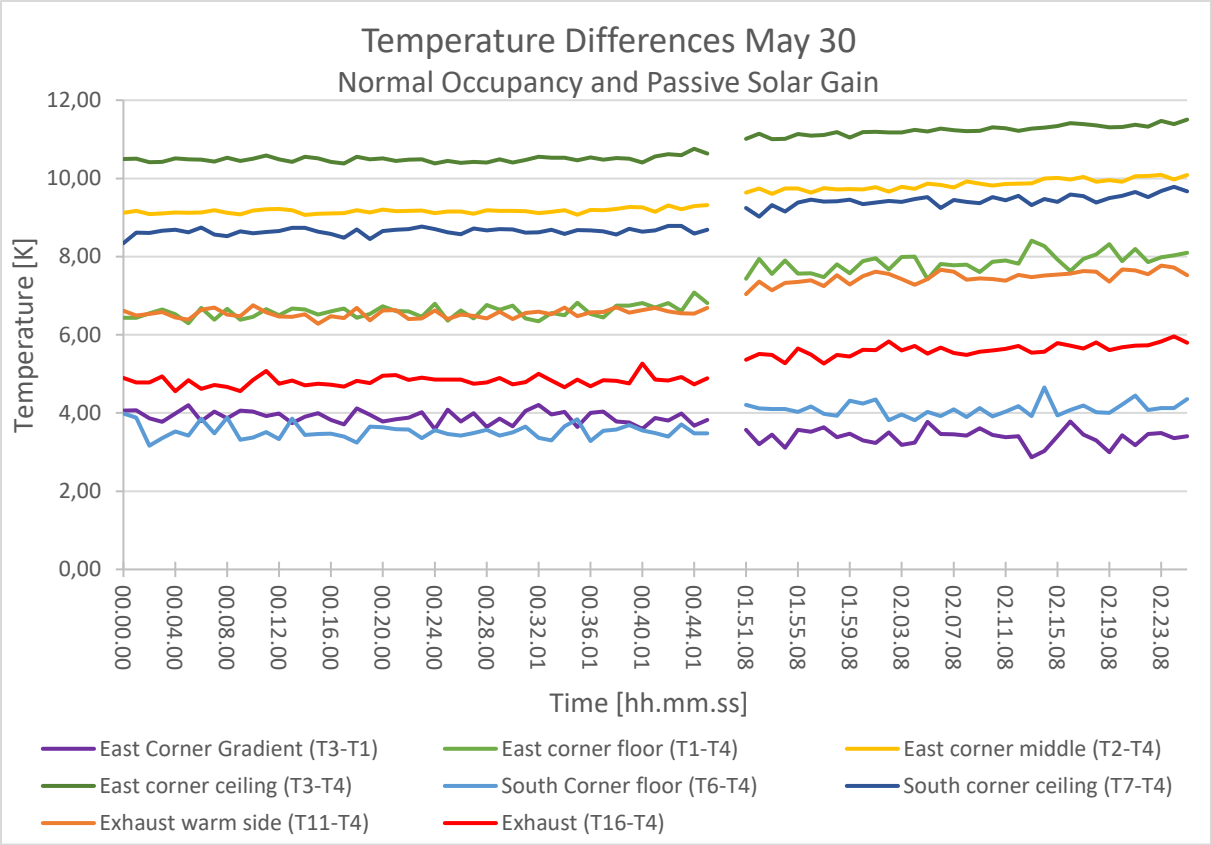

Figure 5.15 Temperature Differences in model and east corner temperature gradient, May 30 2017. Normal occupancy and solar heat gain. Supply temperature as reference temperature. Temperatures on left side of gap with the normal bookshelf. Temperatures on right side with the small bookshelf.

Table 5.9 Mean values and standard deviation for temperature differences and temperature gradients. May 30 2017. N=35 (large bookshelf) and N=46 (small bookshelf) measurements are used to calculate the mean and standard deviations. Supply temperature (T4) as reference temperature.

Mean temperature difference and standard deviation (SD)

Measurement		**Large bookshelf**		**Small bookshelf**		**Difference of mean**
		Mean	*SD*	*Mean*	*SD*	
T3-T1	East Corner Gradient	3,90	0,16	3,38	0,20	-0,51
T7-T6	South Corner Gradient	5,12	0,22	5,34	0,21	0,22
T10-T8	Narrow Passage Gradient	7,36	0,11	7,97	0,12	0,61
T1-T4	East corner floor	6,60	0,16	7,86	0,24	1,26
T3-T4	East corner ceiling	10,49	0,07	11,24	0,13	0,75
T6-T4	South Corner floor	3,53	0,18	4,10	0,18	0,57
T7-T4	South corner ceiling	8,64	0,09	9,44	0,15	0,80
T16-T4	Exhaust	4,81	0,13	5,61	0,15	0,80

Figure 5.15 show the temperature differences in the model and the east corner gradient. The supply temperature (T4) is used as reference temperature. Only the most stable temperatures before and after the bookshelf change are shown. The temperature differences do however still

fluctuate and increase during the experiment, indicating the temperatures have not completely stabilized. Note the jump from in the time axis from 00:44 to 01:51. This caused the gap in between the plots, but makes it easier to see the temperature changes from before and after the bookshelf change. Table 5.9 show the mean temperature differences and standard deviations before and after the bookshelf change, and the difference between them. The standard deviations are a bit larger than previous, indicating the temperature measurements are not as closely centred around the mean value.

All the temperature differences increase, though the east corner floor temperature (T1-T4) increase the most after the bookshelf change. The large increase of the floor temperature causes the east corner temperature gradient to decrease (T3-T1). This can be seen from Figure 5.15 and Table 5.9. The large temperature increase for the east corner floor was not expected. When the bookshelf was changed, it was expected more cool air from the supply diffuser would enter the east corner. The smaller increase of the middle and ceiling temperatures suggests this has happened, but the large increase at floor level suggest otherwise. One cause for the increase of temperature may be due to air exchange with the nearby workstation in northern direction. However, no knowledge on the temperatures here are known. Another possibility is that during the change of bookshelf the thermocouple close to the floor was accidentally pushed down closer to the heated floor. Even though the validity of the floor temperature in the east corner is uncertain, the ceiling temperature has increased less than the other temperatures. This indicate that the air flow pattern in the east corner has changed somehow. Due to the uncertainty of the floor temperature, new measurements, preferably without floor heating, should be performed to validate the current results.

The temperature difference between the exhaust and supply air reaches a mean value of 5,61K (after the bookshelf change). The ventilation heat loss is approximately 233W, and the transmission (and infiltration) heat loss is about 570W. The high transmission heat loss is assumed to be a cause of the extra heat added by the floor heating. A larger heat transfer will occur through the building envelope due to the higher temperatures in the model. In addition, as the heating mats lay directly on the floor, more of the heat is assumed to be transferred trough conduction into the floor beneath. The experiments without the use of the floor mats will have a cool floor and cool air that allow less heat transfer through the floor.

5.4.3 Case III – High Occupancy

This case tested what would happen in the model with a higher internal load. 16 persons, 16 computers and a small amount of solar heat gain is simulated. The temperature for June 5 are presented in Figure 5.16 below. For the first part of the temperature measurements, a low presence was placed in the south corner. For the second half of the experimental run the internal loads simulating humans were moved closer to the south corner. This lead to slightly higher temperatures in the south corner, as expected. As the light bulbs were moved from the east corner, the east corner temperatures decrease slightly. The temperature measurements from June 4 can be found in Appendix B3.

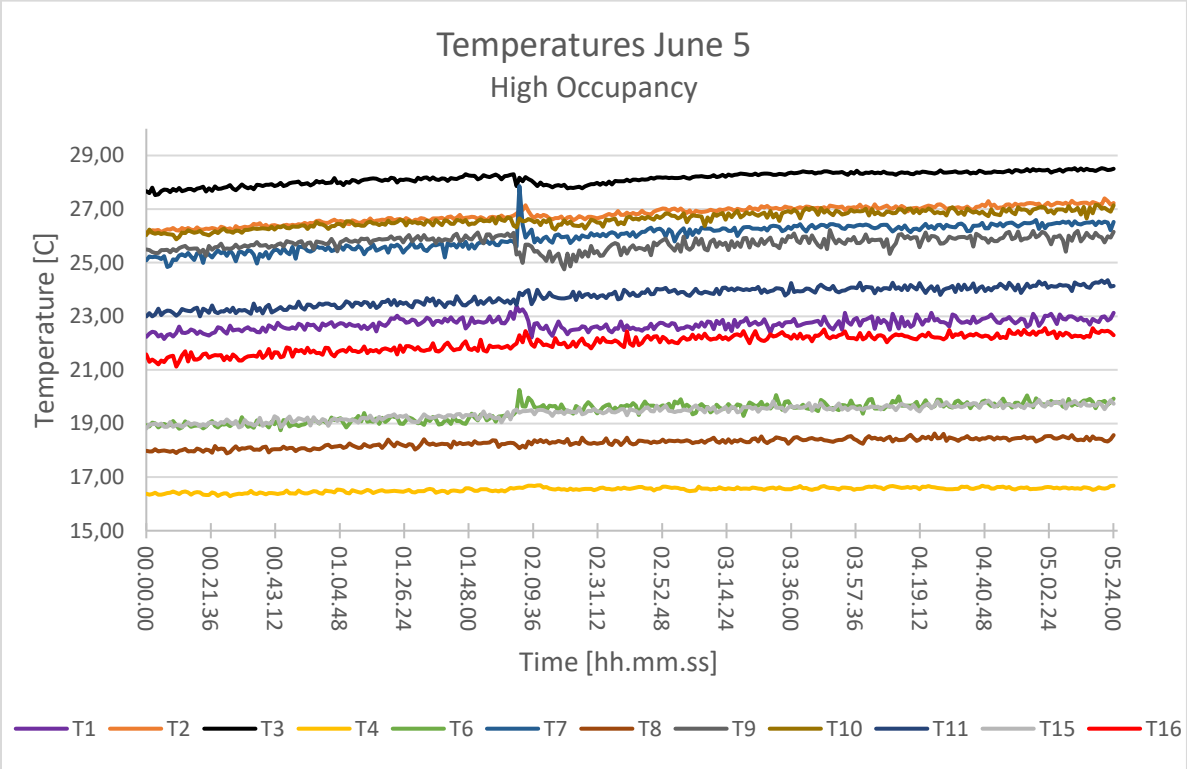

Figure 5.16 Temperatures in model June 5 2017. High Occupancy load.

Figure 5.17 show the temperature differences in the model before the light bulbs are moved. The supply temperature (T4) is used as reference temperature. The temperatures in the model are clearly higher with high occupancy, compared to the normal occupancy (Case I). As the temperatures in the model are higher, it follows that the heat losses will be larger. The difference between the exhaust and supply air reaches a mean difference of 5,3K. The ventilation heat loss is approximately 350W, and the transmission and infiltration heat loss is about 490W. The relative temperature of the air surrounding the model was quite low, increasing the heat loss trough transmission.

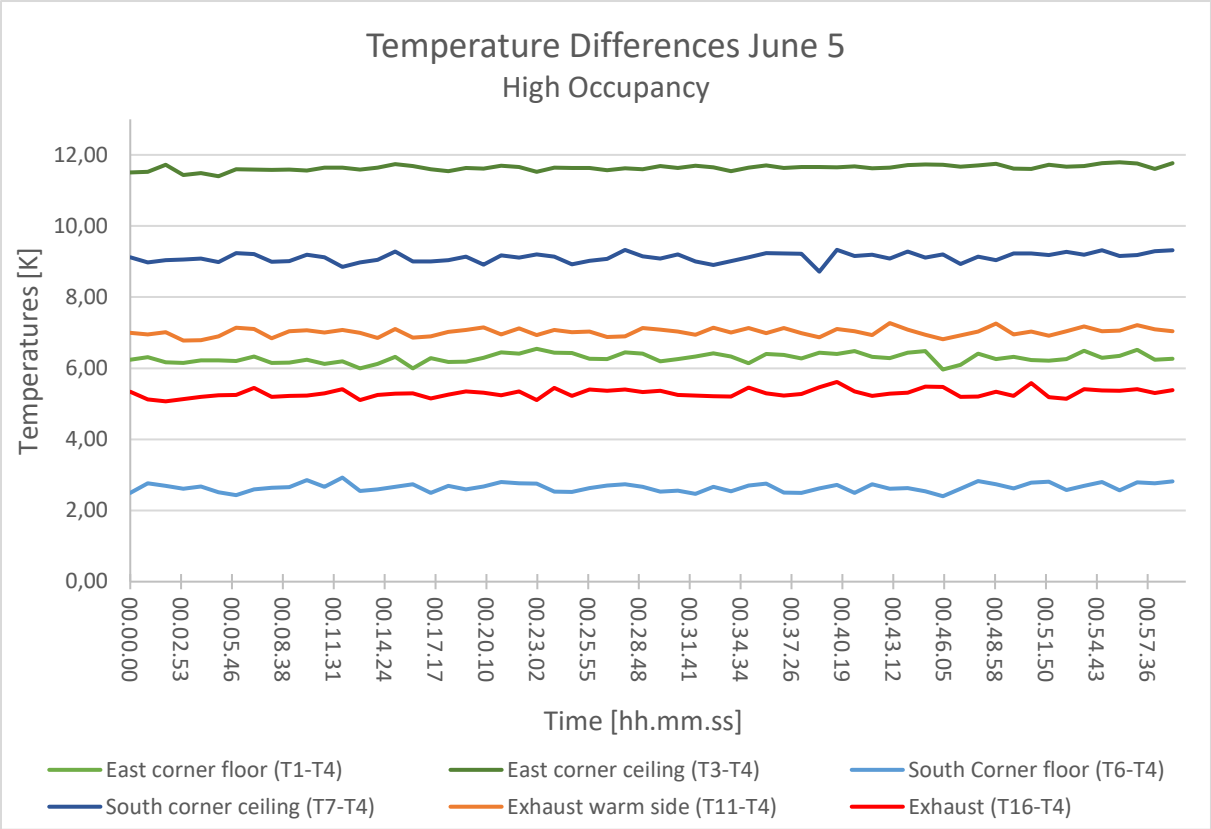

Figure 5.17 Temperature Differences in model, June 5 2017. High occupancy load. Supply temperature (T4) used as reference temperature.

Table 5.10 Summary of temperature differences and temperature gradients in model, June 5 2017. Temperatures from first half of the measurements, N=63 values were used to calculate the mean, median and standard deviation. High occupancy. Supply temperature used as reference temperature.

Measurement		Minimum	Maximum	Mean	Median	Standard deviation
T3-T1	East Corner Gradient	4,98	5,75	5,35	5,32	0,14
T7-T6	South Corner Gradient	5,92	6,80	6,47	6,47	0,16
T10-T8	Narrow Passage Gradient	8,00	8,59	8,28	8,29	0,10
T1-T4	East corner floor	5,96	6,58	6,29	6,29	0,13
T3-T4	East corner ceiling	11,40	11,79	11,64	11,64	0,08
T6-T4	South corner floor	2,40	2,93	2,65	2,66	0,11
T7-T4	South corner ceiling	8,72	9,33	9,12	9,14	0,13
T16-T4	Exhaust	5,07	5,62	5,30	5,29	0,11
T11-T4	Exhaust warm side	6,78	7,27	7,02	7,03	0,11

The temperature gradients in the model are generally quite high, though the temperatures in the east corner are a bit more uniform in height. As for the other experiments, the temperatures in the east corner are higher than elsewhere in the model. The temperature in the south corner increased after the lightbulbs were moved, as can be seen from Figure 5.18.

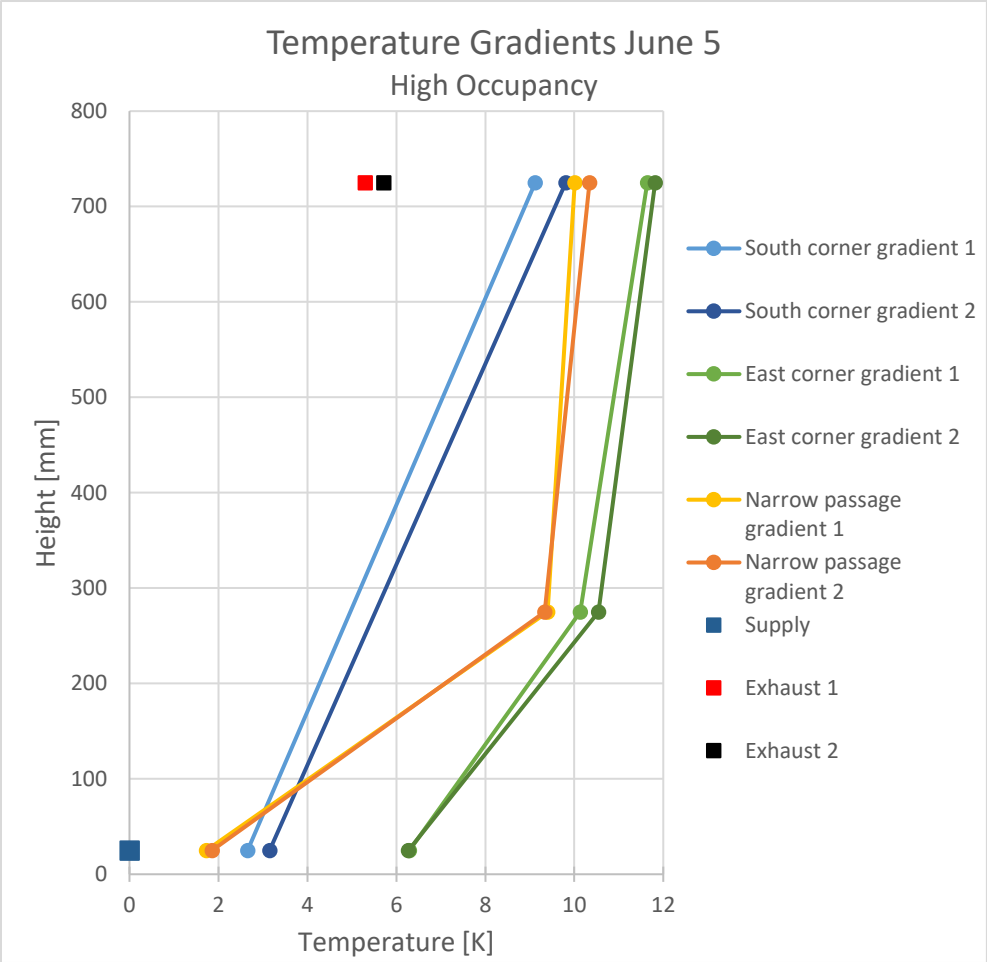

Figure 5.18 Temperature gradients for experiments June 5 2017. High occupancy. Supply temperature (T4) used as reference temperature. Number in series names denote before (1) or after (2) the lightbulbs are moved closer to the south corner. N=63 (before) and N=46 (after) measurements were used to calculate the mean temperatures.

5.4.4 Comparison of Model Results

The temperature differences in the model are highest for the experiments with Normal Occupation and Solar Gain (Case II) and High Occupancy (Case III). This is expected, as the input power is close to double compared to the Normal Occupancy experiment (Case I). However, looking at the south and east corner gradients, there is a lower temperature difference between floor and ceiling air in Case II, when the floor heating was used to simulate solar heat gain. Due to the floor heating, both Case II and Case III has a higher floor temperature than Case I. This can clearly be seen from Figure 5.19(b). The Floor temperature is lowest for the normal occupancy, which has no floor heating added. The high occupancy case has a small amount of floor heat added, causing a slightly higher floor temperature. Finally, the normal occupancy with solar heat gain case has the highest floor heat supplied, causing the highest floor temperature. A warm floor can impact the temperature gradients. As the air is heated

evenly at floor level, the room will get a more uniform temperature. Too much floor heating will cause excess mixing of the air, lowering the ventilation efficiency.

The presence of people has also changed. For the temperature gradients shown in Figure 5.19, the south corner has the same amount of local presence, but the east corner has a presence of two for the normal occupancy and normal occupancy and solar gain, while the presence for the high occupancy is four. The normal occupancy and solar gain and the high occupancy cases has about the same amount of total heat load supplied to the model, though the distribution is different. Even though the south corner has a lower local heat load for the high occupancy compared to the normal occupancy and solar gain (less floor heating), it has a higher temperature gradient. As mentioned above, floor heating can cause more uniform temperatures and smaller temperature gradients.

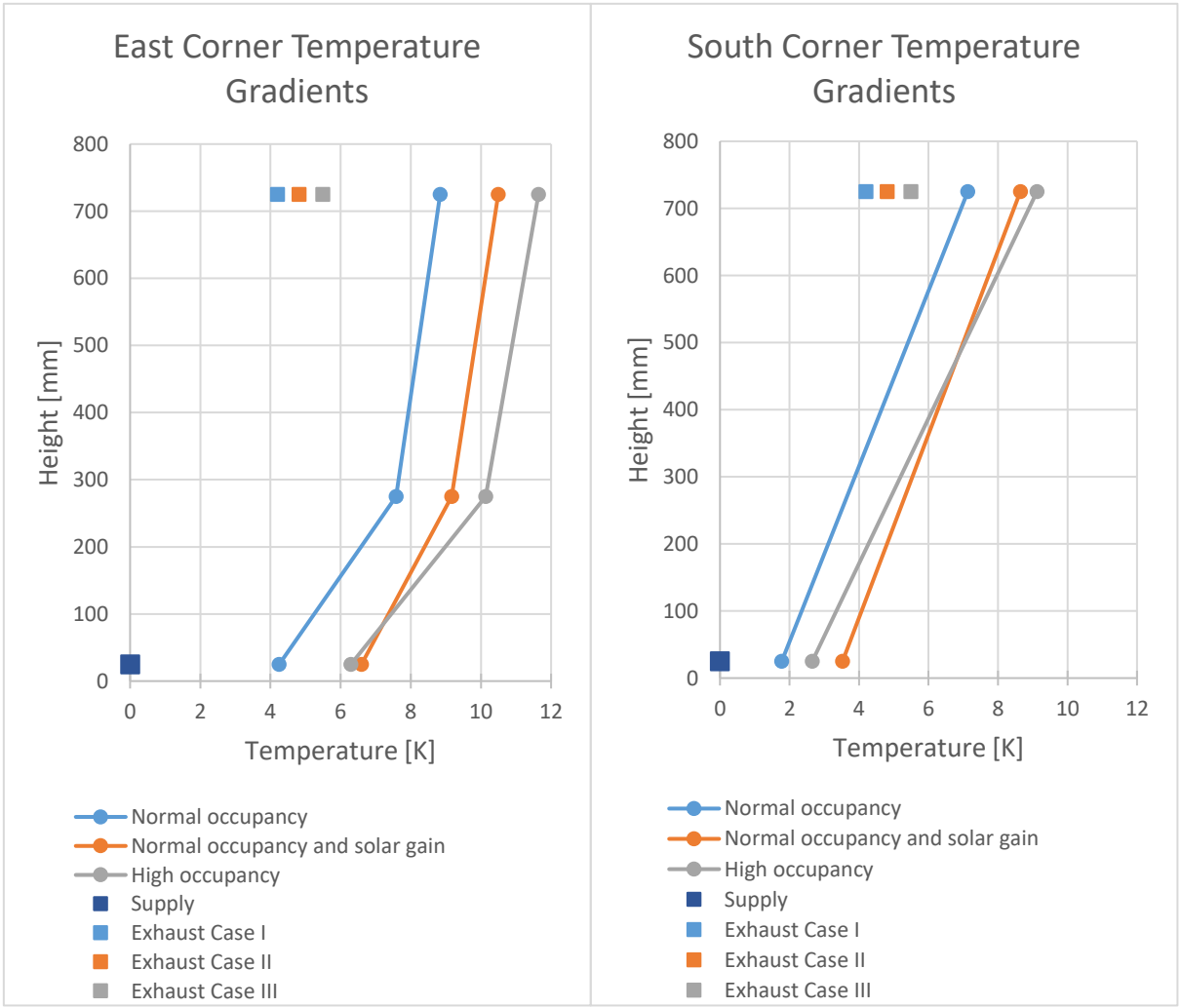

(a) *(b)*

Figure 5.19 East (a) and south (b) corner temperature gradients for the three different heat loads. Measurements done June 2, May 30 and June 5. Supply temperature used as reference.

5.5 Tracer Gas Measurements

The tracer gas measurements were performed in the model at seven different dates, measuring the air change efficiency and local air change index in the model. Three different cases were measured, there the internal heat loads were changed. The local air change index was measured at four different heights in the south and east corner, and at four different location at 375mm height. When talking about these measurement locations, they are named “South Corner”, “East Corner” and “All 375”. In addition, the change in local air change index was measured when changing the divider underneath the desk (Case I) and bookshelf (Case II) in the East Corner, and when moving the heat sources closer to the South Corner (Case III). The cross-section diffusers are not used for any of the tracer gas measurements. See Chapter 5.1 for description of the different experimental cases. See Chapter 4.4.2 for further description of the tracer gas setup.

The tracer gas equipment has the possibility to measure six points at one time. Two of these were needed for the exhaust and supply concentrations, leaving four measurement points in the model. However, to get a sufficient amount of measurements, only one location in the model is measured at a time. As the tracer gas volume flow is controlled manually, the supply air concentration is never exactly the same. The plots showing the exhaust and room concentration have been multiplied by a constant, to see if they look similar from experiment to experiment. Some of the concentration curves are presented in the section below. All the values used to calculate the air change efficiency, mean age of air, nominal time constant, local air change efficiency and local age of air, and a few examples of the concentration curves for one measurement set can be found in Appendix C. The supply concentration curves are not shown in the concentration figures presented below, but can be found for some examples in Appendix C.

5.5.1 Case I – Normal Occupancy

This case measure the ventilation efficiency for when 10 people are present, each using a computer. No passive solar gain is simulated. The local air change index in the east corner is measured at four different heights, for two different setups. First the normal desk is used, then the divider underneath the desk is removed. The first measurement set in the east corner, with the normal desk, was performed June 2. The second measurement set in the east corner, without the divider underneath the desk, was done June 11. Two different sets were measured June 8.

The first set measured four different heights in the south corner, the second set measured four different locations (south, south-east, east and north) at 375mm height. All the values used to calculate the air change efficiency, mean age of air, nominal time constant, local air change efficiency and local age of air can be found in Appendix C1.

Figure 5.20 show the concentration decay curves for the exhaust measured June 2. Figure 5.21 show the logarithmic representations of these curves. As the conditions for the experiments ideally should be the same, the concentration decay curves for the exhaust should overlap completely. Some small differences can be seen from Figure 5.20, but overall the exhaust curves follow each other closely. The logarithmic representations of the exhaust curves are straight, providing good values for the calculation of the air change efficiency. Only the curves from June 2 are shown here, though curves from June 8 and June 11 also follow the curves from June 2 closely.

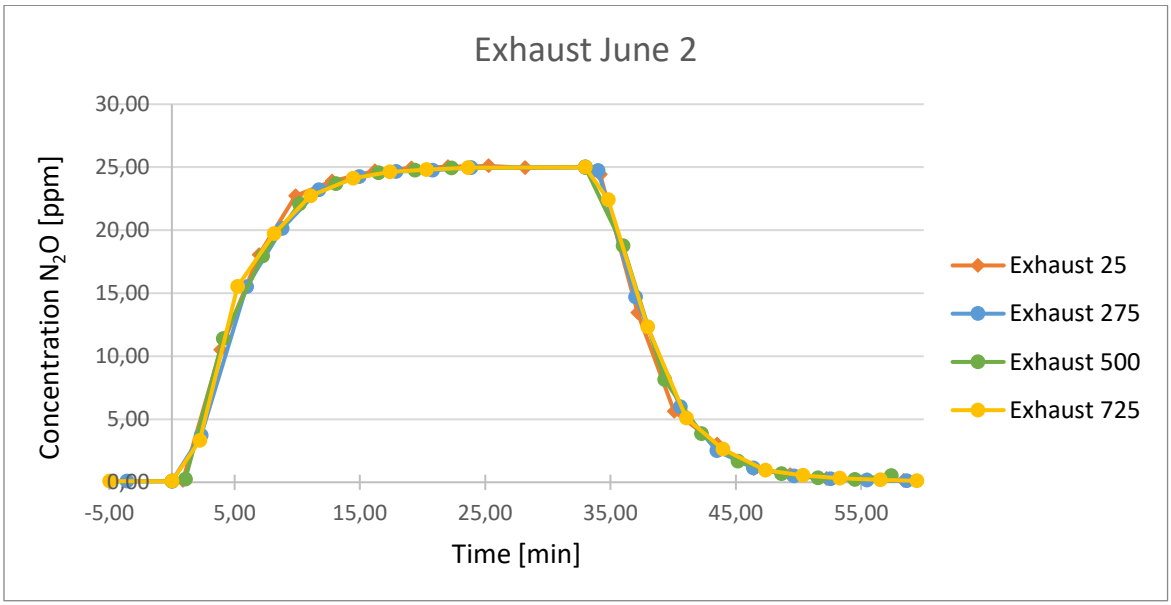

Figure 5.20 Step-up and step-down concentration decay curves for the exhaust June 2 2017. Number in series names represent the height of the east corner local measurement that was taken. Normal occupancy.

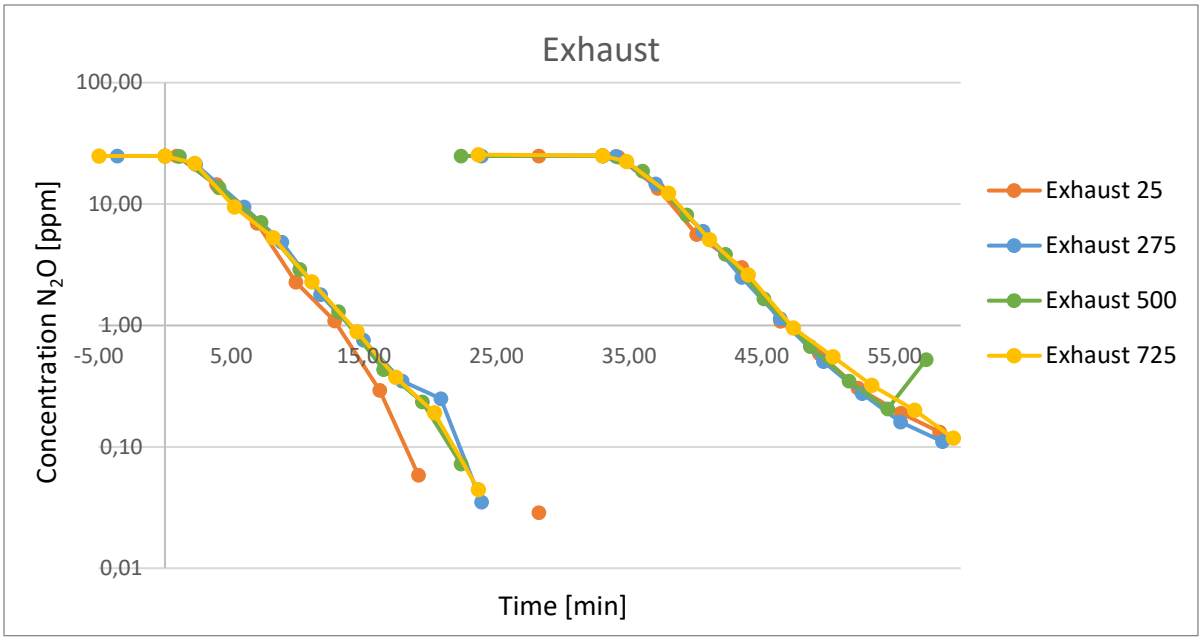

Figure 5.21 Logarithmic presentation of the step-up and step-down concentration decay curves for the exhaust June 2 2017. Step up curve inverted. Number in series names represent the height of the east corner local measurement that was taken. Normal occupancy.

Figure 5.22 show the concentration curves for the measurements of all heights in the east corner June 2. The exhaust concentration curve is from the East 275 measurement. The curves behave as expected for displacement ventilation, where the concentration close to the floor increase (step-up) and decrease (step-down) the fastest. The exhaust concentration is the last to increase and decrease. If the ventilation efficiency was mixing ventilation, the curves would follow each other more closely, overlapping the exhaust concentration. The logarithmic representation in Figure 5.23 are fairly straight. The line for the East 25 step-down line curve somewhat, which can be caused by a small change in the supply air volume.

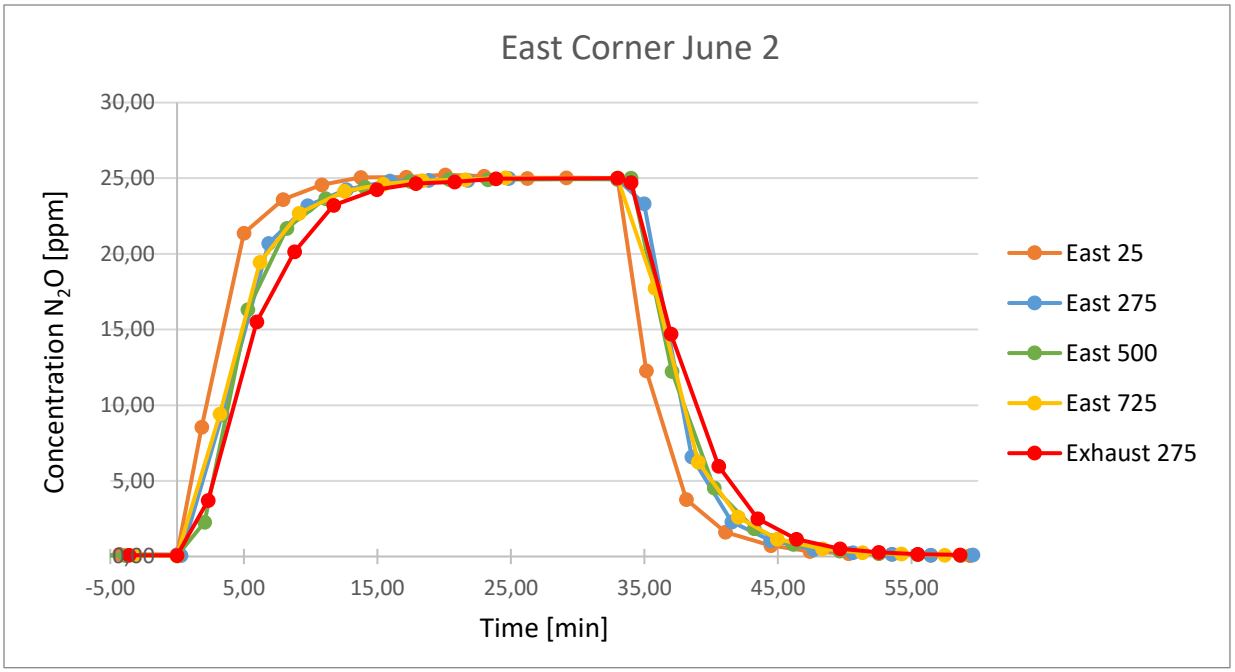

Figure 5.22 Step-up and step-down concentration decay curves for the east corner June 2 2017. Normal bookshelf. Numbers in series names represent height [mm]. Normal occupancy.

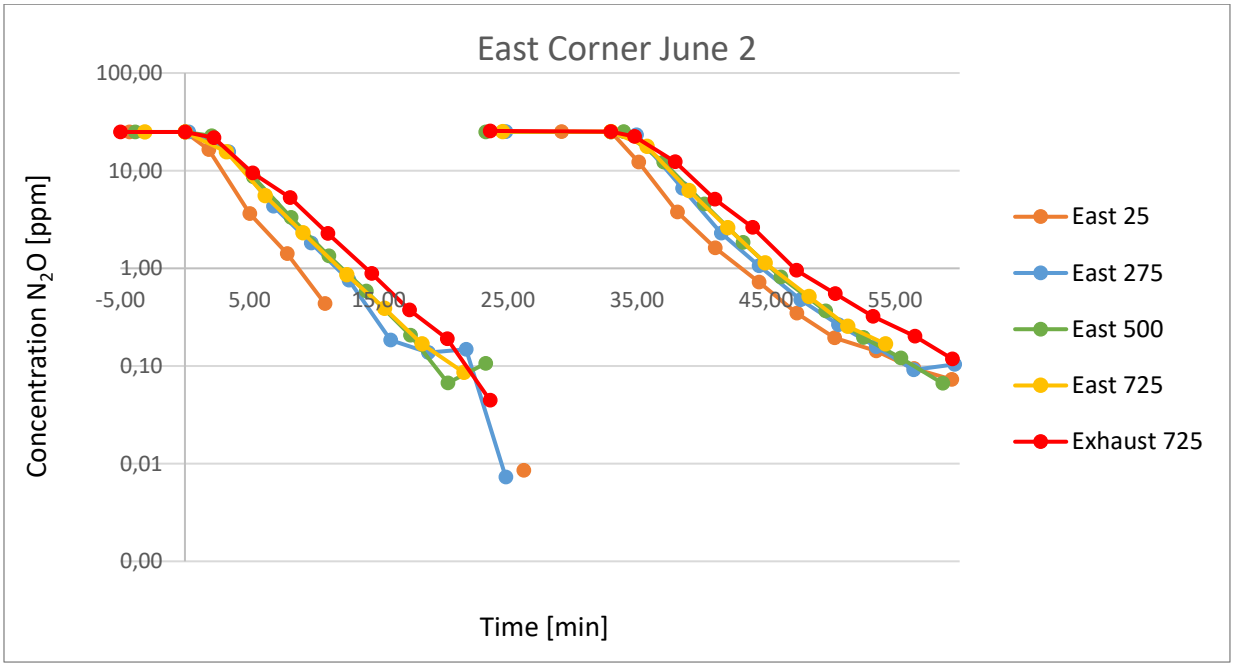

Figure 5.23 Logarithmic presentation of the step-up and step-down concentration decay curves for the East Corner, June 2 2017. Step up curve inverted. Normal bookshelf. Numbers in series names represent height [mm]. Normal occupancy.

Table 5.11 Summary of tracer gas measurements, June 2, June 8 and June 11 2017. N=30 measurements was used for calculating the mean, median and standard deviation.

	Minimum	Maximum	Mean	Median	Standard deviation
Air change efficiency [%]	61,94	68,23	64,54	64,51	1,43
Nominal time constant	5,73	6,25	5,97	5,98	0,13
Mean age of air	4,41	4,90	4,63	4,63	0,11

Table 5.11 presents the minimum, maximum, mean and median values of the ventilation effectiveness. Both the minimum and the maximum air change efficiency indicate that the ventilation in the model works as displacement ventilation. The standard deviation is small, indicating the measurements are gathered close around the mean value.

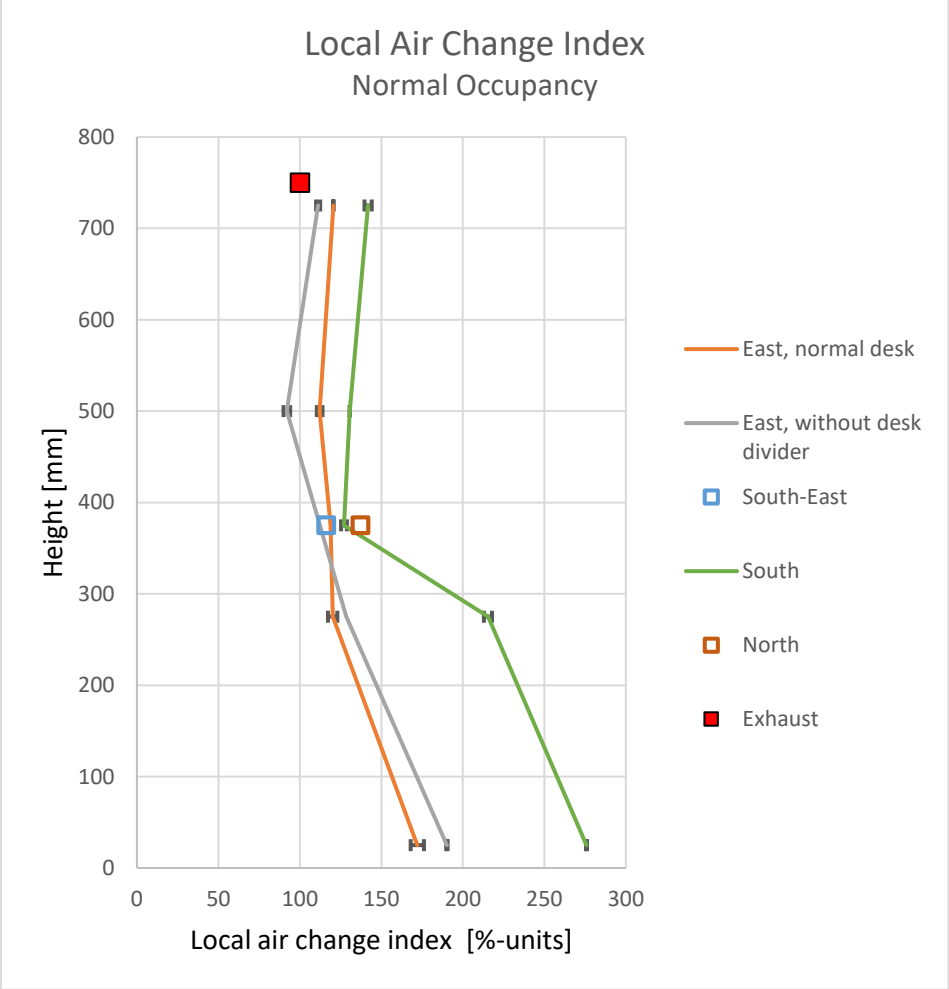

Figure 5.24 Measurement of Local air change index by Height, compared to Exhaust (at 750mm). Normal occupancy. Mean value of step-up and step-down measurements presented, bars show minimum and maximum value. "East, normal desk – 375mm", "East, without desk divider – 275mm" and "North – 375mm", only one measurement each. "South-East" has two measurements at 375mm only, error bar smaller than marker.

Figure 5.24 show the local air change index for all the measured locations, plotted as a function of height. The mean value from the step-up and step-down measurements are used if both values are acceptable. As only one or two measurements are taken, the uncertainty of the mean values may be significant. Horizontal bars show the measured minimum and maximum values if both values are acceptable. The values showed in Figure 5.24 show very little variation. The largest is at East 25, where the maximum and minimum value differ 4,1 %-units from the mean. This is difference is considered very small, as the mean local air change index is 172 %-units.

The local air change index show high values, consistent for displacement ventilation. It is largest at floor level and decrease with height, suggesting the air is supplied at floor level, then brought to the ceiling via thermal plumes. The east corner has a lower air change than the south corner, as can be seen from Figure 5.24. However, the local air change index for both corners indicate displacement ventilation. The local air change index in the east corner without the divider is slightly larger at 25mm and 275mm (18 %-units and 8 %-units respectively). As the smoke experiments showed quite clearly that the divider underneath the desk hindered the air, a larger improvement on the local air change index was expected.

As the tracer gas experiments were performed on three different dates, the temperature conditions for the measurements were not constant. The supply temperature varied, and the temperature of the air surrounding the model changed during the day, as the outside temperature increased. As mentioned in Chapter 5.4.1, the temperature difference between the air inside the model and the ambient room air outside the model was larger for the measurements June 8 and June 11, compared to June 2. This caused larger thermal losses June 8 and June 11, leading to smaller temperature differences in the model. However, looking at the air change efficiency, it changes little from date to date. All measurements show the ventilation efficiency is consistent with displacement ventilation.

5.5.2 Case II – Normal Occupancy and Solar Gain

This case measure the ventilation efficiency for when 10 people are present, each using a computer. Solar gain is simulated by the electric floor heating. The local air change index in the east corner is measured at four different heights, for two different setups. First the normal bookshelf facing north is used, then it is changed to a smaller one, half the size. Both bookshelves are shown in Figure 5.2. The local air change index for the east corner was measured May 30, first with the normal bookshelf, then with the smaller bookshelf. May 31 the local air change index for the south corner and All 375 was measured. All the values used to

calculate the air change efficiency, mean age of air, nominal time constant, local air change efficiency and local age of air can be found in Appendix C2.

Table 5.12 Summary of tracer gas measurements, May 30 and May 31 2017. N=30 measurements are used for calculating the mean, median and standard deviation.

	Minimum	**Maximum**	**Mean**	**Median**	**Standard deviation**
Air change efficiency [%]	61,46	71,69	66,38	65,66	2,73
Nominal time constant	5,27	6,21	5,66	5,68	0,24
Mean age of air	4,02	4,68	4,26	4,24	0,16

Table 5.12 present the minimum, maximum, mean and median values of the ventilation effectiveness. The measurements show the ventilation efficiency is consistent for displacement ventilation. However, the standard deviation for the air change efficiency is almost doubled compared Case I, meaning the values are not as closely centred around the mean. The values varying the most are from May 30, when the supply temperature increased by 4,5K from morning to mid-day, then decreased by 1,5K in the evening.

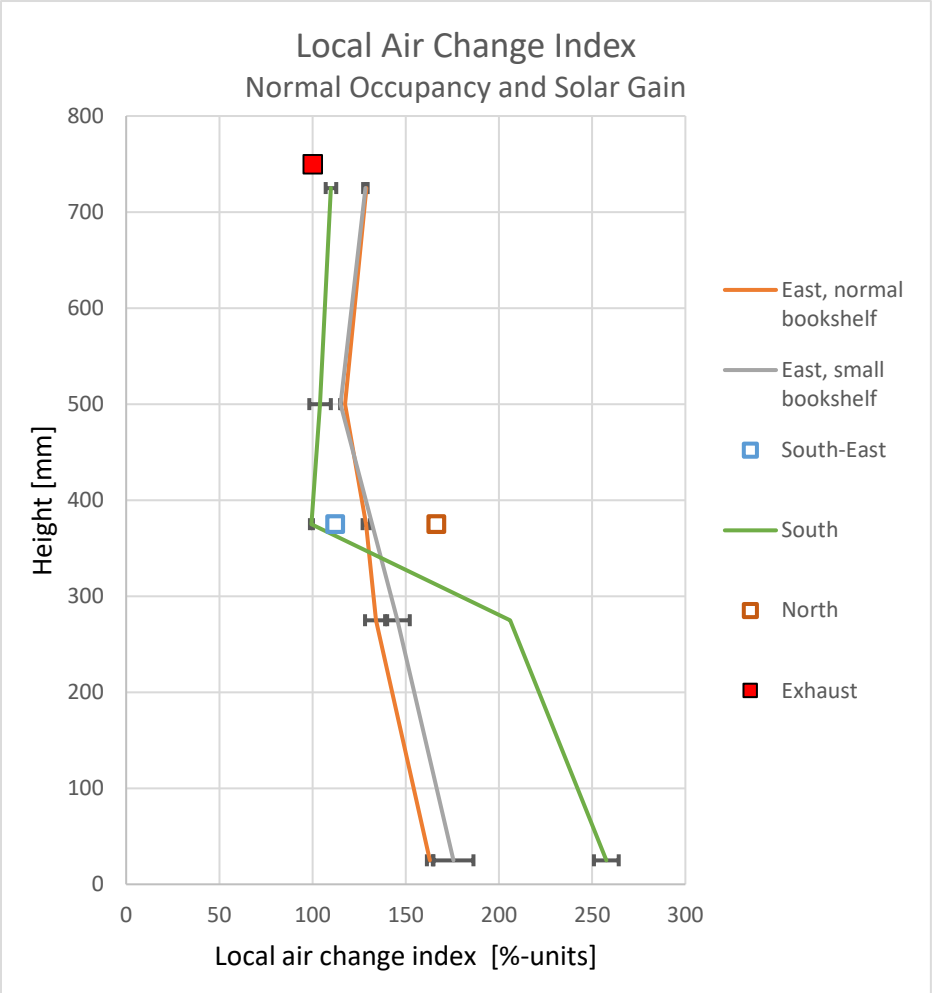

Figure 5.25 Measurement of Local air change index by Height, compared to Exhaust (at 750mm). Normal occupancy and solar heat gain. Mean value of step-up and step-down measurements presented, bars show minimum and maximum value. "South – 275mm", "East, normal bookshelf – 500mm" and "North – 375mm" only one measurement each. "South-East" has two measurements at 375mm only, error bar smaller than marker.

Figure 5.25 show the local air change index for the measured locations, plotted as a function of height. The mean value from the step-up and step-down measurements are used if both values are acceptable. As only one or two measurements are taken, the uncertainty of the mean values may be significant. The horizontal bars show the measured minimum and maximum values if both values are acceptable. The largest difference between the step-up and step-down measurements is at East, small bookshelf at 25mm, where the maximum and minimum value differ 10,7 %-units from the mean. This is difference is considered small, as the mean local air change index is 176 %-units.

The local air change index show values consistent with displacement ventilation. The local air change index is largest at floor level and decrease with an increased height. Similar to Case I, the south corner has a higher local air change than the east corner. The local air change index

in the east corner is slightly larger at 25mm and 275mm when using the smaller bookshelf. However, as the difference between the large and small bookshelf is small, and the error bars of the measurements overlap, the change is neglectable. As displacement ventilation is driven by thermal plumes, the experiment should be performed with varying local presence (and solar heat gain) in the east corner, to see how the presence impact the local air change index. This experiment was performed with a local presence of two people.

5.5.3 Case III – High Occupancy

This case measure the ventilation efficiency for when a high load of 16 people are present, each using a computer. In addition, a small amount of solar gain is simulated by the electric floor mats. June 4 the local air change index for the south corner and All 375 was measured. The local air change index in the south corner is measured at four different heights, for two different setups. First a small local load is present in the south corner, then some lightbulbs are moved closer, increasing the local presence. The local air change index for the south corner was measured June 5, first with the normal presence (South 1), and then with the increased local presence (South 2). All the values used to calculate the air change efficiency, mean age of air, nominal time constant, local air change efficiency and local age of air can be found in Appendix C3.

The ventilation has high local air change at low heights in the south corner (25mm and 275mm), but as the height increase the ventilation look more like mixing ventilation (500mm and 725mm). As the fresh air need heat to rise to the ceiling, a situation where a corner has little local heat can cause stagnant zones. This seem to be happening in the south corner. The fresh, cold air easily enters the corner at floor level, but little driving force hinders the air from moving in height. Instead, warm air from other parts of the model moves into the south corner at ceiling height, causing this mixing effect. However, the air quality for a person working here should be good, as there is ample fresh air at floor level. As mentioned in Chapter 2.2.1, the air will rise along the person bringing fresh air into the breathing zone. To test and see if the local air change index would improve with a higher local load, the person load was moved closer to the south corner (South 2). The local air change index for the south corner seen in Figure 5.26 clearly show that it has increased for all heights.

Table 5.13 Summary of tracer gas measurements, June 4 and June 5 2017. N=30 measurements are used for calculating the mean, median and standard deviation.

	Minimum	Maximum	Mean	Median	Standard deviation
Air change efficiency [%]	63,00	70,90	66,81	67,06	1,70
Nominal time constant	5,57	6,13	5,79	5,80	0,14
Mean age of air	4,14	4,52	4,34	4,33	0,10

Figure 5.13 present the minimum, maximum, mean and median values of the ventilation effectiveness. Both the minimum and the maximum air change efficiency indicate that the ventilation in the model works as displacement ventilation. The standard deviation is small, indicating the measurements are gathered close around the mean value.

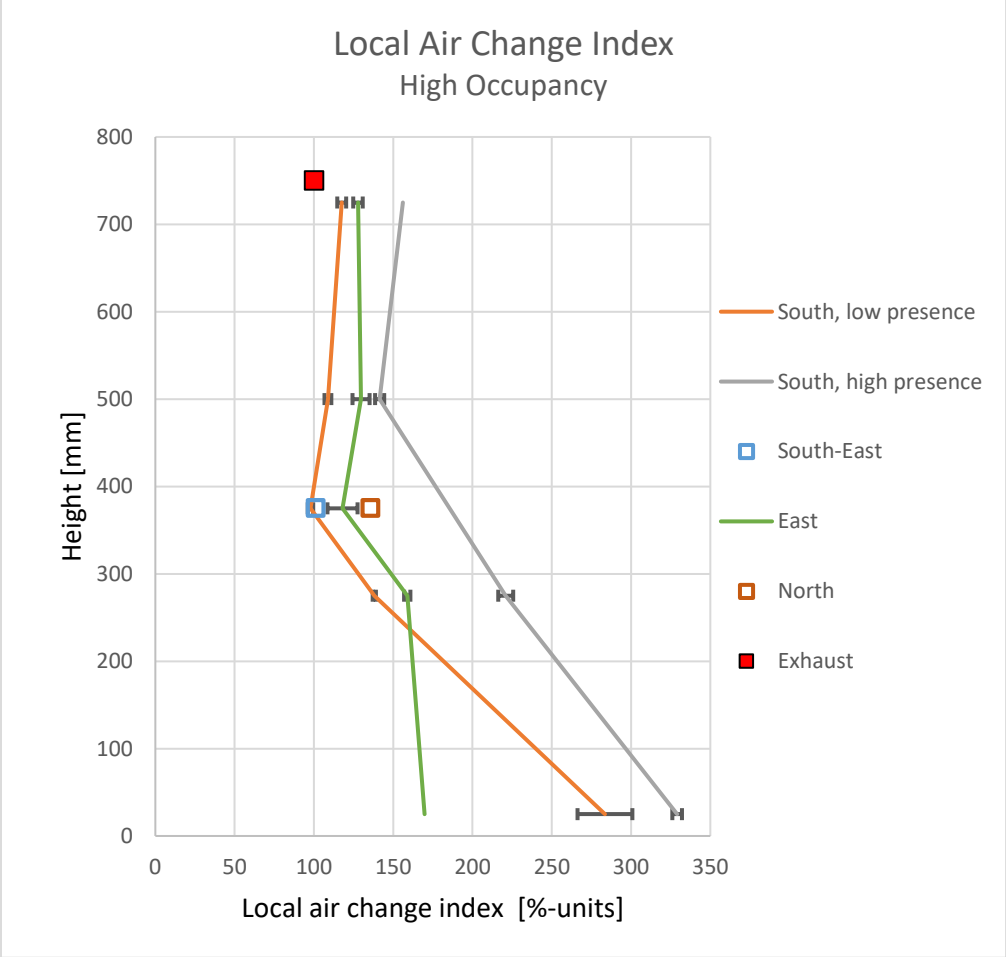

Figure 5.26 Measurement of Local air change index by Height, compared to Exhaust (at 750mm). High occupancy. Mean value of step-up and step-down measurements presented, bars show minimum and maximum value. "South – 725mm" and "East – 25mm" only one measurement each. "South-East" and "North" have two measurements at 375mm only, error bar smaller than marker.

Figure 5.26 show the local air change index for all the measured locations, plotted as a function of height. The mean value from the step-up and step-down measurements are used if both values are acceptable. As only one or two measurements are taken, the uncertainty of the mean values may be significant. The horizontal bars show the measured minimum and maximum values. The values showed in Figure 5.26 show little variation. The largest is at South, low presence at 25mm, where the maximum and minimum value differ 17,3 %-units from the mean. This is difference is considered small, as the mean local air change index is 284 %-units.

The local air change index show high values, consistent for displacement ventilation. The values in the lower half of the model are very high, and decrease in the upper part of the model. The presence in the south corner was changed, and the measurements clearly show the local air change index has increase with an increased presence. Comparing the mean values, the local air change index in the south corner is 45,5 %-units larger at 25mm and 82,9 %-units larger at 275mm with two people present.

5.5.4 Comparison of Model Results

Figure 5.27 show a box plot of the air change efficiencies for the three different experimental cases. 30 values were used for calculating each data set, 90 in total for the three data sets. For each data set, the line in the centre of the box show the mean value, the box show the standard deviation of the measurements, and the vertical bars show the minimum (lower bar) and maximum (upper bar) value of the data set. The standard deviation of "Normal occupancy with solar gain" is notably larger than for the two other measurements, indicating the spread of measurements were larger.

Normal plots on the air change efficiency measurements were constructed for the three different cases. The normal probability plots showed that they were normally distributed (Appendix C).

The values varying the most were from May 30, when the supply temperature was very unstable. Looking at the confidence intervals from the different cases (Figure 5.28), the air change efficiency from "Normal occupancy" was significantly smaller than for the other two measurements. As "Normal occupancy" had the lowest heat load, this indicate a lower ventilation efficiency with a lower heat load. This is logical, as displacement ventilation is driven by the buoyancy effect of warm objects. The extra heat increases the thermal differences, amplifying the overall buoyancy effect. However, as the difference of the mean values were low (about 2 %-units), and the ventilation functions as good displacement ventilation for all the Cases, the difference of air change efficiency has little practical significance.

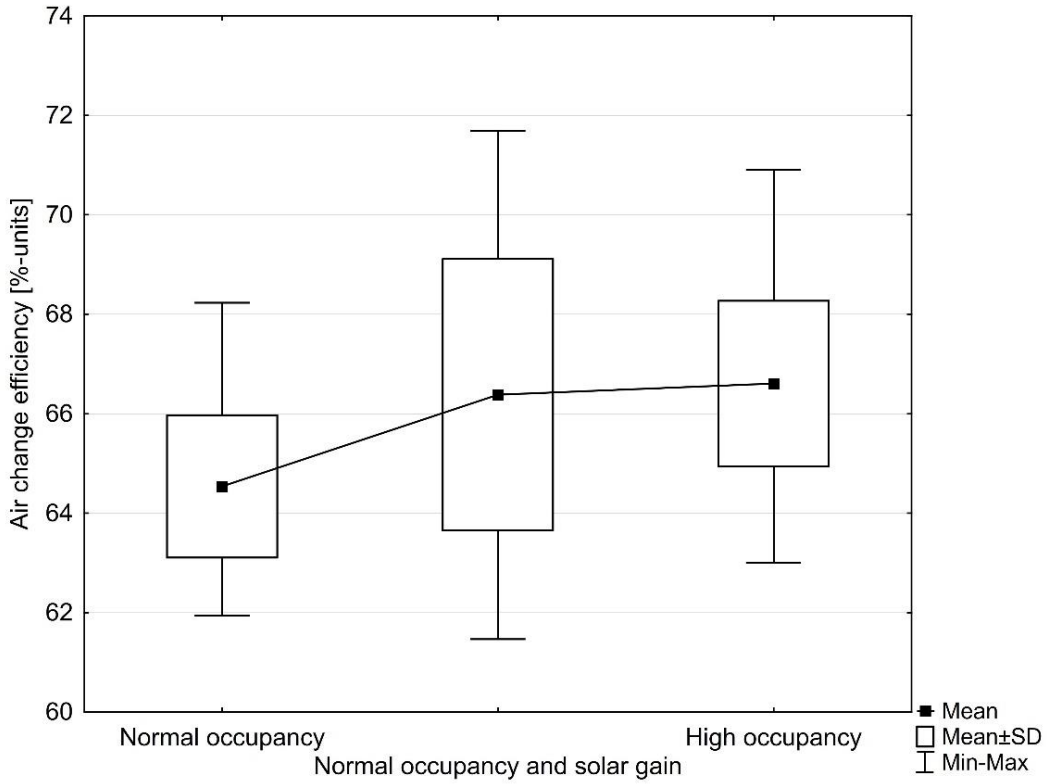

Figure 5.27 Box plot of air change efficiencies for the three different cases. N=30 for each box plot, 90 in total.

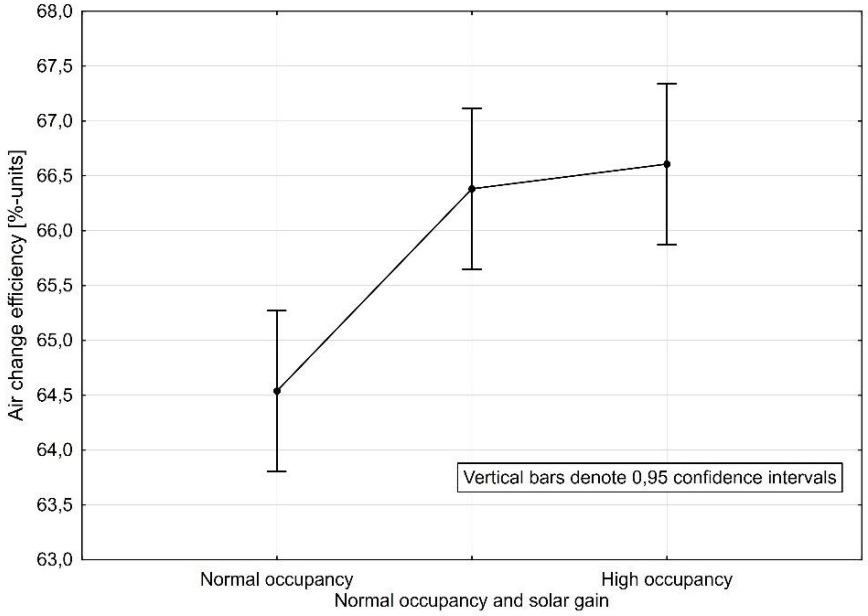

Figure 5.28 Mean air change efficiency for the different experimental cases. Vertical bars denote 95% confidence intervals.

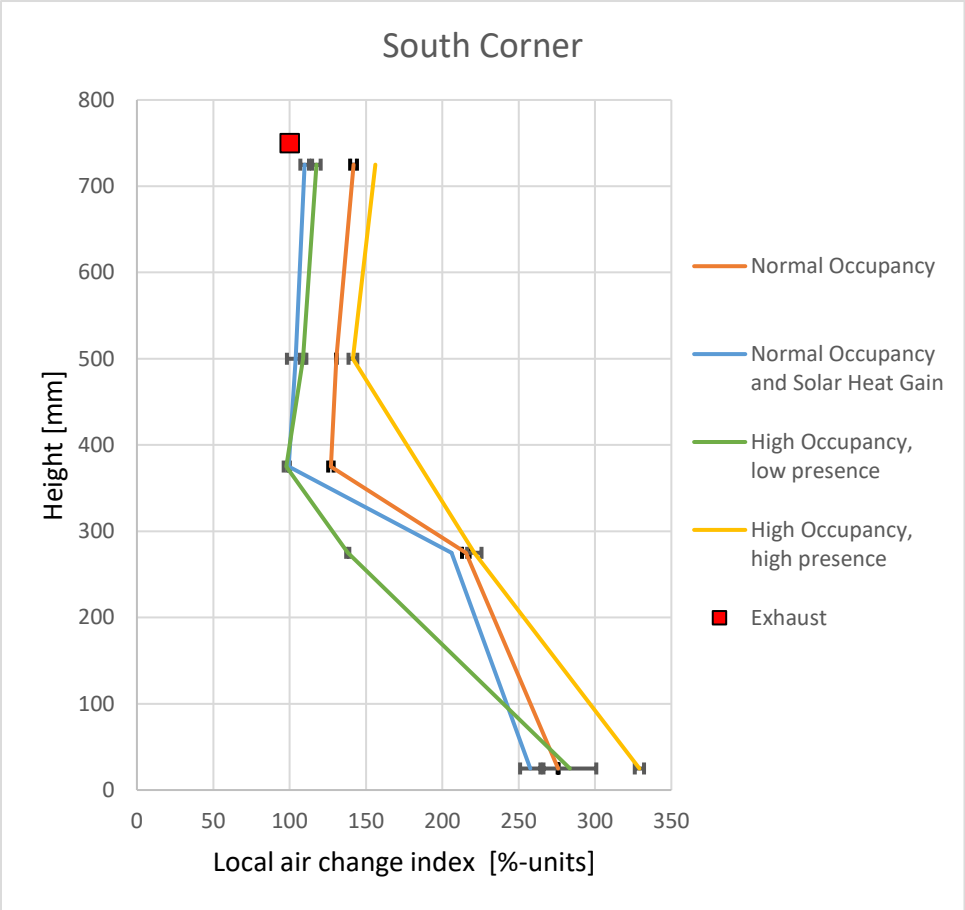

Figure 5.29 Local air change index in the south corner for different heat loads.

Figure 5.29 show the local air change index for the south corner. The local presence in the south corner was one person for all the experiments, except the second part of Case III (High occupancy, high presence), when to people were present. The local air change was highest when the local presence was high. As a larger local heat gain will heat more air, causing it to rise, the local air change will naturally be higher. However, when only one person was present in the south corner, the floor heating and temperature distribution in rest of the model seemed to affect the local air change index in the upper part here. As the temperatures in the ceiling were higher toward the east, it is possible that it hindered the slightly colder air from the south corner from moving toward the exhaust. The difference between the east and south corner ceiling temperatures were smallest with “Normal occupancy”, when no floor heating was used, and highest for “High occupancy”, when the local presence in the south corner was low. Nevertheless, the local air change in the south corner was very good. The higher mixing in the upper, contaminated zone is expected.

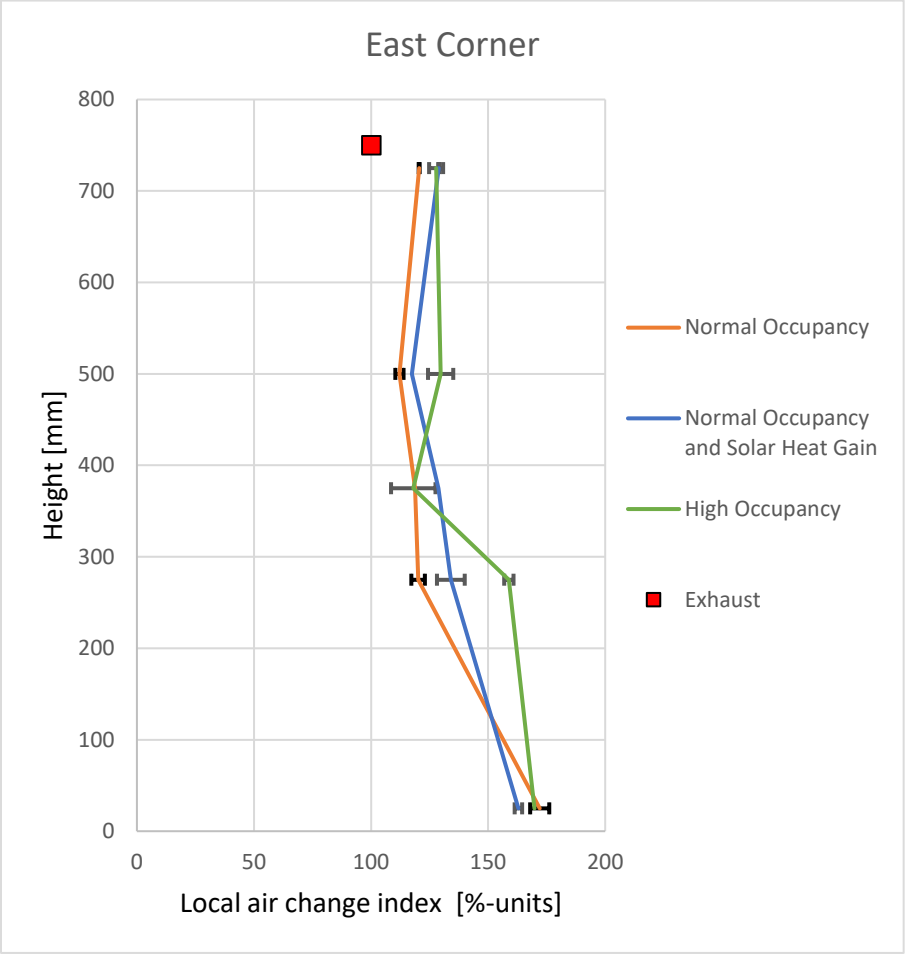

Figure 5.30 Local air change index in the east corner for different heat loads. All measurements with the normal bookshelf.

Figure 5.30 show the local air change index for the east corner at different heat loads. “Normal occupancy” and “Normal occupancy and solar gain” had a local presence of two people, while “High occupancy” had a local presence of four people. The local air change index was quite similar for the three different cases, though seem to be a bit higher with a higher presence. The measurements show working displacement for all the measurements in the east corner, though significantly lower than in the south corner. The measurements at 375mm height were located just above the bookshelf height, where air from other parts of the open office can cause additional mixing.

5.6 Results from Prototype

The prototype results were found by Sangnes (2016) and Alonso et al. (in preparation) in March 2016.

The supply air temperature in the prototype is quite high for displacement ventilation, as can be seen from Table 5.14. There is no measurement on the supply temperature from the south-east diffuser in the office landscape, but the supply temperature 37, located in the south part of the floor must travel approximately the same distance as the supply to the south-east diffuser. As the supply air travels from the main supply duct in uninsulated ducts in a warm ceiling, the longer the air has to travel, the warmer it will be. This can be seen by the supply temperatures in Table 5.14, where the supply temperatures have risen 0,3K on the shortest distances (location 38 and 39) and 0,8K on the longest distance (location 37). The location of the temperature measurements in the prototype can be seen in Appendix F. The exhaust temperature in the staircase between the second and third floor (location 35) is only 1,2K warmer than the supply temperature in the south diffuser (location 37). The supply temperature should be 2-3K colder than the ambient room temperature to get properly working displacement ventilation (see Chapter 2.2). However, from the measurements March 9 2016, the supply temperature (37) is only 0,6K lower than the room mean temperature. If the supply temperature is not cold enough, the air will not distribute itself properly along the floor. With a supply temperature that is only slightly colder than the ambient air, only a small amount of heat will cause it to rise to the ceiling, mixing with old air. As the distance from the south-east supply diffuser to the east corner is quite long, the air will have gained heat before it reaches the east corner. Before it reaches the east corner, it will be dragged toward the exhaust. Smoke tests conducted by Alonso et al. (in preparation) suggested this can be happening. If the air does not reach the east corner, surplus heat on warm days will not be removed. On cold days, there is a possibility that heat from the radiators will not reach the east corner, supplying required heat.

Table 5.14 Mean temperatures in prototype from 12:00 to 15:00. Measurements done March 9 2016 by Søgnen and Sangnes (2016)

Measurement point		**Mean temperature [C]**
Supply	Main supply	21,51
	37	22,32
	38	21,83
	39	21,84
Room average at 1,1m height	8, 11, 14, 31	22,93
Exhaust	35	23,53

As a stagnant zone, the contaminated air will not be removed, causing poor local air quality. The CO_2 concentration was measured in the prototype by Alonso et al. (in preparation). The

measurements suggest the east corner as a stagnant zone. The concentration is found to be constant in height, and higher than the exhaust concentration at all heights. For a displacement ventilated room, the CO_2 concentration is expected to be low at floor height (close to the supply concentration), and increase to exhaust concentration above the occupancy zone. The east corner has been suggested as a problem area due to the long distance to the closest supply diffuser and the confinement due to the bookshelves.

The prototype CO_2 concentration is generally quite low in the open office area. This suggest the ventilation flow rate is controlled by the temperature sensors, not the CO_2 sensors. Lowering the supply temperature can decrease the supply air flow rate required to keep the air quality and thermal environment good, consequently reducing the required fan power. In addition, a lower supply air temperature will enable the air to distribute itself along the floor, increasing the ventilation efficiency. The model experiment show the prototype building has the possibility of achieving good displacement ventilation, even in the east corner.

Tracer gas measurements were performed in the prototype by Sangnes (2016). The results for the air change efficiency and local air change index was tried calculated by Alonso et al. (in preparation), but found non-consistent with each other and the observations from the concentration decay curves. However, the decay curves suggest the overall ventilation efficiency is suboptimal, looking more like mixing ventilation than displacement ventilation.

5.6.1 Comparison of Model and Prototype Results

The model and prototype measurements show dissimilar results, most likely caused by the different supply temperatures. As the difference between the supply temperature and the ambient air temperature is crucial to get a functioning displacement ventilation system, a difference here can have a great impact on the air distribution in the model and prototype. The relative model supply temperature is colder than in the prototype, which can give better air efficiency than in the prototype. However, the model does not give wrong results, but rather show a situation with a lower supply temperature in the prototype.

The model air change efficiency show the ventilation functions as displacement ventilation. Results from the prototype indicate a ventilation efficiency closer to mixing ventilation. As the prototype supply temperature is too warm (only 0,6K lower than the ambient room temperature), there is a high probability that the air will overly heat before it reaches the east corner. The east corner is an area of interest, due to its confinement. CO_2 concentration measurements in the prototype show the east corner is a stagnant zone. Tracer gas experiments

in the model show the east corner has well-functioning displacement ventilation. However, there are some factors in the prototype that can cause further mixing, the model does not consider. People are moving about, mixing thermal stratified layers, and cold surfaces, such as cold supply ducts in the ceiling, can cause additional mixing of the upper layers. Objects located in the upper layer close to the ceiling, can also hinder the air moving toward the exhaust, causing further mixing.

Figure 5.31 show the model temperatures for Case I, scaled to prototype dimensions. All the temperature gradients are within the recommended maximum vertical temperature difference of 3K (Arbeidstilsynet, 2016). The narrow passage has the highest temperature gradient, 1,3K, well within the recommendations. Even for the largest temperature gradient measured (narrow passage for High occupancy case), the gradient is 1K lower than the maximum recommended value.

The model temperature results, scaled to prototype dimensions, show the east corner is up to 0,5K warmer than the south corner (assuming the south corner gradient will have a similar bend as the east corner and narrow passage gradients). However, the model east corner has functioning displacement ventilation, while prototype CO_2 concentration measurements show the east corner as a stagnant zone. As a stagnant zone there is a possibility that the thermal climate will be unsatisfactory. Too hot temperatures can occur if excess heat is not be removed during warm days, and if the required heat is not brought into the area in the heating season, the temperature may be too low.

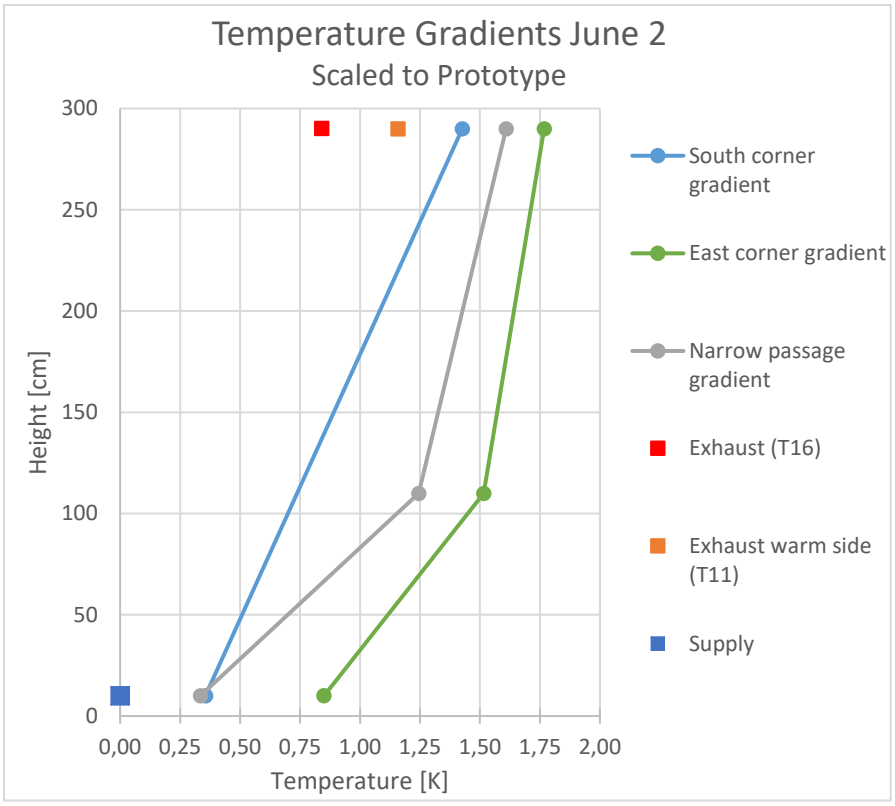

Figure 5.31 Temperature differences June 2 2017, scaled down to prototype.

5.7 Discussion

The results shown above, must be interpreted in light of limitations of the experimental setup.

The heat gain from the lighting and radiators has not been simulated. Only about half of the scaled heat gains are supplied to the model. As discussed in Chapter 4.5.2, the temperature differences in the model will vary from the calculated differences. The south part of the model has no heat gains, meaning the temperatures will be low. The exhaust temperature is lower than expected, as the warm temperature from the east part and the cold temperature from the south part mix. As the light armatures are installed in the ceiling of the prototype, the gained heat would have strengthened the thermal stratification, possibly amplifying the ventilation efficiency.

The heating load delivered to the model is controlled by two different Variacs and one dimmer. The actual delivered voltage has been measured for the different regulators, to better control the supplied heat. However, the voltage is controlled by manually rotating a disk, so the exact voltage delivered will differ some from the desired voltage. Consequently, the heat delivered to the model will differ some from the calculated heat required.

5.7.1 Temperature

The new cooling unit for the AHU was not able to deliver a cold stable supply temperature to the model. To maximize the cooling load, the cooling unit was set to cool the glycol in a storage tank during the night, while the cold night air cooled the air ducts connected to the model. The outside temperature changed from a rather cool night temperature, to a warm summer temperature in the day. As experiments was performed continuously for up to 12 hours, and the new cooling unit did not have sufficient capacity, the glycol was warmed until it had little or no cooling capacity. This lead to the AHU not being able to keep the supply temperature cold and stable. Some sudden rises and falls can be seen in the supply temperature for some of the experiments, and it is assumed the cooling is turned off and on by the control system.

The temperature differences in the model both increase and decrease during the experiments, suggesting it does not reached steady state. The change is thought mainly due to the unstable supply temperature. In addition, there is no control on the ambient air surrounding the model. The relative temperature difference between the ambient air surrounding the model and the temperature inside the model is therefore not the same for each experiment. A higher temperature difference between the inside and the outside of the model result in larger transmission heat losses through the envelope. This lead to relative cool surfaces in the model, which can increase the mixing of the old and new air in the model. The temperature differences in the model should be equal for the experiments with the same heat loads. However, they vary due to the varying supply and ambient room temperatures. As both physical objects and internal heat gains are changed for the experiments, a better control of the supply and ambient air temperatures will make the experimental results more comparable. It will be easier to see exactly how the changes impact the thermal climate and indoor environment.

As mentioned in Chapter 5.6, the supply temperature used as reference temperature in the prototype is the main supply temperature. The difference between the main supply temperature and the exhaust is 2K. However, as the supply temperature increase from the main supply duct to the supply diffuser, the temperature difference is only 1,2K. The model supply temperature is measured in the supply diffuser. Consequently, the model temperature difference should be 6K. However, the temperature increase of the supply temperature is not as large for the two supply diffusers located closer to the main supply duct. Assumed the south-east diffuser has the same supply temperature as the south diffuser, the temperature difference between the average supply temperature and the exhaust temperature is ΔT_P = 1,45K. This correspond to ΔT_M = 7,25K in the model if all the heat gains and thermal losses correspond. Ideally, the diffuser

supply temperatures in the model should reflect the different diffuser supply temperatures in the prototype.

The supply temperature (T4) on the experiments run June 8 (and other dates) was not stable. This caused unstable temperatures in the model. However, the unstable supply temperature showed that the floor temperature in the east corner was less affected by the change in supply air temperature, compared to the south corner and narrow passage floor temperatures. This suggest that less air enters the east corner, compared to other areas. This was also found from the smoke visualization in the east corner, which showed less smoke entered the east corner, compared to other areas. The tracer gas measurements show that the east corner has a lower air change than the south corner. However, it also shows the local air change index is good, consistent for displacement ventilation.

All the temperature results presented above were performed without the use of the cross-section diffusers. Temperature measurements with the use of the cross-section diffusers were performed for Normal occupancy. The measurements are not presented in the results above, but can be found in Appendix B1. The cross-section diffuser air simulates old air, and should have the same temperature as the exhaust air. Poor control on the cross-section air temperature lead to too hot air supplied. At 7,5K difference from the supply air, it suggests that the "not built half" of the building has no heat loss through the building envelope. Calculation on the measured temperatures show that the heat loss in the model is approximately 400W for these conditions. Comparing the temperature results from when using and when not using the cross-section diffusers, the temperature in the south-east part of the office landscape is not visibly affected. Consequently, it is assumed that experiments run without the cross-section diffusers will have similar air movements in this area. As the south-east open office landscape is the area of interest for the model experiments and the measurements made with the use of the cross-section diffusers presented no new or better results in this area, only the results from when not using the cross-section diffusers are presented in the results.

5.7.2 Tracer Gas

The tracer gas equipment has the possibility to measure six points at one time. Two of these were needed for the exhaust and supply concentrations, leaving four measurement points in the model. One measurement set consist of measuring the concentration in these four points in the model, and in the exhaust and supply air, as mentioned in Chapter 4.4.2. However, as the time move more than 4 times as fast in the model (S_t = 0,22) compared to in the prototype, the air

change in the model is very fast. To get as many tracer gas concentration measurements as possible, the measurement sets were divided in four. In other words, only one point in the model (three in total with supply and exhaust concentration) was measured per step-up and step-down measurement. As each measurement took about one hour to complete, measuring up to sixteen points for each case took a long time. Usually, eight measurements (two locations) were completed consecutively in one day. As the supply air temperature and ambient air temperature changed during the day, and from day to day, the conditions for each measurement was not equal. Ideally the boundary conditions for the model experiments should have been identical.

Some of the tracer gas measurements get very few measurements per step-up and step-down concentration curve, when there is a high local air change. In addition, the tracer gas concentration sinks to a low ppm very fast, increasing the risk of measurement error. This is generally for the South 25 measurement, though happens to most of the measurements to some degree. It is not ideal to measure the tracer gas concentration with the available equipment at such high air changes per hour. Due to the fast air change, the calculations for the local age of air and air change index vary from the step-up and step-down measurement. However, even though the exact value for the local air change index may be wrong, it is still known that it is very high.

The desired tracer gas concentration is 25ppm N_2O. The supply flow of tracer gas is manually controlled, meaning the concentration is not equal from experiment to experiment. The plots showing the exhaust and room concentration have been multiplied by a constant, to see if they look similar from experiment to experiment. For the step-up measurements, the exhaust and local room concentrations increase to the supply concentration. This suggest that there is little or no air leakage from the model, confirming that the taping of the openings has worked to tighten the model.

Some of the tracer gas logarithmic plots curve slightly. They should be completely straight. This curving suggests the supply air volume flow is not completely stable, or that there is a signal disturbance in the equipment. As the air volume from the AHU have been observed changing a small amount previously, this is thought to be the main reason for the curving. This can also be observed by the nominal time constant for the different experiments. As the air change rate of a room is the inverse of the nominal time constant, at steady state, with the exact same volume flow, it should be equal for each measurement. However, it varies for each measurement. A change in the supply air volume will impact the air efficiency and local air change index. However, the curving is generally minimal, and the results for all the

measurements mostly have similar values. Even though the results may not have the exact correct value, they still are valid and say something about the general ventilation effectiveness of the model.

The cross-section diffusers are not used for any of the tracer gas measurements. As mentioned previously, it will give the wrong results for the step-up and step-down decay curves. The air from the cross-section diffuser is not thought to influence the air flow pattern in the south-east part of the open office landscape. The distance between these two areas are quite large, and the path toward the exhaust (the narrow passage) is located between them. The air is thought to move from the cross-section diffuser through the narrow passage and to the exhaust. The results for the tracer gas measurements are thought to be valid for the open office landscape modelled. However, the exhaust concentration will be influenced by the lack of half the floor. If there is a stagnant zone in the not built part, or if the air change is better than in the built part, both the nominal time constant and the mean age of air will be affected. It is assumed that the not built part of the model will have the same air change efficiency as the built part.

As the AHU was unable to keep a stable supply temperature for most of the experiments, the temperatures in the model varied for all of them. This variation can cause different air flow patterns in the model, affecting the air change efficiency. The standard deviation of the measured temperatures show the temperatures are relatively stable for parts of the measurements. However, as the tracer gas measurements ran for a long time, the temperatures during these measurements varied quite a lot. Still, the air change efficiencies measured during each step-up and step-down measurement set (32 in total per experimental case) varied relatively little.

To many simplifications in the model compared to the prototype building will prevent the experimental results from being transferable to the prototype building. CFD modelling may be a better method for calculating the ventilation efficiency and thermal climate in the prototype. CFD simulations can more easily take into account varying boundary conditions. However, creating a CFD model for a large complex building also requires simplifications, and the simulations can give unstable results. The scaled model used for the experiments in this thesis is not thought to give results that are completely transferrable to the prototype. The experimental measurements from the model does not correspond to the available prototype measurements. This means that the model cannot be validated against the prototype. However, the results achieved are thought to show results for a very similar, smaller building, which can be compared to the prototype.

The ventilation system seems to be functioning well for the scaled model, indicating the prototype can achieve good displacement ventilation. The ventilation system chosen, with few supply diffusers for a large office landscape can function well for a zero emission building. However, as for other buildings with displacement ventilation, supplying air at a relatively low temperature, and placing the furniture so that it does not hinder the air flow is important. As displacement ventilation requires a lower air supply, using a lower amount of power for the fans (SFP), it is ideal for ZEB.

Chapter 6 Conclusion

Reduced scaled model experiments can give valuable insight into the air movements of the full-scale prototype, if conducted properly. To better the similarity of the model and prototype, improvements have been made in the model. Experiments measuring the diffuser air velocity, temperature and ventilation efficiency have been performed in the model. The results have been compared to the prototype.

Some simplifications have been made when modelling the prototype. The most significant that half of the 2nd floor has not been built, but is simulated as air supplied through two large cross-section diffusers. The cross-section diffusers have not been used, as they cannot be used when performing tracer gas experiments. In addition, all the internal heat gains are not simulated and the heat transfer through the building envelope vary from experiment to experiment. Due to these simplifications, the results cannot be directly transferred to the prototype. The model has not been validated to the prototype, thus the validity of the model cannot be certain. However, the results are deemed similar enough, and it is thought that the air movements in the open office landscape in the model show results for a smaller building similar to the prototype.

The diffuser air velocity mapping show the supply patterns for the model and prototype differs. The model air is supplied at relatively cold temperatures, creating the negative buoyant effect of the air. This can be seen from the velocity mapping. The air supplied by the prototype diffuser does not have this effect, suggesting the supplied air temperature is too high. Temperature measurements from the prototype show the supply air increases by 0,8K from the main supply duct to a supply diffuser similar to the one used for velocity mapping. The air supplied here is only 0,6K colder than the ambient room temperature.

Smoke visualization experiments show the air distribution in the model is unstable. The supplied air does not always travel the same path. Small changes in the boundary conditions can impact the air distribution pattern in the model. However, tracer gas experiments show the ventilation efficiency is as expected for displacement ventilation. The air change efficiency is higher than 64 %-units for the three different experimental cases. The local air change index indicates the south and east corner has good displacement ventilation. The local air change in the east corner is nevertheless lower than in the south corner. The lowest east corner local air change index at 25mm was above 160 %-units.

The model results show the prototype has the possibility of achieving good displacement ventilation, even in the east corner. The largest difference between the model and prototype is

identified to be the supply temperature. CO_2 concentration measurements at Powerhouse Kjørbo indicate the ventilation air flow is controlled by the temperature sensors. Decreasing the supply temperature at Powerhouse Kjørbo can both increase the ventilation efficiency and decrease the required supply air volume, thus reducing the fan power needed. To find whether the ventilation can improve at Powerhouse Kjørbo, while still maintaining a satisfactory thermal environment, measurements should be conducted for a lower set point temperature in the AHU.

6.1 Recommendations for Further Work

Further measurements should be performed in the prototype, checking the supply air temperatures in the diffusers, to see if the air has been excessively heated in the ducts in the ceiling. In addition, a new velocity mapping should be performed on the supply diffuser, to validate the current results. If the supply temperature is decreased in the prototype, a new velocity mapping should be performed to see how the air behaves. As only one supply diffuser has been mapped, there is no control on how the air from the other VAV diffusers in the open office area behave. The diffusers which were not the focus of this thesis, should also be mapped, to see whether the air behave according with displacement ventilation theory. The ventilation efficiency and local air change index in the east corner should be measured at Kjørbo for a lower supply temperature, to see if the ventilation efficiency can be improved, while still keeping an acceptable thermal environment.

To get a better understanding of the air movements in the model, some further experiments and improvements are recommended performed. Below some suggestions for further work in the model is stated:

- Rise the thermal cylinders, to allow air moving underneath.
- Include heat in model to simulate light and radiators.
- Gain better control of the ambient room temperature outside the model. This is to gain control on the transmission heat transfer in the model.
- Perform experiments in the east corner, changing the furnishing. The local air change index with different local presences should be measured. The bookshelves can be raised above the floor or removed completely.
- See if the ventilation efficiency increase with an additional exhaust in the ceiling of either in the south or east corner.
- Add personal ventilation in the east corner.

Chapter 7 References

ALONSO, M. J., MATHISEN, H. M. & COLLINS, R. Ventilative cooling as a solution for highly insulated buildings in cold climate. Energy Procedia, 2015. 3013-3018.

ALONSO, M. J., MATHISEN, H. M., SØGNEN, O. B. & LIU, P. in preparation. Lessons learned about Powerhouse-Kjørbo Block 4.

ARBEIDSTILSYNET 2016. *Veiledning om klima og luftkvalitet på arbeidsplassen,* Oslo, Arbeidstilsynet.

AWBI, H. B. 2003. *Ventilation of buildings,* London ;, Spon Press.

BRE, B. R. E. 2016. *Why BREEM* [Online]. Available: http://www.breeam.com/why-breeam [Accessed 8th November 2016].

CABLE, A., MYSEN, M. & THUNSHELLE, K. 2014. Can demand controlled ventilation replace space heating in office buildings with low heating demand. *Proceedings of Indoor Air,* 3**,** 434-441.

CAUSONE, F., BALDIN, F., OLESEN, B. W. & CORGNATI, S. P. 2010. Floor heating and cooling combined with displacement ventilation: Possibilities and limitations. *Energy and Buildings,* 42**,** 2338-2352.

COMMTECH GROUP, T. 2003. *Achieving the desired indoor climate : energy efficiency aspects of system design,* Lund, Studentlitteratur.

ETHERIDGE, D. & SANDBERG, M. 1996. *Building ventilation : theory and measurement,* Chichester, Wiley.

FME ZEB, T. R. C. O. Z. E. B. 2016. *ZEB Definitions* [Online]. Available: http://www.zeb.no/index.php/en/about-zeb/zeb-definitions [Accessed 8th November 2016].

FORN, O. 2008. *Ventilasjon av klasserom.* Master Master Thesis, NTNU.

GEORGES, L. 2017. *RE: Effect of emissivity and heat transfer.* Type to TRYDAL, H. J.

HERMAN, I. P. 2016. *Physics of the human body*, Springer.

HOSNI, M. H., JONES, B. W. & XU, H. 1999. Experimental results for heat gain and radiant/convective split from equipment in buildings. *ASHRAE Transactions,* 105**,** 527.

INGEBRIGTSEN, S., STENSAAS, L. I. & STÄHLI, M. B. 2015. *Ventilasjonsteknikk : Del 1,* Oslo, Skarland press.

MATHISEN, H. M. 10 november 2016. *RE: Personal communication: Power use of a laptop and an extra screen.* Type to TRYDAL, H. J.

MATHISEN, H. M. 2017. *RE: Personal communication: Displacement ventilation efficiency.* Type to TRYDAL, H. J.

MIDTBUST, H.-M. 2014. *Simulation of indoor climate in ZEB in relation to heating and cooling system.* Master Master Thesis, NTNU.

MUNDT, E., MATHISEN, H. M., NIELSEN, P. V. & MOSER, A. 2004. *Ventilation effectiveness,* Brussels, Rehva.

NGBC, N. G. B. C. 2016. *Hva er BREEM?* [Online]. Available: http://ngbc.no/breeam-nor/ [Accessed 8th Novemner 2016].

NIELSEN, P. V. 1993. *Displacement Ventilation*, Dept. of Building Technology and Structural Engineering, Aalborg University.

NOVOSELAC, A. & SREBRIC, J. 2002. A critical review on the performance and design of combined cooled ceiling and displacement ventilation systems. *Energy and Buildings,* 34**,** 497-509.

POWERHOUSE. 2016a. *Om Powerhouse* [Online]. Available: http://www.powerhouse.no/om/ [Accessed 8th November 2016].

POWERHOUSE. 2016b. *The Powerhouse definition* [Online]. Available: http://www.powerhouse.no/content/uploads/2014/02/2016.06.14_Powerhouse-definition_til-publisering.pdf [Accessed 8th November 2016].

POWERHOUSE. 2016c. *Powerhouse Kjørbo - Trinn 1* [Online]. Available: http://www.powerhouse.no/prosjekter/kjorbo/ [Accessed 8th November 2016].

PRICE INDUSTRIES 2016. Engineering Guide Displacement Ventilation. Price Industries Limited.

RÅDSTOGA, O. 2014. Ventilasjonsaggregat 360.405 - ventilasjon blokk 4 kontorarealer. (Projectplace).
SANGNES, M. O. 2016. *Analysis of Ventilation Strategies for ZEB.* Master Master thesis, NTNU.
SEPPÄNEN, O., FISK, W. J. & LEI, Q. H. Room temperature and productivity in office work. HB 2006 - Healthy Buildings: Creating a Healthy Indoor Environment for People, Proceedings, 2006. 243-247.
SINTEF & NTNU, N. T.-N. U. 2007. *ENØK i bygninger : effektiv energibruk,* Oslo, Gyldendal undervisning.
SKISTAD, H. E., MUNDT, E., NIELSEN, P. V., HAGSTRÖM, K. & RAILIO, J. 2004. *Displacement ventilation in non-industrial premises,* Brussels, REHVA SINTEF energiforskning distributør.
STANDARD NORGE 2006. Ergonomi i termisk miljø: analytisk bestemmelse og tolkning av termisk velbefinnende ved kalkulering av PMV- og PPD-indeks og lokal termisk komfort (ISO 7730:2005). 3. utg. ed. Lysaker: Standard Norge.
STANDARD NORGE 2012. NS 3701:2012, Kriterier for passivhus og lavenergibygninger Yrkesbygninger.
STATENS BYGNINGSTEKNISKE ETAT 2012. Veiledning til forskrift om tekniske krav til byggverk (TEK10:2012). *Veiledning til forskrift om tekniske krav til byggverk (byggteknisk forskrift).* Oslo: Norsk byggtjenestes forlag.
STATENS BYGNINGSTEKNISKE ETAT 2016. Veiledning til forskrift om tekniske krav til byggverk (TEK10:2016). *Veiledning til forskrift om tekniske krav til byggverk (byggteknisk forskrift).* Oslo: Norsk byggtjenestes forlag.
SØGNEN, O. B. 2015a. *Indoor climate at Powerhouse Kjørbo.* Project Thesis, NTNU.
SØGNEN, O. B. 2015b. *Indoor climate in a zero energy building. An analysis of the thermal environment and indoor air quality.* Master Master Thesis, NTNU.
SØGNEN, O. B. & SANGNES, M. O. 2016. iButton temperature measurements at Powerhouse Kjørbo, January 11 to March 10.

Tracer gas experiments March 9 and 10.
TAHTI, E. & GOODFELLOW, H. D. 2001. *Industrial Ventilation Design Guidebook,* Burlington, Elsevier Science.
THERMOCOUPLE INFO. 2016. *Type T thermocouple* [Online]. Available: http://www.thermocoupleinfo.com/type-t-thermocouple.htm [Accessed 9 December 2016].
THERMOWORKS. 2017. *Emissivity Table* [Online]. Available: http://www.thermoworks.com/learning/emissivity_table [Accessed March 2017].
THOMSEN, J. & BERGE, M. 2012. Inneklima i energieffektive boliger-en litteraturstudie.
THYHOLT, M. 2014. BREEAM NOR: Ene 1 - Energieffektivitet (Projectplace).
TRYDAL, H. J. 2016. *Displacement ventilation in Zero Emission Office Buildings (ZEB)* Project Project Thesis, NTNU.
WARGOCKI, P., WYON, D. P., BAIK, Y. K., CLAUSEN, G. & FANGER, P. O. 1999. Perceived air quality, sick building syndrome (SBS) symptoms and productivity in an office with two different pollution loads. *Indoor air,* 9**,** 165-179.
WARGOCKI, P., WYON, D. P., SUNDELL, J., CLAUSEN, G. & FANGER, P. 2000. The effects of outdoor air supply rate in an office on perceived air quality, sick building syndrome (SBS) symptoms and productivity. *Indoor air,* 10**,** 222-236.
WING, R. D. 2008. Smart energy houses of the future - Self- Supporting in energy and zero emission. *Future Energy.*
YUAN, X., CHEN, Q. & GLICKSMAN, L. R. 1998. A critical review of displacement ventilation. *ASHRAE transactions,* 104**,** 78.
ZOHURI, B. 2015. *Dimensional Analysis and Self-Similarity Methods for Engineers and Scientists,* Cham, Springer International Publishing.
ZUKOWSKA, D., MELIKOV, A. & POPIOLEK, Z. 2012. Impact of geometry of a sedentary occupant simulator on the generated thermal plume: Experimental investigation. *HVAC and R Research,* 18**,** 795-811.

Appendix

Appendix A. Air Velocity Mapping

A1. Model

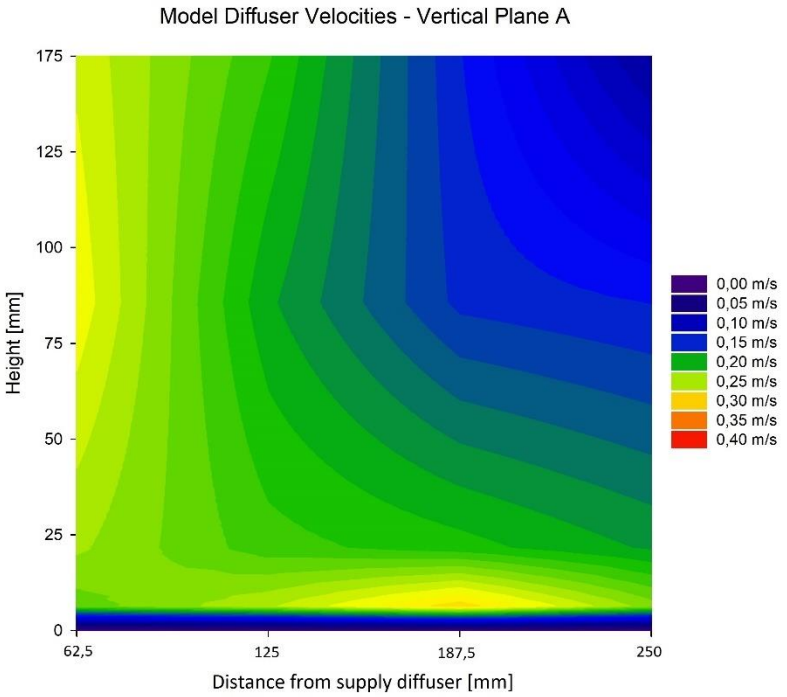

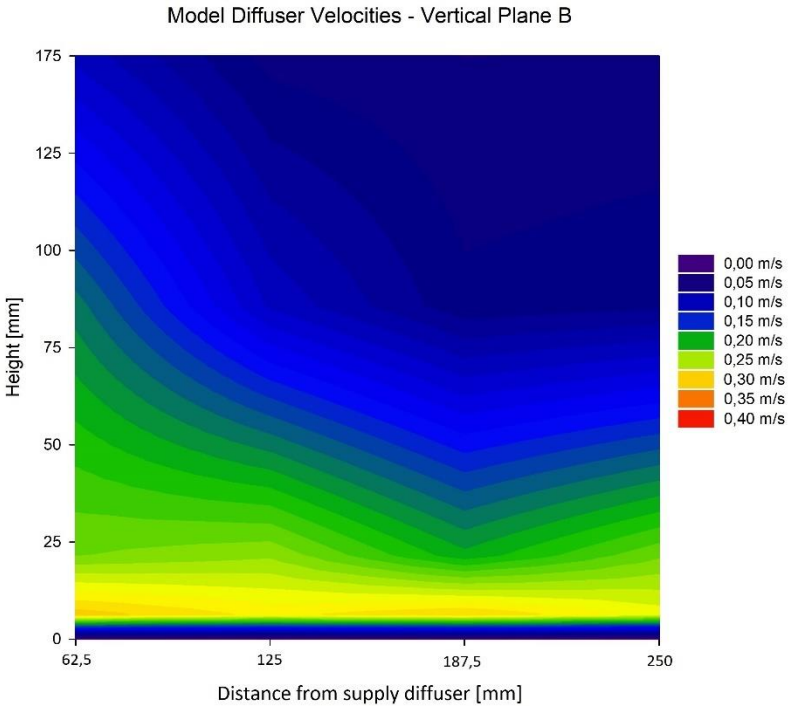

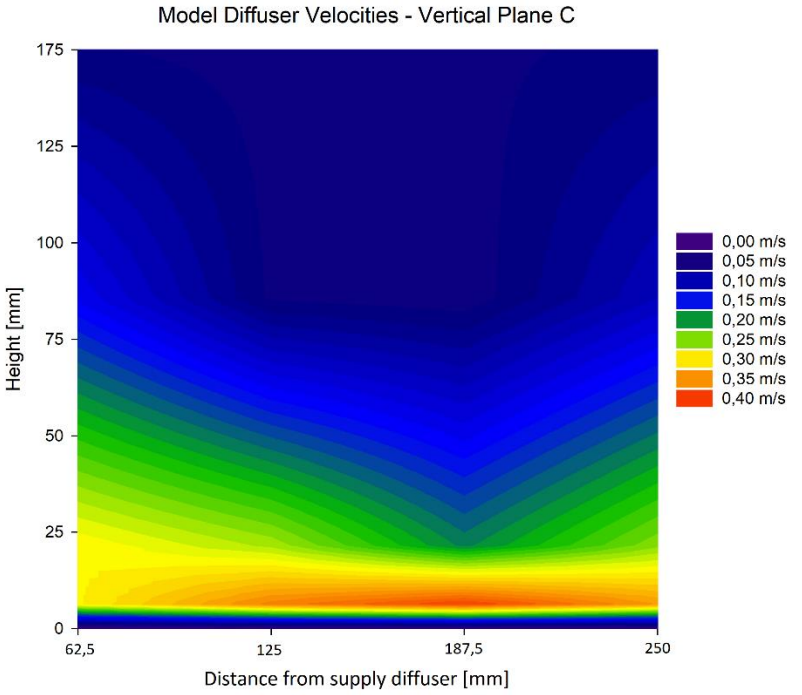
Model Diffuser Velocities - Vertical Plane C
175
125
100
75
50
25
0
Height [mm]
62,5
125
187,5
250
Distance from supply diffuser [mm]
0,00 m/s
0,05 m/s
0,10 m/s
0,15 m/s
0,20 m/s
0,25 m/s
0,30 m/s
0,35 m/s
0,40 m/s

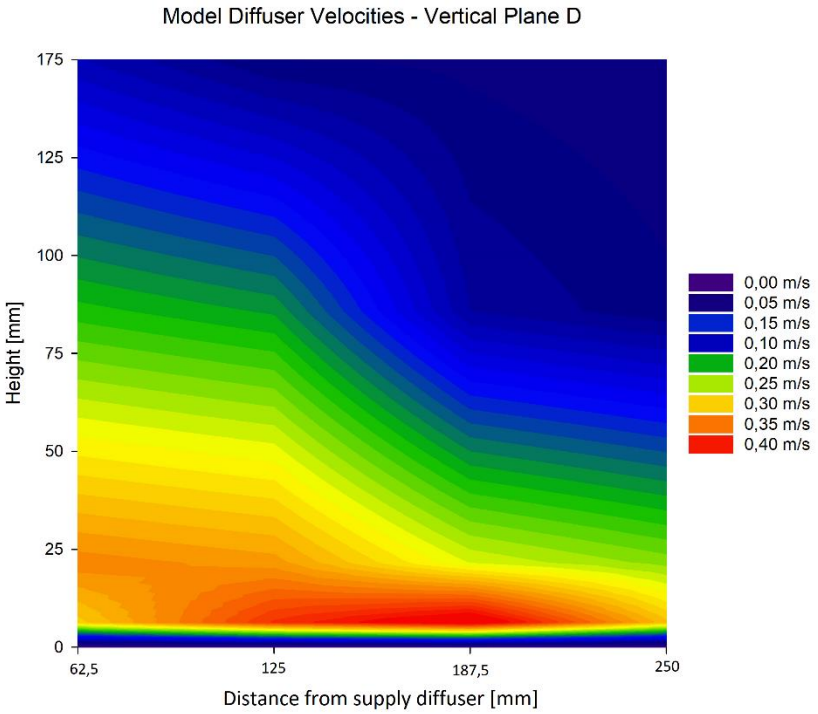
Model Diffuser Velocities - Vertical Plane D
175
125
100
75
50
25
0
Height [mm]
62,5
125
187,5
250
Distance from supply diffuser [mm]
0,00 m/s
0,05 m/s
0,15 m/s
0,10 m/s
0,20 m/s
0,25 m/s
0,30 m/s
0,35 m/s
0,40 m/s

Model Diffuser Velocities - Vertical Plane E

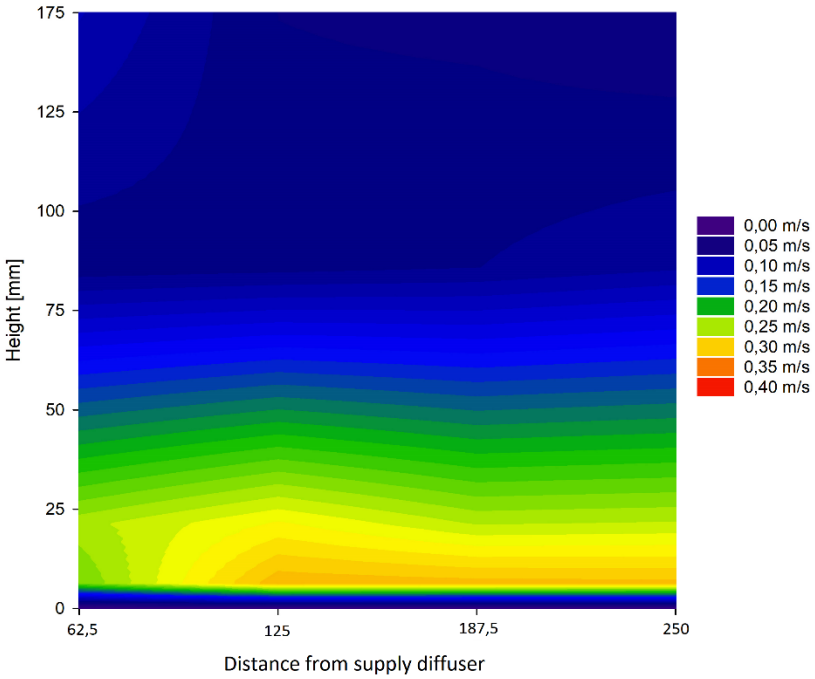

Model Diffuser Velocities - Vertical Plane F

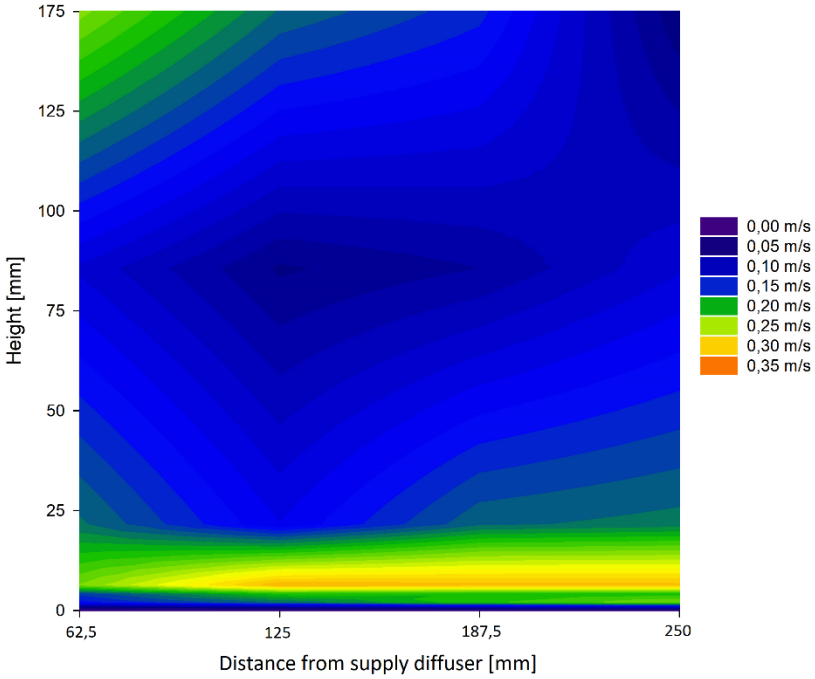

A2. Prototype

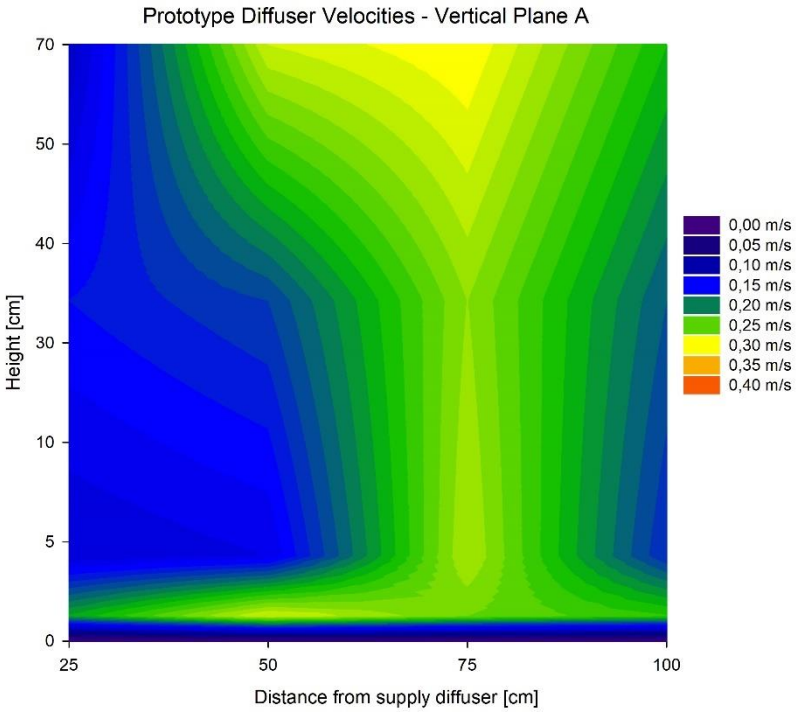

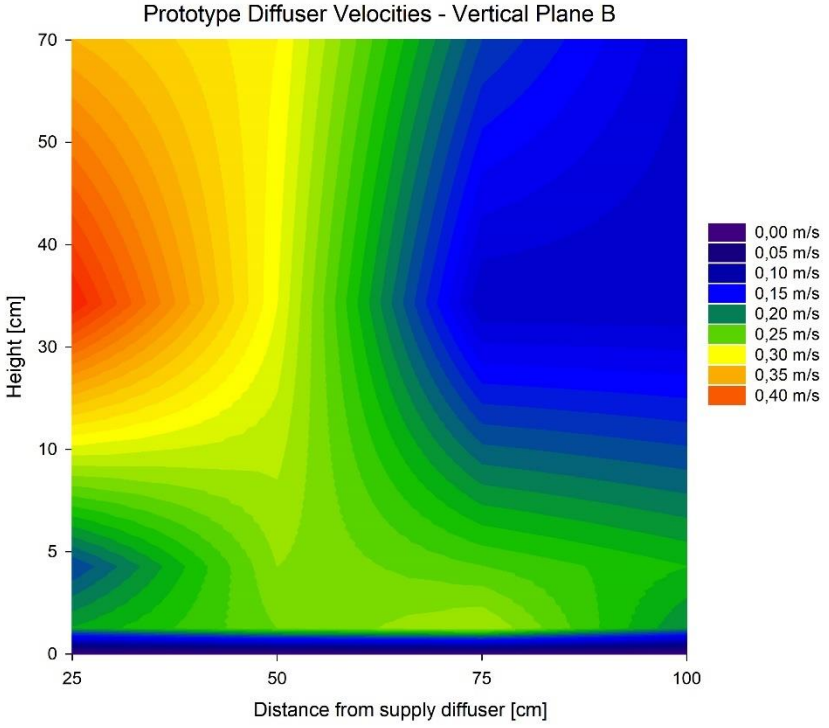

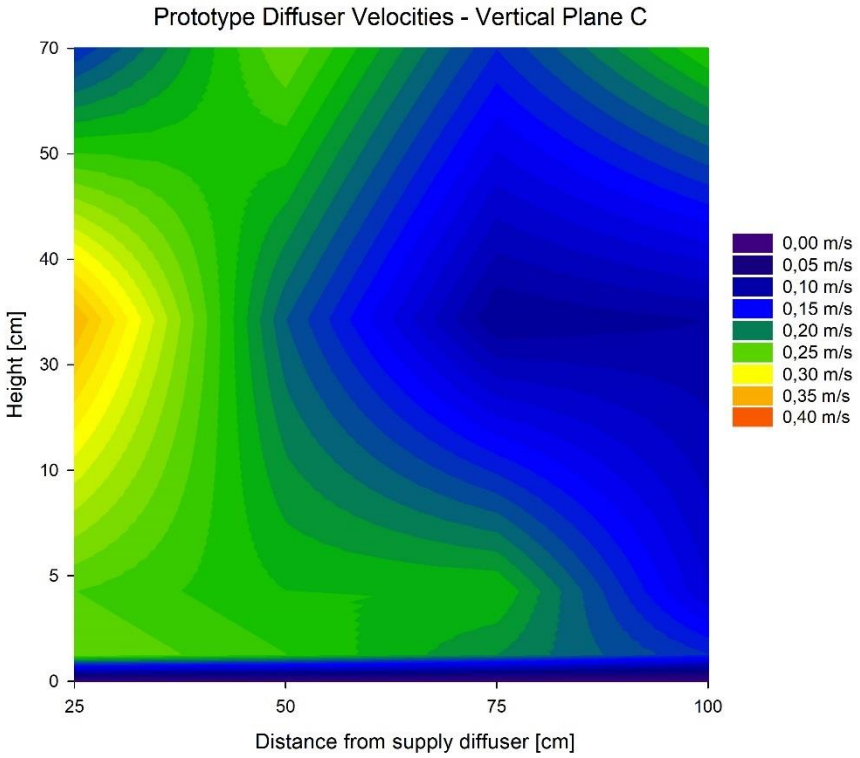
Prototype Diffuser Velocities - Vertical Plane C
Height [cm]
70
50
40
30
10
5
0
25
50
75
100
Distance from supply diffuser [cm]
0,00 m/s
0,05 m/s
0,10 m/s
0,15 m/s
0,20 m/s
0,25 m/s
0,30 m/s
0,35 m/s
0,40 m/s

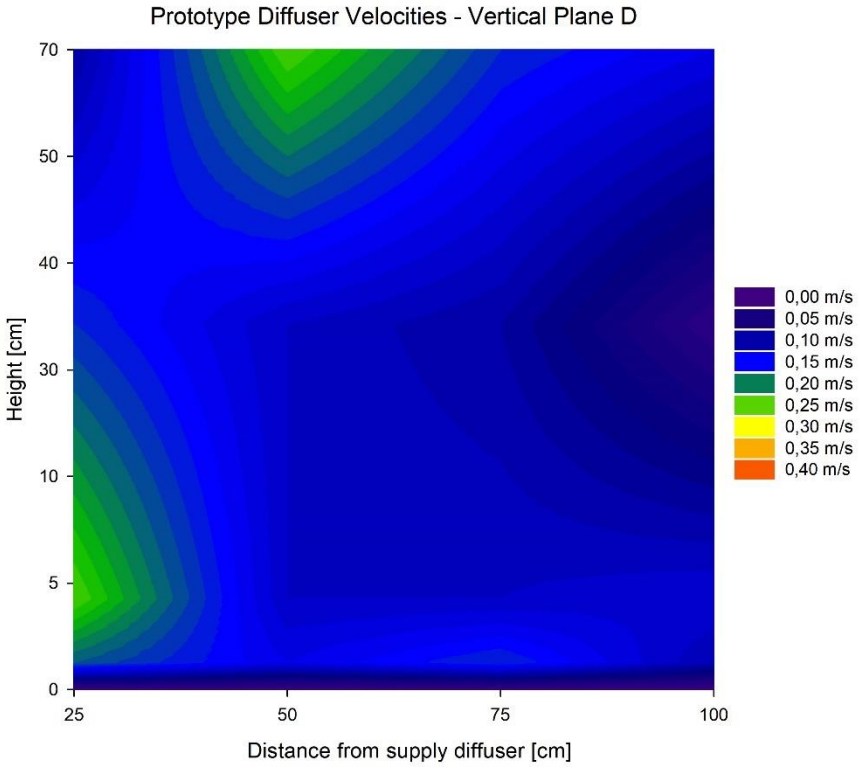
Prototype Diffuser Velocities - Vertical Plane D
Height [cm]
70
50
40
30
10
5
0
25
50
75
100
Distance from supply diffuser [cm]
0,00 m/s
0,05 m/s
0,10 m/s
0,15 m/s
0,20 m/s
0,25 m/s
0,30 m/s
0,35 m/s
0,40 m/s

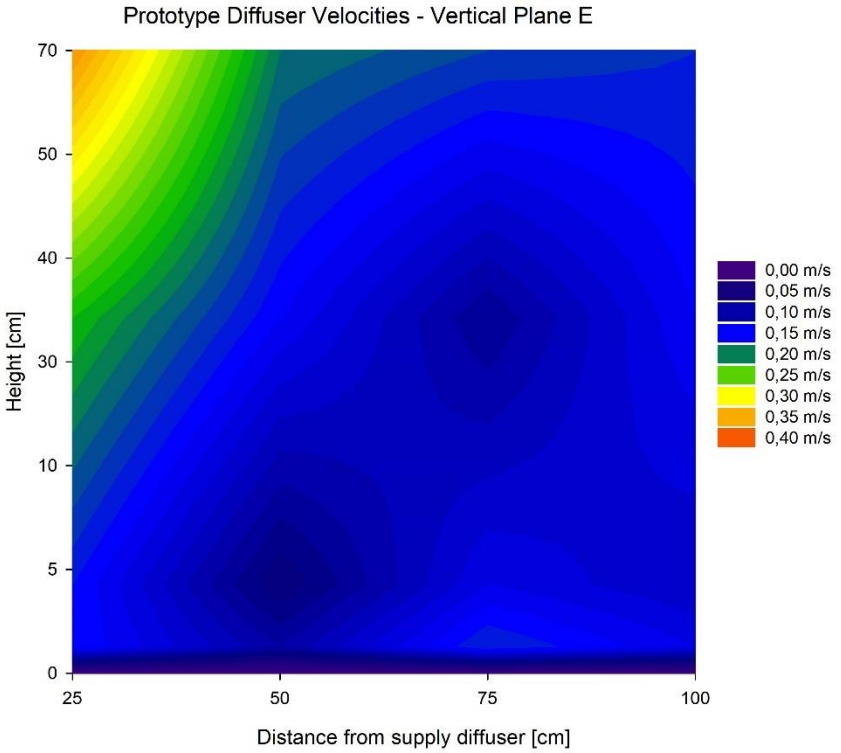
Prototype Diffuser Velocities - Vertical Plane E
Height [cm]
70
50
40
30
10
5
0
25
50
75
100
Distance from supply diffuser [cm]
0,00 m/s
0,05 m/s
0,10 m/s
0,15 m/s
0,20 m/s
0,25 m/s
0,30 m/s
0,35 m/s
0,40 m/s

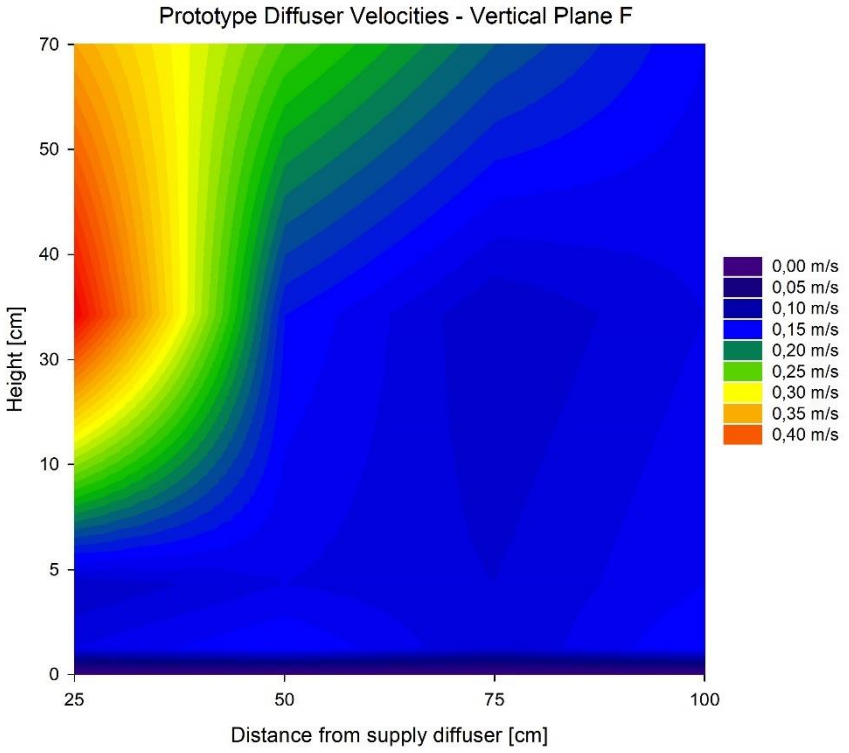
Prototype Diffuser Velocities - Vertical Plane F
Height [cm]
70
50
40
30
10
5
0
25
50
75
100
Distance from supply diffuser [cm]
0,00 m/s
0,05 m/s
0,10 m/s
0,15 m/s
0,20 m/s
0,25 m/s
0,30 m/s
0,35 m/s
0,40 m/s

Appendix B. Temperature Measurements

B1. Case I – Normal Occupancy

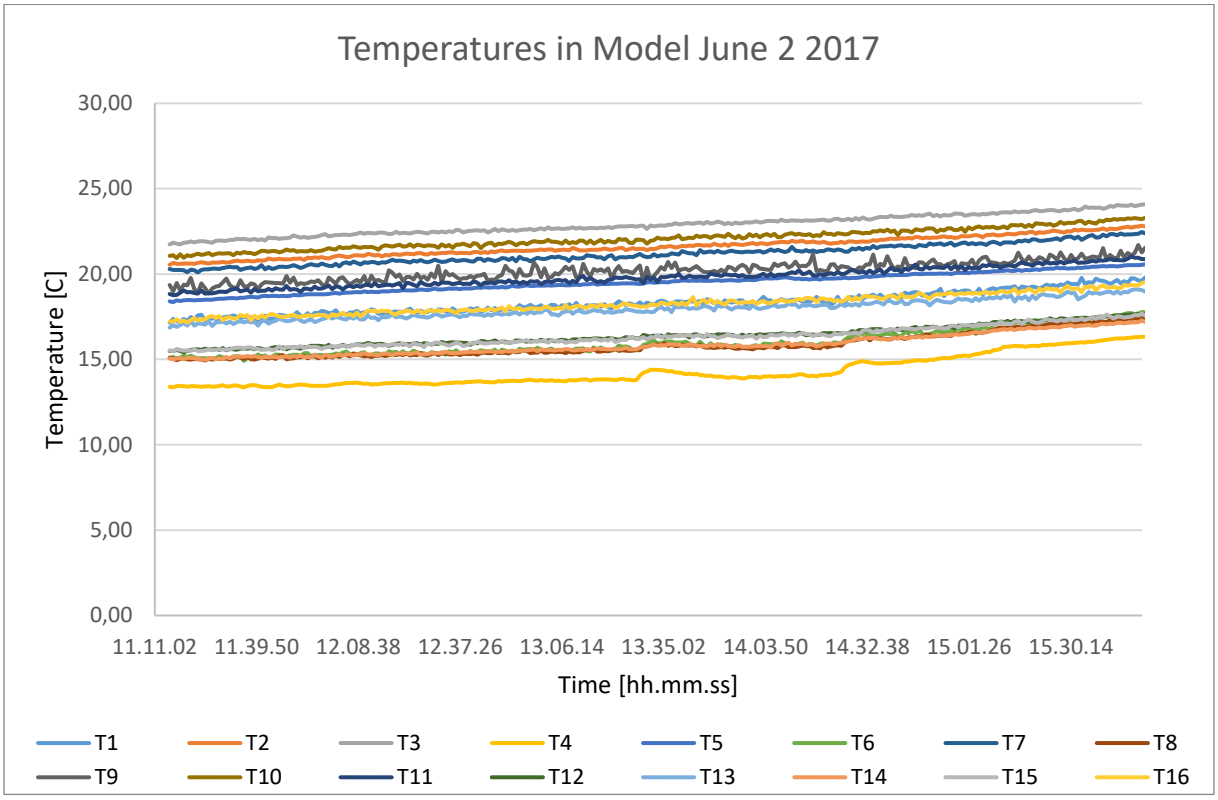

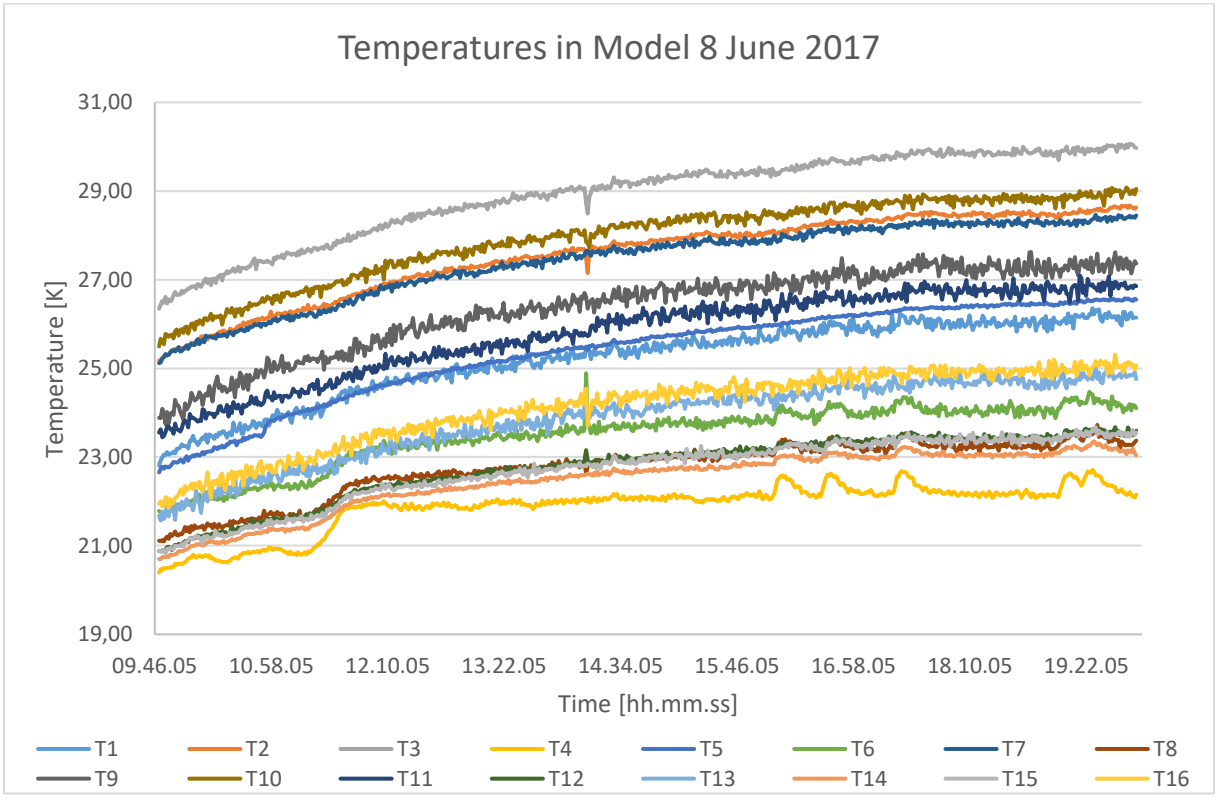

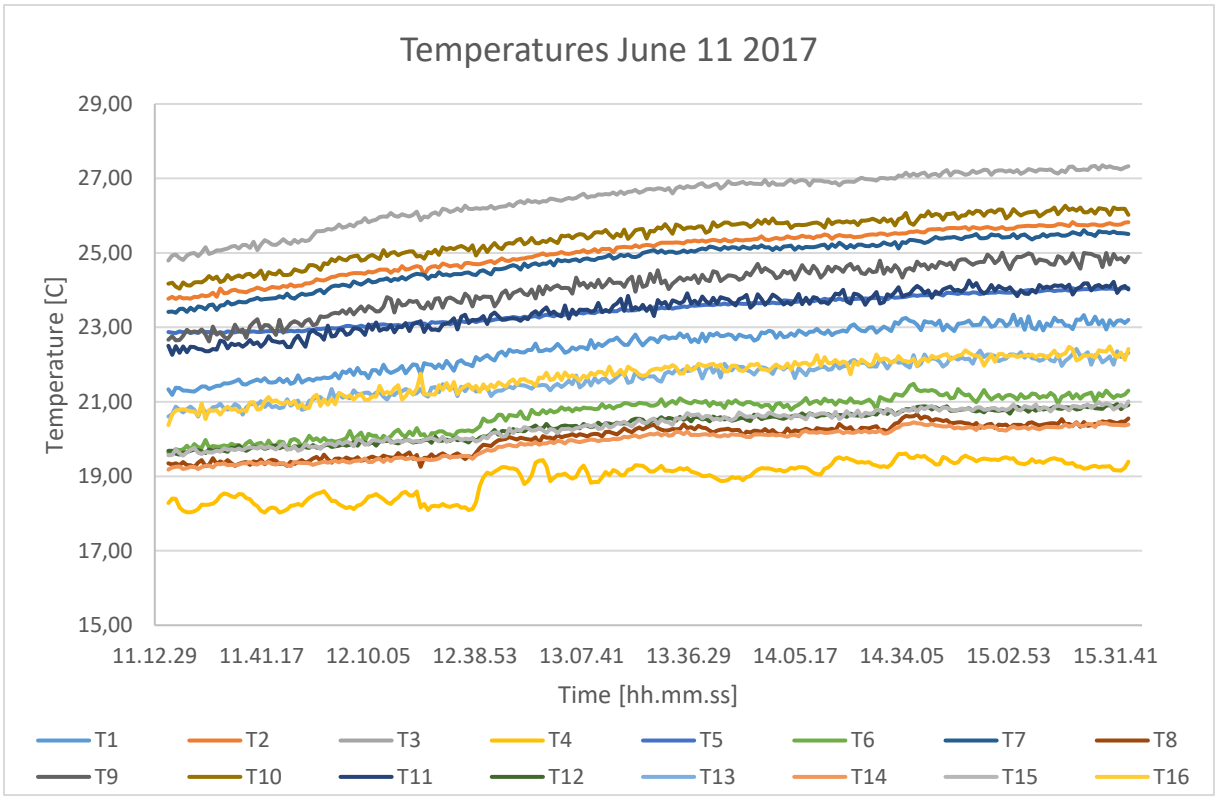
Temperatures June 11 2017
29,00
27,00
25,00
23,00
21,00
19,00
17,00
15,00
Temperature [C]
11.12.29
11.41.17
12.10.05
12.38.53
13.07.41
13.36.29
14.05.17
14.34.05
15.02.53
15.31.41
Time [hh.mm.ss]
T1
T2
T3
T4
T5
T6
T7
T8
T9
T10
T11
T12
T13
T14
T15
T16

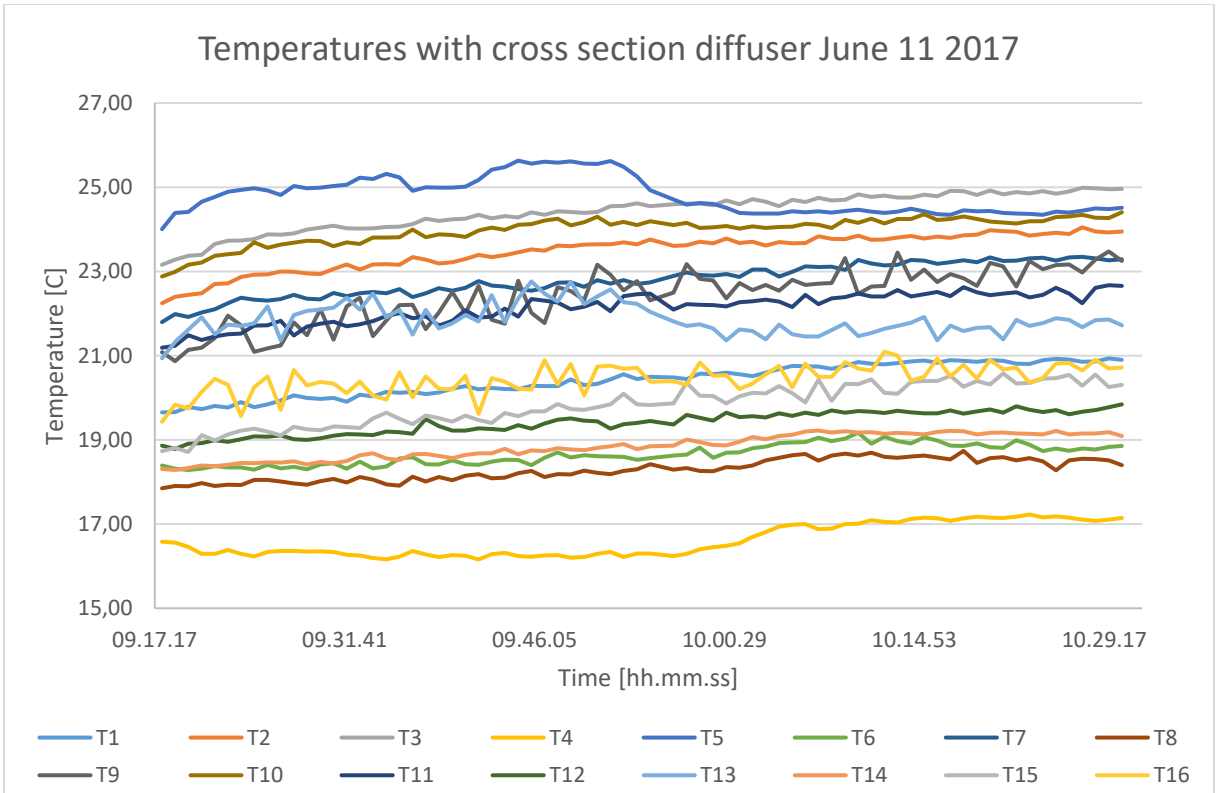
Temperatures with cross section diffuser June 11 2017
27,00
25,00
23,00
21,00
19,00
17,00
15,00
Temperature [C]
09.17.17
09.31.41
09.46.05
10.00.29
10.14.53
10.29.17
Time [hh.mm.ss]
T1
T2
T3
T4
T5
T6
T7
T8
T9
T10
T11
T12
T13
T14
T15
T16

B2. Case II – Normal Occupancy, with Solar Heat Gain

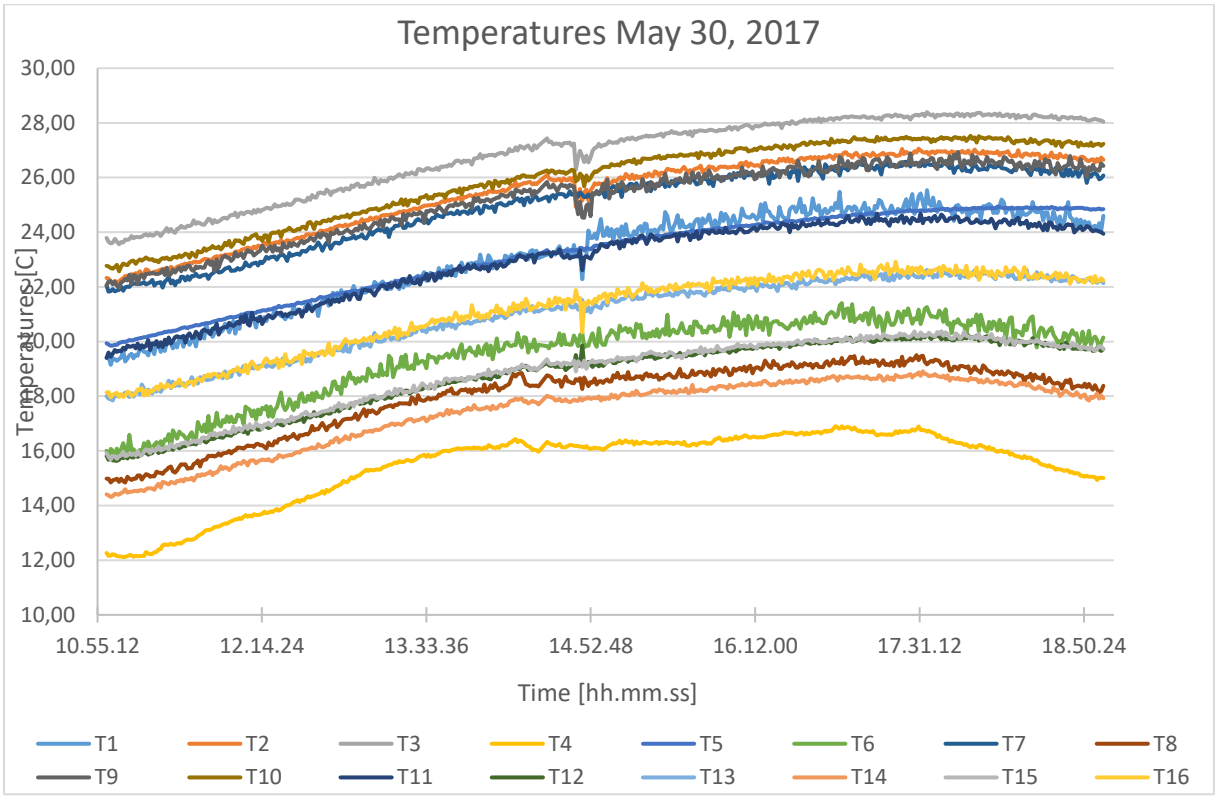

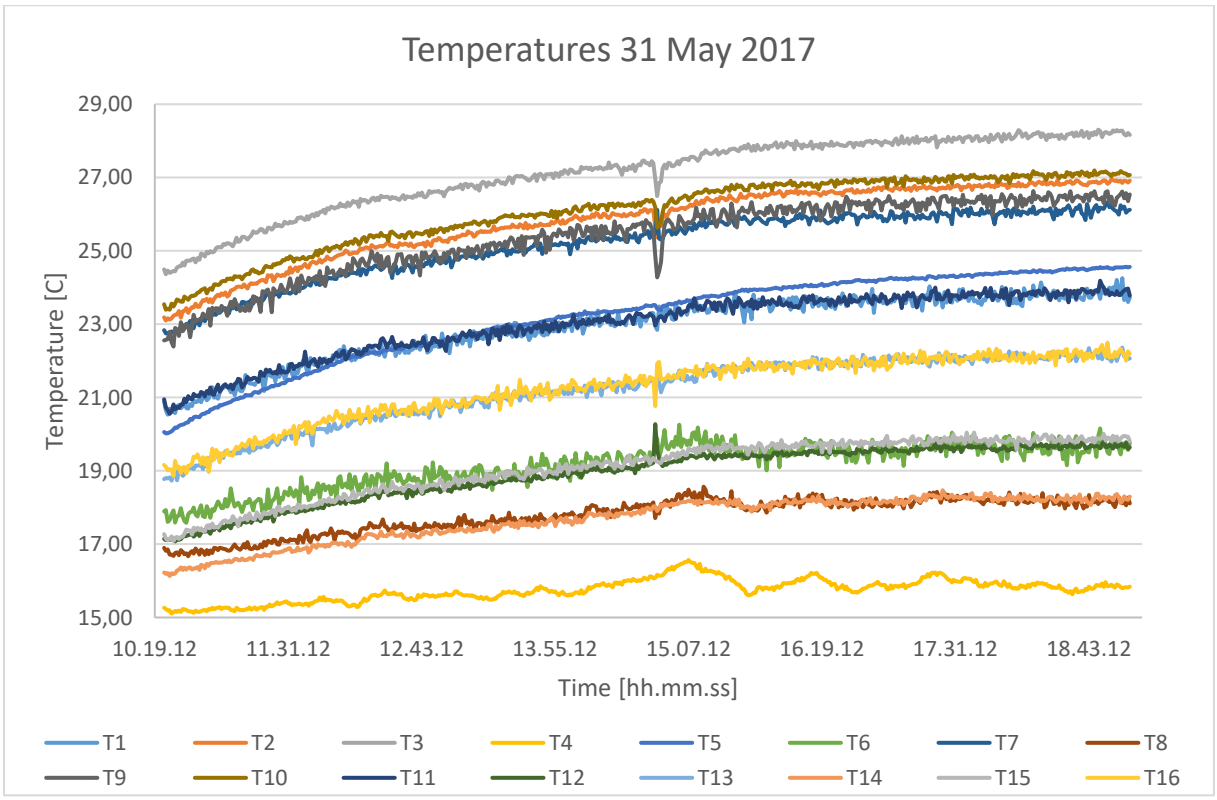

B3. Case III – High Occupancy

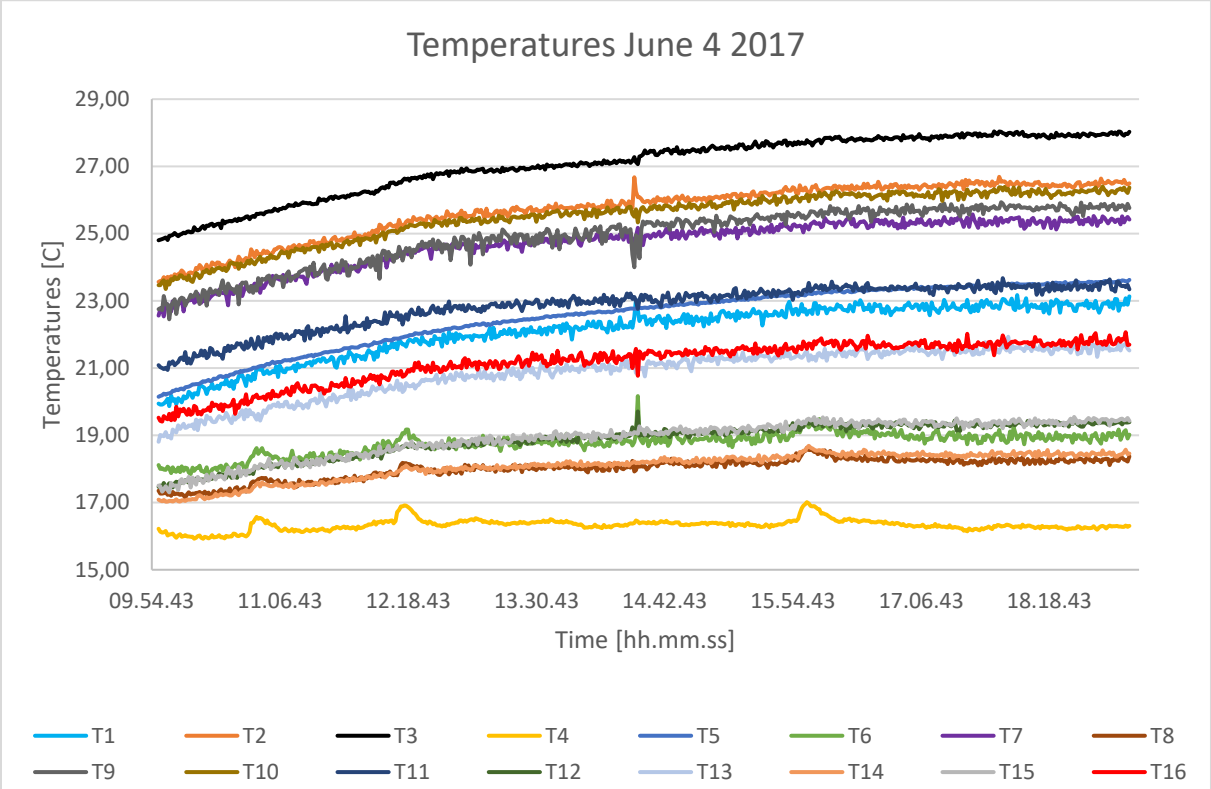

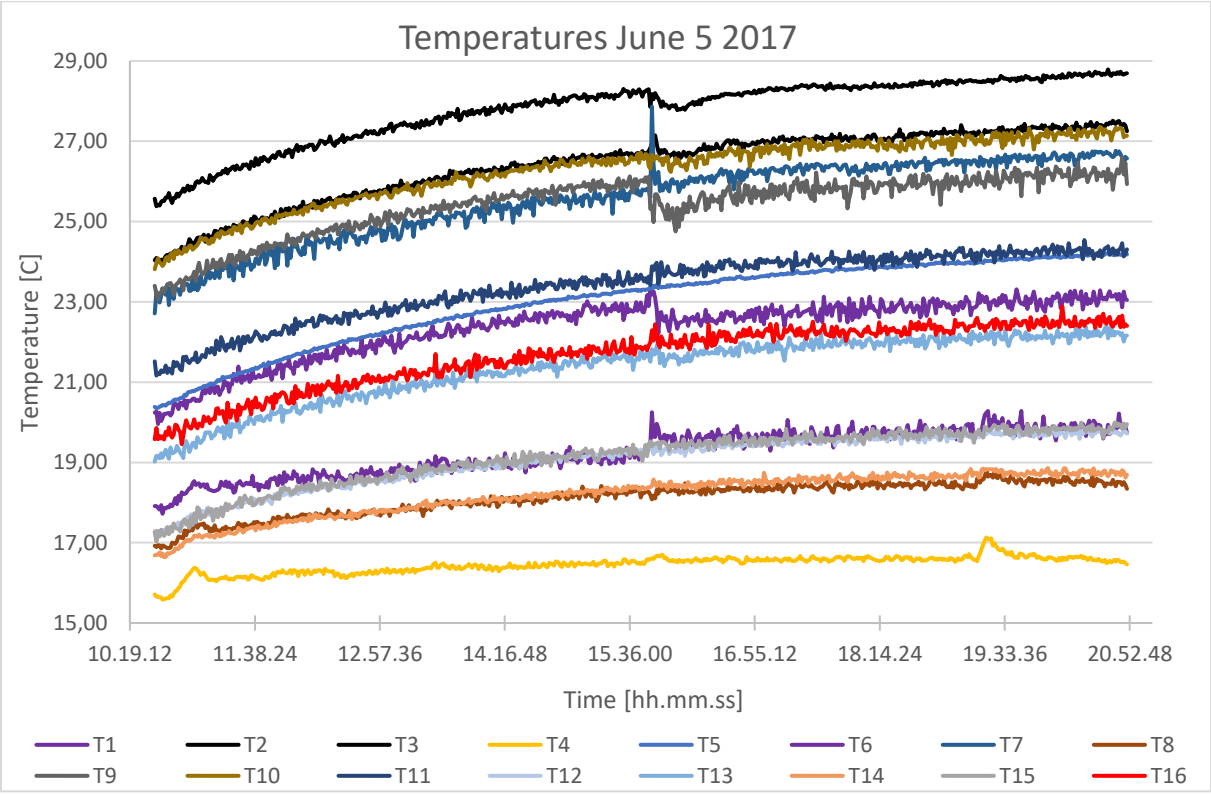

Appendix C. Tracer Gas measurements

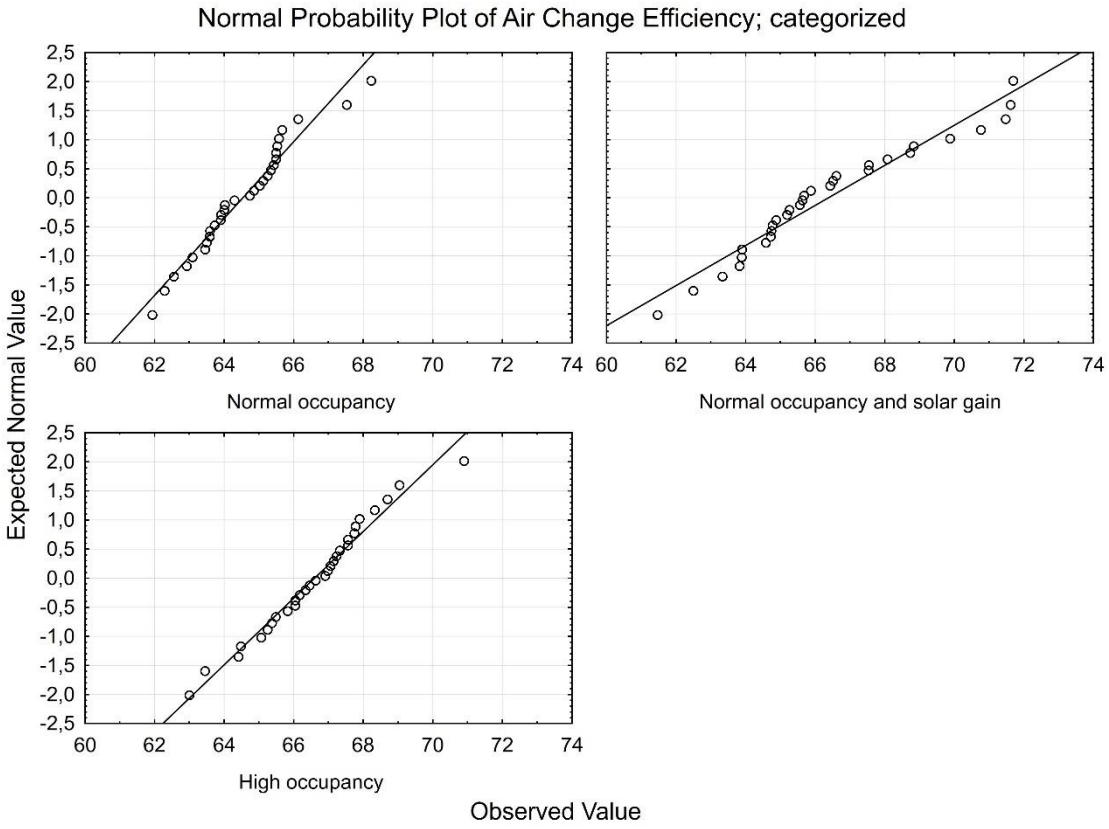

Figure C-1 Normal probability plots of the air change efficiencies for the three different experimental cases.

C1. Case I – Normal Occupancy

	Air Change Efficiency [%-units]					***Mean Age of Air [min]***			
	Set 1	*Set 2*	*Set 3*	*Set 4*		*Set 1*	*Set 2*	*Set 3*	*Set 4*
June 2	64,00	65,34	65,25	63,59		4,48	4,65	4,51	4,57
	64,02	64,85	63,50	65,12		4,48	4,57	4,65	4,63
June 8, setup 1	65,02	65,49	65,66	64,29		4,65	4,56	4,61	4,67
	65,49	63,09	65,58	63,90		4,55	4,55	4,63	4,68
June 8, setup 2	65,53	62,93	-	61,94		4,50	4,80	-	4,82
	66,13	63,45	63,91	64,74		4,58	4,72	4,74	4,70
June 11	68,35	-	62,56	63,72		4,40	-	4,64	4,68
	67,53	63,59	62,29	65,43		4,62	4,90	4,80	4,54

	Nominal Time Constant			
	Set 1	*Set 2*	*Set 3*	*Set 4*
June 2	5,74	6,07	5,88	5,81
	5,73	5,92	5,91	6,03
June 8, setup 1	6,04	5,97	6,05	6,01

	5,97	5,74	6,07	5,98
June 8, setup 2	5,90	6,05	-	5,97
	6,05	6,00	6,06	6,09
June 11	6,01	-	5,81	5,97
	6,25	6,23	5,98	5,94

	Local Air Change Index [%-units]					***Local Age of Air***			
	Set 1	*Set 2*	*Set 3*	*Set 4*		*Set 1*	*Set 2*	*Set 3*	*Set 4*
June 2, normal desk	**East 25**	**East 275**	**East 500**	**East 725**		**East 25**	**East 275**	**East 500**	**East 725**
	167,96	122,98	110,38	120,34		3,41	4,94	5,33	4,83
	176,11	117,21	113,87	120,75		3,25	5,05	5,19	4,99
June 8, setup 1	**South 25**	**South 275**	**South 500**	**South 725**		**South 25**	**South 275**	**South 500**	**South 725**
	275,52	217,86	130,69	144,09		2,19	2,74	4,63	4,17
	276,17	212,91	130,48	139,65		2,16	2,69	4,66	4,28
June 8, setup 2	**South 375**	**South-East 375**	**East 375**	**North 375**		**South 375**	**South-East 375**	**East 375**	**North 375**
	125,25	115,05	-	137,10		4,71	5,25	-	4,35
	128,83	117,36	118,76	-		4,70	5,11	5,11	-
June 11, without desk divider	**East 25**	**East 275**	**East 500**	**East 725**		**East 25**	**East 275**	**East 500**	**East 725**
	189,65	-	89,96	109,94		3,17	-	6,46	5,43
	190,62	128,40	94,02	112,44		3,28	4,85	6,36	5,29

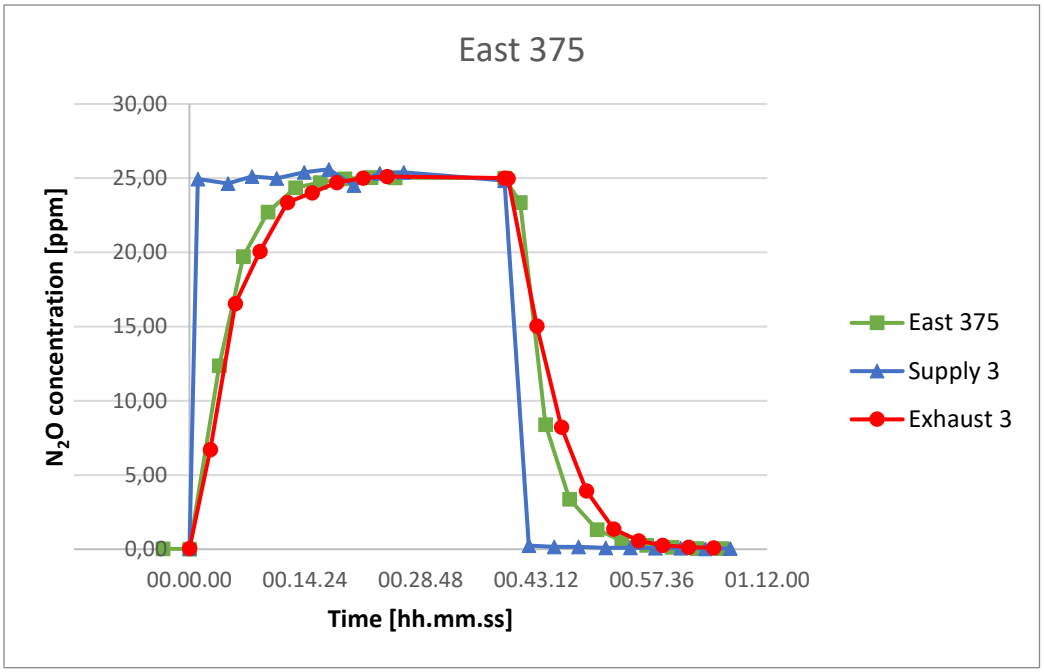

Figure C-2 Tracer gas concentration for one step-up and step-down measurement set. East 375 measured June 8. Normal desk, normal occupancy.

C2. Case II – Normal Occupancy, with Solar Heat Gain

	Air Change Efficiency [%-units]					***Mean Age of Air***			
	Set 1	*Set 2*	*Set 3*	*Set 4*		*Set 1*	*Set 2*	*Set 3*	*Set 4*
May 30, setup 1	68,83	68,73	-	71,48		4,18	4,18	-	4,22
	64,58	61,46	63,88	65,56		4,34	4,49	4,45	4,35
May 30, setup 2	71,61	70,77	69,88	71,69		4,23	4,17	4,13	4,06
	64,74	67,54	65,25	66,60		4,39	4,46	4,41	4,26
May 31, setup 1	-	64,87	63,89	65,63			4,06	4,13	4,04
	66,43	65,87	65,19	62,49		4,68	4,28	4,41	4,22
May 31, setup 2	68,08	66,51	63,34	67,54		4,17	4,03	4,38	4,02
	63,83	65,68	64,77	64,72		4,25	4,26	4,39	4,22

	Nominal Time Constant			
	Set 1	*Set 2*	*Set 3*	*Set 4*
May 30, setup 1	5,75	5,74	-	6,03
	5,60	5,52	5,69	5,71
May 30, setup 2	6,05	5,90	5,77	5,83
	5,68	6,02	5,75	5,68
May 31, setup 1	-	5,27	5,28	5,31
	6,21	5,64	5,75	5,28
May 31, setup 2	5,67	5,37	5,55	5,43
	5,43	5,59	5,68	5,47

	Local Air Change Index [%-units]					*Local Age of Air*			
	Set 1	*Set 2*	*Set 3*	*Set 4*		*Set 1*	*Set 2*	*Set 3*	*Set 4*
May 30, setup 1	**East 25**	**East 275**	**East 500**	**East 725**		**East 25**	**East 275**	**East 500**	**East 725**
	164,53	140,01	-	129,22		3,50	4,10	-	4,67
	161,33	128,15	117,44	128,67		3,47	4,31	4,84	4,44
May 30, setup 2	**East 25**	**East 275**	**East 500**	**East 725**		**East 25**	**East 275**	**East 500**	**East 725**
	186,30	138,91	114,92	129,54		3,25	4,25	5,02	4,50
	164,86	152,15	115,10	127,13		3,45	3,96	5,00	4,47
May 31, setup 1	**South 25**	**South 275**	**South 500**	**South 725**		**South 25**	**South 275**	**South 500**	**South 725**
	-	206,01	109,80	112,69		-	2,56	4,81	4,71
	250,95	-	98,25	107,04		2,48	-	5,85	4,93
May 31, setup 2	**South 375**	**South-East 375**	**East 375**	**North 375**		**South 375**	**South-East 375**	**East 375**	**North 375**
	100,19	109,49	126,85	-		5,66	4,90	4,37	-
	98,59	114,83	130,73	166,89		5,51	4,87	4,35	3,28

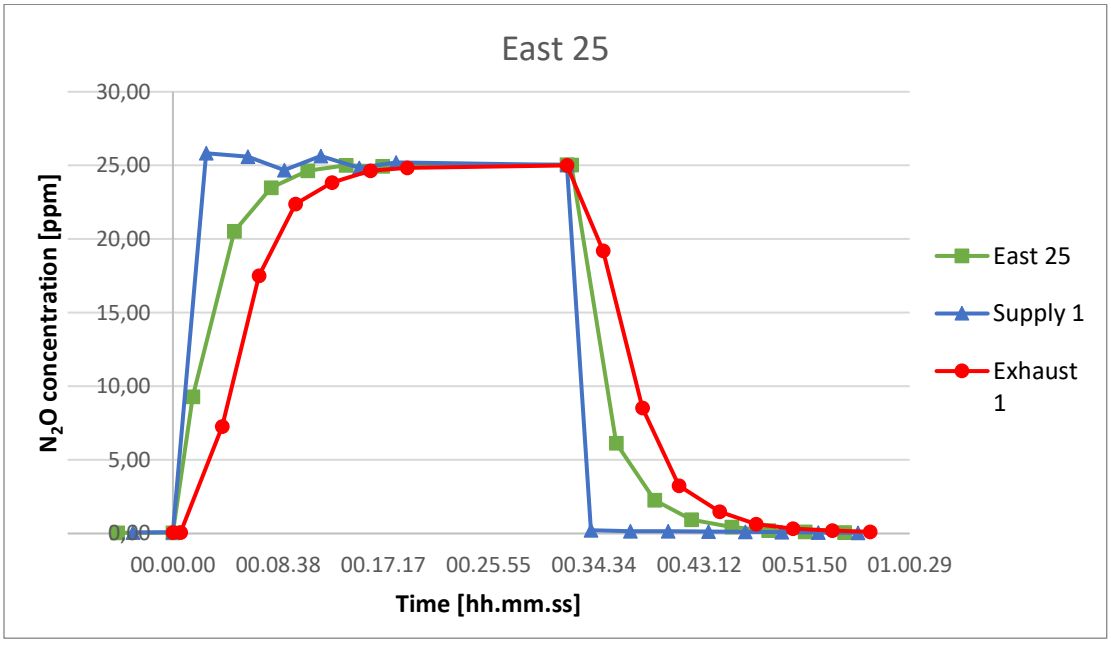

Figure C-3 Tracer gas concentration for one step-up and step-down measurement set. East 25 measured May 30. Normal occupancy and solar gain, small bookshelf in east corner.

C3. Case III – High Occupancy

	Air Change Efficiency [%-units]					*Mean Age of Air*			
	Set 1	*Set 2*	*Set 3*	*Set 4*		*Set 1*	*Set 2*	*Set 3*	*Set 4*
June 4, setup 1	67,63	67,05	66,53	69,04		4,39	4,46	4,52	4,35
	64,62	66,98	63,00	67,32		4,38	4,39	4,52	4,39

June 4, setup 2	-	67,45	66,34	65,75		-	4,14	4,28	4,43
	63,02	65,32	67,74	66,07		4,42	4,33	4,34	4,38
June 5, setup 1	69,31	65,11	67,00	65,13		4,21	4,45	4,26	4,33
	67,62	67,29	66,61	67,31		4,30	4,24	4,40	4,34
June 5, setup 2	65,19	67,06	68,07	-		4,33	4,20	4,15	-
	67,52	70,90	68,46	67,89		4,30	4,32	4,28	4,25

	Nominal Time Constant			
	Set 1	*Set 2*	*Set 3*	*Set 4*
June 4, setup 1	5,94	5,98	6,02	6,01
	5,66	5,88	5,70	5,90
June 4, setup 2	-	5,58	5,67	5,83
	5,57	5,66	5,88	5,79
June 5, setup 1	5,84	5,80	5,72	5,64
	5,82	5,71	5,87	5,85
June 5, setup 2	5,65	5,64	5,64	-
	5,81	6,13	5,86	5,77

	Local Air Change Index [%-units]					***Local Age of Air***			
	Set 1	*Set 2*	*Set 3*	*Set 4*		*Set 1*	*Set 2*	*Set 3*	*Set 4*
June 4, setup 1	**South 375**	**South-East 375**	**East 375**	**North 375**		**South 375**	**South-East 375**	**East 375**	**North 375**
	99,55	101,11	127,52	133,12		5,97	5,91	4,72	4,52
	96,11	101,21	108,54	138,15		5,89	5,81	5,25	4,27
June 4, setup 2	**East 25**	**East 275**	**East 500**	**East 725**		**East 25**	**East 275**	**East 500**	**East 725**
	-	156,87	124,33	130,78		-	3,56	4,56	4,45
	169,79	160,84	135,11	124,80		3,28	3,52	4,35	4,64
June 5, setup 1	**South 25**	**South 275**	**South 500**	**South 725**		**South 25**	**South 275**	**South 500**	**South 725**
	266,25	139,09	110,97	114,73		2,19	4,17	5,15	4,92
	300,85	137,05	106,68	120,34		1,93	4,16	5,50	4,86
June 5, setup 2	**South 25**	**South 275**	**South 500**	**South 725**		**South 25**	**South 275**	**South 500**	**South 725**
	326,04	216,26	138,58	-		1,73	2,61	4,07	-
	332,11	225,67	144,31	156,18		1,75	2,72	4,06	3,69

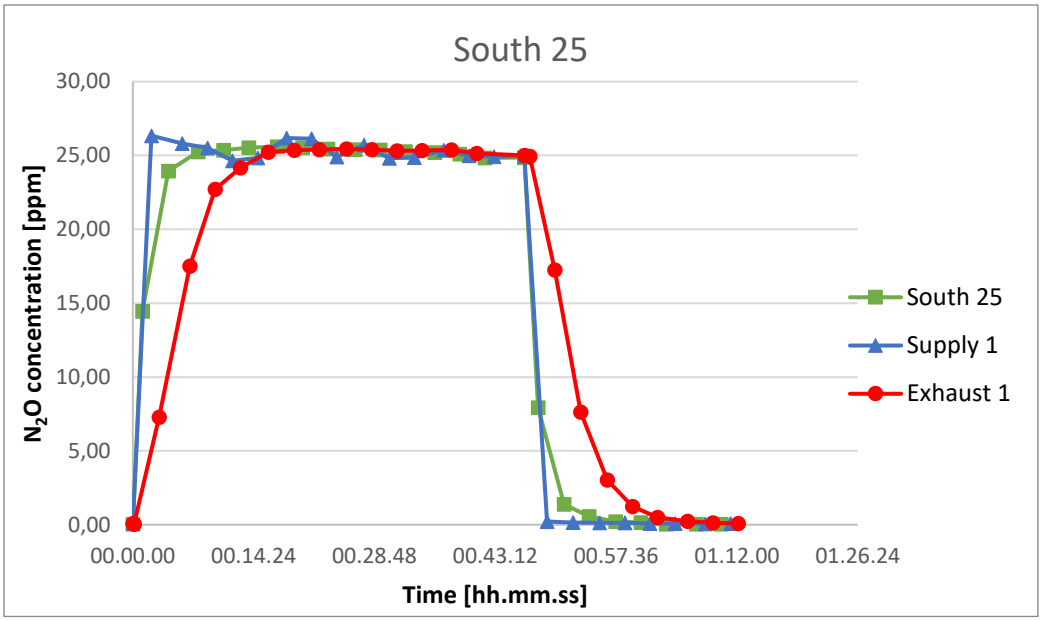

Figure C-4 Tracer gas concentration for one step-up and step-down measurement set. South 25 measured June 5, high local occupancy.

Appendix D. Worksheet for Tracer Gas Calculation

The Excel data sheet for calculating the air change efficiency presented below. Local air change index calculated in a similar sheet, where the local age of air is calculated and the local air change index can be calculated from the local age of air and the nominal time constant. The tracer gas calculations presented for the three cases in this thesis is made up of 48 data sheets similar data sheets calculating the step-up and step-down concentrations for the exhaust, and 48 measurements calculation the step-up and step-down concentration for the local points in the model. The following sheet present the step-up calculations for the Exhaust concentration for the East 725 measurement in the model on June 2 2017. The step-up concentration has been inverted to show a decay curve.

Exhaust 4		**C∞**	25,00
Time	**N2O**	**C∞-C(x)**	0,43
00:00:00	0,08	24,92	
00:02:18	3,31	21,69	
00:05:23	15,54	9,46	
00:08:23	19,72	5,28	
00:11:23	22,72	2,28	
00:14:53	24,11	0,89	
00:17:53	24,62	0,38	
00:20:53	24,81	0,19	
00:24:18	24,96	0,04	
00:33:55	25,00	0,00	
00:35:48	22,42	2,58	
00:39:03	12,34	12,66	
00:42:13	5,11	19,89	
00:45:13	2,62	22,38	
00:48:43	0,96	24,04	
00:51:48	0,55	24,45	
00:54:48	0,32	24,68	
00:58:08	0,20	24,80	
01:01:08	0,12	24,88	

SLOPE		Exhaust 4		Calculated values		
-0,237		**Time (min)**	**PPM N2O**		Area under the curve	Weighted area under the curve
00.00.00	00.00.00	0,00	24,92			
00.02.18	00.02.18	2,30	21,69		53,6073	61,6484224
00.05.23	00.05.23	5,38	9,46		48,0209	184,480105
00.08.23	00.08.23	8,38	5,28		22,1086	152,180814
00.11.23	00.11.23	11,38	2,28		11,3512	112,187803
00.14.53	00.14.53	14,88	0,89			
00.17.53	00.17.53	17,88	0,38			
00.20.53	00.20.53	20,88	0,19			
00.24.18	00.24.18	24,30	0,04			
00.33.55	00.33.55	33,92	0,00			
00.35.48	00.35.48	35,80	2,58			
00.39.03	00.39.03	39,05	12,66			
00.42.13	00.42.13	42,22	19,89			
00.45.13	00.45.13	45,22	22,38			
				Tail	9,6349	
				Weighted tail		150,331167
				sum area	144,72	
				Sum weighted area under the curve		660,83
						IN TIME
				Mean age of air	4,57	00.04.34
				Nominal time constant	5,81	00.05.48
				Air change efficiency, %	63,59	

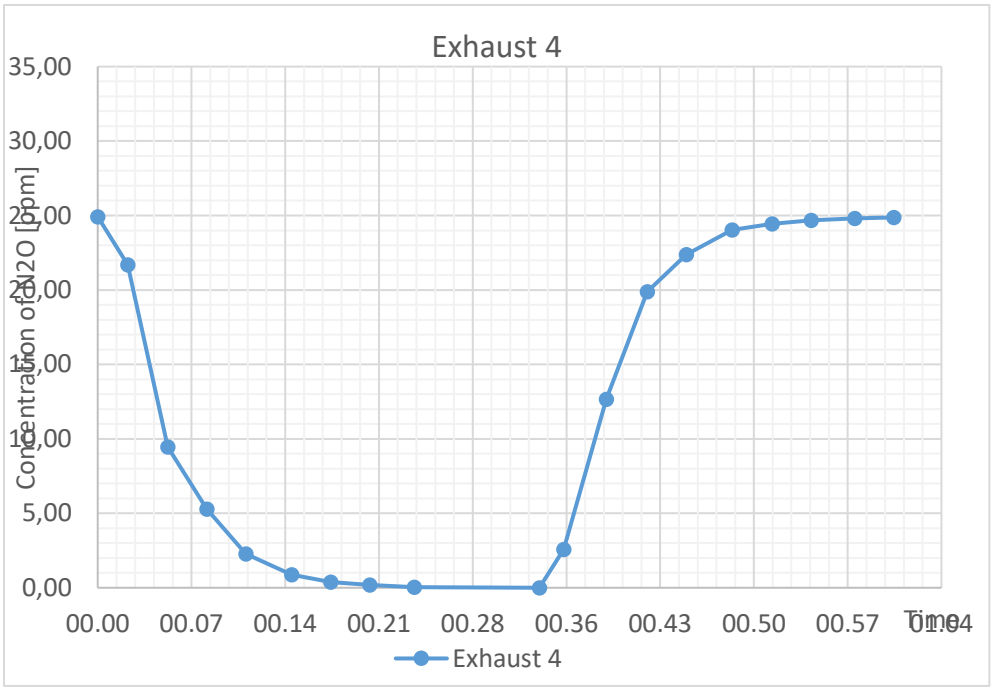

Figure D-1 Inverted concentration curve

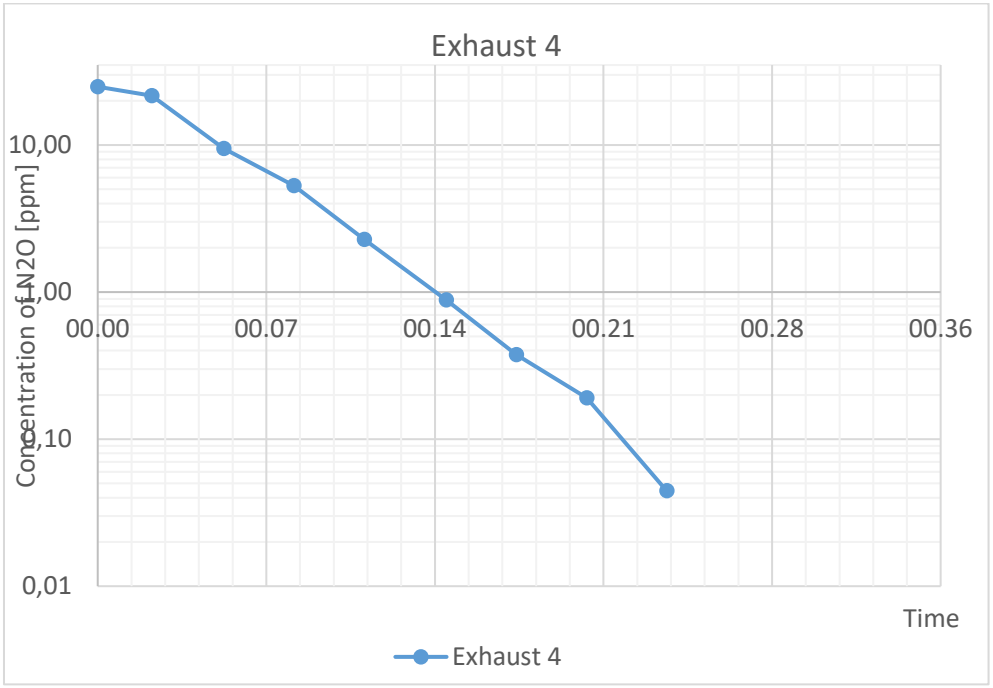

Figure D-2 Logarithmic representation of the inverted step-up concentrations.

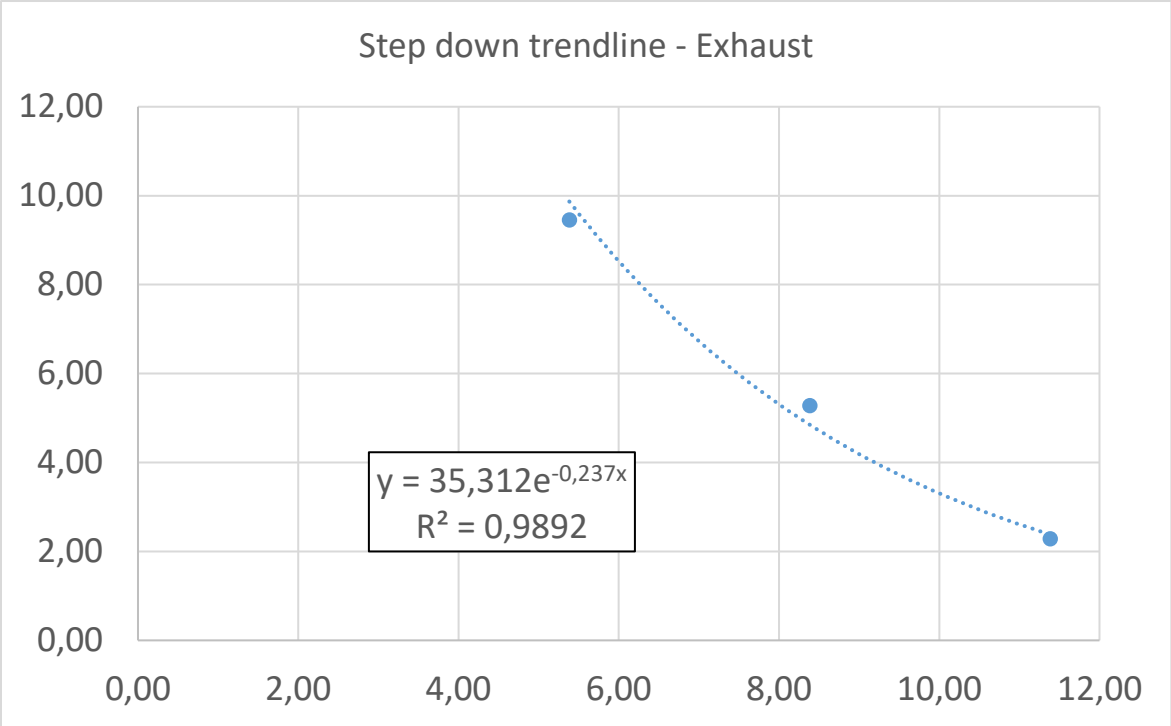

Figure D-3 Trend line from straight logarithmic representation calculate the slope for the tail.

Appendix E. Equipment

E1. Thermocouples

The temperatures have been measured with TSI thermocouples of Type-T (copper/constantan), with extension wires. The thermocouples consist of two wires of different metals, welded at one end, making a junction. When the junction measures a temperature change, a voltage is created, which can be interpreted into a temperature. Thermocouple Type-T is very stable, and can measure temperatures from -270°C to +300°C (-200°C to +200°C with good repeatability). The extension cable has a temperature range of 0°C to +200°C. (Thermocouple Info, 2016)

E2. Air Velocity Transducers

Hot-Wire anemometers are used to measure the air velocities. The models used are of type 8465 (windowless) and 8475 (omnidirectional). The anemometers have been calibrated in a TSI compression air calibrator.

Table 0.1 Air Velocity Transducer Specifications (TSI, 2016)

	TSI 8465	**TSI 8475**
Range	0,125 - 50 m/s	0,05 - 0,5 m/s
Accuracy	±2,0% of reading ±0,5% of full scale of selected range	±3,0% of reading ±1,0% of full scale of selected range
Response time to flow	0,2 seconds	5 seconds

E3. LabVIEW

Temperature and velocity meters are connected to a logging system by National Instruments. The data are sent to and logged in a computer program, LabVIEW. The data stored can be exported to an excel file for further processing. The temperatures have been logged once every 60 seconds, and the air velocities have been logged once every 2 seconds.

E4. Tracer Gas Equipment

Figure E-1 Sampler (left) and monitor (right) system from Brüel & Kjær.

A sampler and monitor system by Brüel & Kjær was used to measure the tracer gas concentrations in the model. The system is fitted with filters to measure different types of gasses. The sampler is a multi-point sampler of type 1303, and the monitor is a multi-gas monitor of type 1302. The sampler has six channels for measuring the concentration, which is done at regular time intervals. The sampler has a possibility of dosing tracer gas at regular intervals, but as the tracer gas was supplied at a constant flow rate in these experiments, the dosing channels was not used. Both the sampler and monitor was remotely controlled by LumaSense Technologies Application Software – Innova 7620. The software has the application to activate the different sampler channels and gas filters. For these experiments the filter for N_2O was activated, with water compensation. Innova 7620 also log the measured concentrations in a database, which then can be exported for further analysing.

The sampler and monitor system uses speakers to measure the concentration of tracer gas in the air. The system does not measure zero concentration when there is no tracer gas present in the air. Some disturbances or static noise can register as a small amount of tracer gas. This amount must be subtracted from the tracer gas measurements. In addition, water compensation can be turned on, to exclude the water vapour in the air. However, if the system is not properly calibrated, giving linear results, the different amount of vapour in the air at different days can give some differences.

Appendix F. Placing of iButton Sensors at Prototype

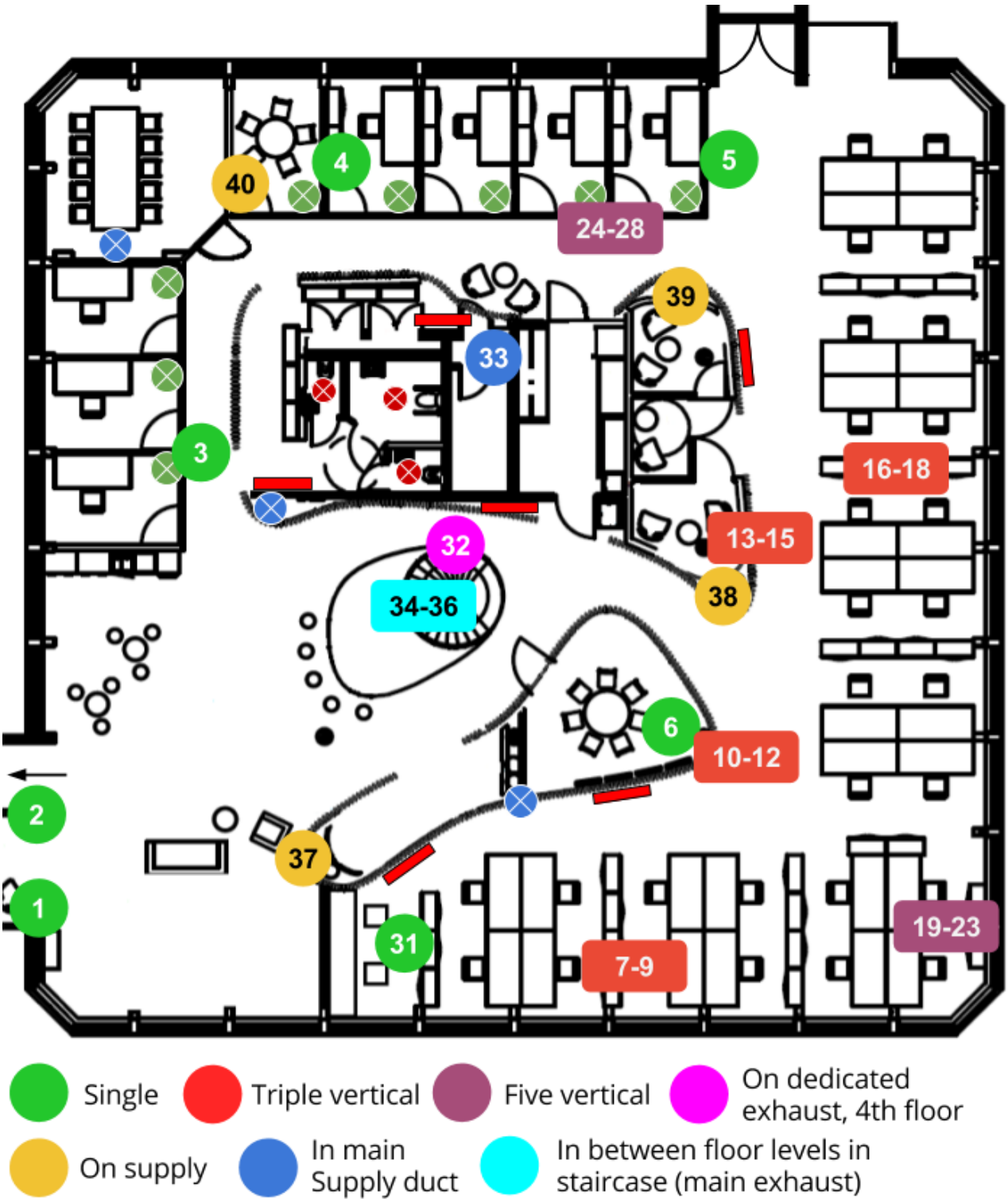

Figure F-1 Individual placing of iButton sensors at Powerhouse Kjørbo, 2nd floor. (Søgnen, 2015b)

Table F-1 Individual placing of iButton temperature sensors at Powerhouse Kjørbo. (Søgnen, 2015b)

Floor	Number	Room	Use	Specific position	Height (cm)	Area
2nd	1	Open landscape	Entrance area	On wall	110	S
2nd	2	Open landscape	Entrance area	On wall	110	S
2nd	3	Open landscape	Hallway	On wall	110	SW
2nd	4	4208	Cell Office	On wall	110	NW
2nd	5	Open landscape	Open office	On wall	110	N
2nd	6	4239	Meeting room	On wall	110	C
2nd	7	Open landscape	Open office	Vertical (attached from the ceiling with a string)	10	SE
2nd	8	Open landscape	Open office		110	SE
2nd	9	Open landscape	Open office		170	SE
2nd	10	Open landscape	Open office	Vertical (attached from the ceiling with a string)	10	E
2nd	11	Open landscape	Open office		110	E
2nd	12	Open landscape	Open office		170	E
2nd	13	Open landscape	Open office	Vertical (attached from the ceiling with a string)	10	NE
2nd	14	Open landscape	Open office		110	NE
2nd	15	Open landscape	Open office		170	NE
2nd	16	Open landscape	Open office	Vertical (attached from the ceiling with a string)	10	NE
2nd	17	Open landscape	Open office		110	NE
2nd	18	Open landscape	Open office		170	NE
2nd	19	Open landscape	Open office	Vertical (attached from the ceiling with a string)	10	E
2nd	20	Open landscape	Open office		110	E
2nd	21	Open landscape	Open office		170	E
2nd	22	Open landscape	Open office		230	E
2nd	23	Open landscape	Open office		300	E
2nd	24	Open landscape	Hallway	Vertical (attached from the ceiling with a string)	10	NW
2nd	25	Open landscape	Hallway		110	NW
2nd	26	Open landscape	Hallway		170	NW
2nd	27	Open landscape	Hallway		230	NW
2nd	28	Open landscape	Hallway		300	NW
AHU	29	Technical 4th floor	Vent. unit	Venstre tillufstvifte	-	-
AHU	30	Technical 4th floor	Vent. unit	Høyre tillufstvifte	-	-

2nd	31	Open landscape	Open office	south part	110	SE
4th	32	4th floor	Dedicated Exhaust 4th	Not staircase exhaust	270	-
2nd	33	Main supply duct	Inside one supply duct		-	-
2nd	34	Central stair	-	Etasjeskille 1-2	0	C
3rd	35	Central stair	-	Etasjeskille 2-3	0	C
4th	36	Central stair	-	Etasjeskille 3-4	0	C
2nd	37	Open landscape	On supply duct	South supply	30	S
2nd	38	Open landscape	On supply duct	NE supply	30	NE
2nd	39	Open landscape	On supply duct	North supply	30	N
2nd	40	Cell office	On supply duct -4207	4207 supply	20	W

Flödesmätspjäll DIRU

Beskrivning

DIRU är ett irisspjäll för mätning och injustering av luftflöden. DIRU har följande egenskaper: låg ljudnivå, centriskt flöde, fasta mätuttag som ger noggrann flödesmätning samt är utrustad med regleringsfunktion som kan öppnas helt, vilket betyder att det inte krävs någon renslucka.
Klarar täthetsklass C.

Dimensioneringsdiagrammen ska användas för att bestämma tryckfallet över flödesmätspjället samt ge information om ljudeffektnivå vid olika inställningar.

Vid injustering av spjället ska injusteringsdiagrammen användas. För flödesmätspjäll finns en monterings-, mätnings-, injusterings- och skötselanvisningen (MMIS).

Reglerskivorna bildar en mätfläns som möjliggör flödesmätning. Avläst tryckfall över donets mätnipplar ger luftflödet efter utträkning med k-faktor. K-faktor och spjällinställning är sammat tal, vilket innebär att man slipper avläsa diagram för att få fram k-faktorn utifrån en viss spjällinställning. Luftflödet regleras med spjällets handtag.

Utförande
Spjället är tillverkat i galvaniserad stålplåt

Montering
DIRU injusteringsspjäll monteras så att störningsavståndet beaktas.

Rensning
Genom att ställa spjället i öppet läge kommer man åt att rensa kanalen. Kom ihåg att återställa spjället efter rensning.

Dimensioner

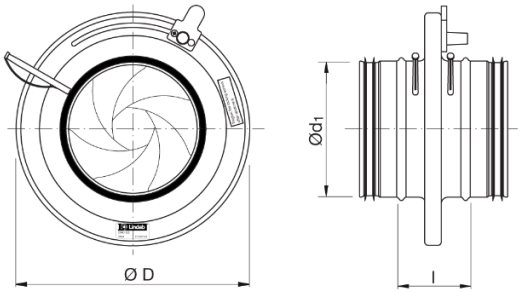

Ød1 nom	ØD mm	l mm	m kg
80	135	52	0,60
100	163	54	0,80
125	210	63	1,20
160	230	60	1,40
200	285	62	2,00
250	333	62	2,60
315	406	63	3,40
400	560	70	6,90
500	644	60	7,90
630	811	60	11,9

Beställningsexempel

DIRU	160
Produkt	
Dimension Ød1	

Appendix H. Risk Assessment

Experiments are conducted in a scaled model in the Indoor Climate Lab at the Thermal Energy Building (VATL). The description of the model can be seen in Chapter 4.2. There is equipment set up for tracer gas experiments, smoke air tubes will be used for smoke experiments, and the lightbulb effect is controlled by a Variac. There are some risk factors connected to these experiments, and a Risk Assessment has been conducted. The results are summarized in Table H-1. The full version is sent electronically to the supervisor.

Table H-1 Risk factors in model experiments

Risk source	**Risk**	**Risk assessment**	**Action**
Tracer gas (N_2O)	Excessive gas leakage	D1	Handle according to safe handling of gas
Lightbulbs	Overheating	C2	Do not cover or touch when in use
Variac	Electrical shock	D1	Use according to user manual
Smoke ampule (Sulfuric acid)	Burns or stains due to leakage	B2	Handle according to user manual

Conclusion: The risks of the activity are acceptable. No special safety equipment is needed. Unit Responsible should have training in safe handling of gas.

Table H-2 Risk Matrix

CONSEQUENSES	Catastrophic	**E1**	**E2**	**E3**	**E4**	**E5**
	Major	**D1**	**D2**	**D3**	**D4**	**D5**
	Moderate	**C1**	**C2**	**C3**	**C4**	**C5**
	Minor	**B1**	**B2**	**B3**	**B4**	**B5**
	Insignificant	**A1**	**A2**	**A3**	**A4**	**A5**
		Rare	Unlikely	Possible	Likely	Almost
		PROBABILITY				

Shutdown procedure consist by switching off the channel fan in the test room and the air handling system placed on the floor directly below the test room. Delivered air is stopped by switching off the fans. The tracer gas supply is stopped by turning the valve on top of the tank

clockwise until it is shut. The heat sources are disconnected by unplugging them. Used smoke ampoules should be disposed of according to proper procedures.

Action on rig before evacuation:

- Shut off the N_2O gas supply by closing valve on the tank
- Switch off the fan connected to the model
- Unplug the heat sources